Saturation, the Color Glass Condensate and Glasma:
What Have we Learned from RHIC?

RIKEN BNL Research Center Workshop
May 10-12, 2010 at Brookhaven National Laboratory

Dependence of Single Particle Distributions on Rapidity and Centrality

R. Debbe BNL

BROOKHAVEN NATIONAL LABORATORY

Outline of talk

- The physics context of d+Au collisions.
- What was measured so far at RHIC.
- Mid-rapidity measurements.
- Forward measurements.
- Descriptions of high y measurements
- Summary

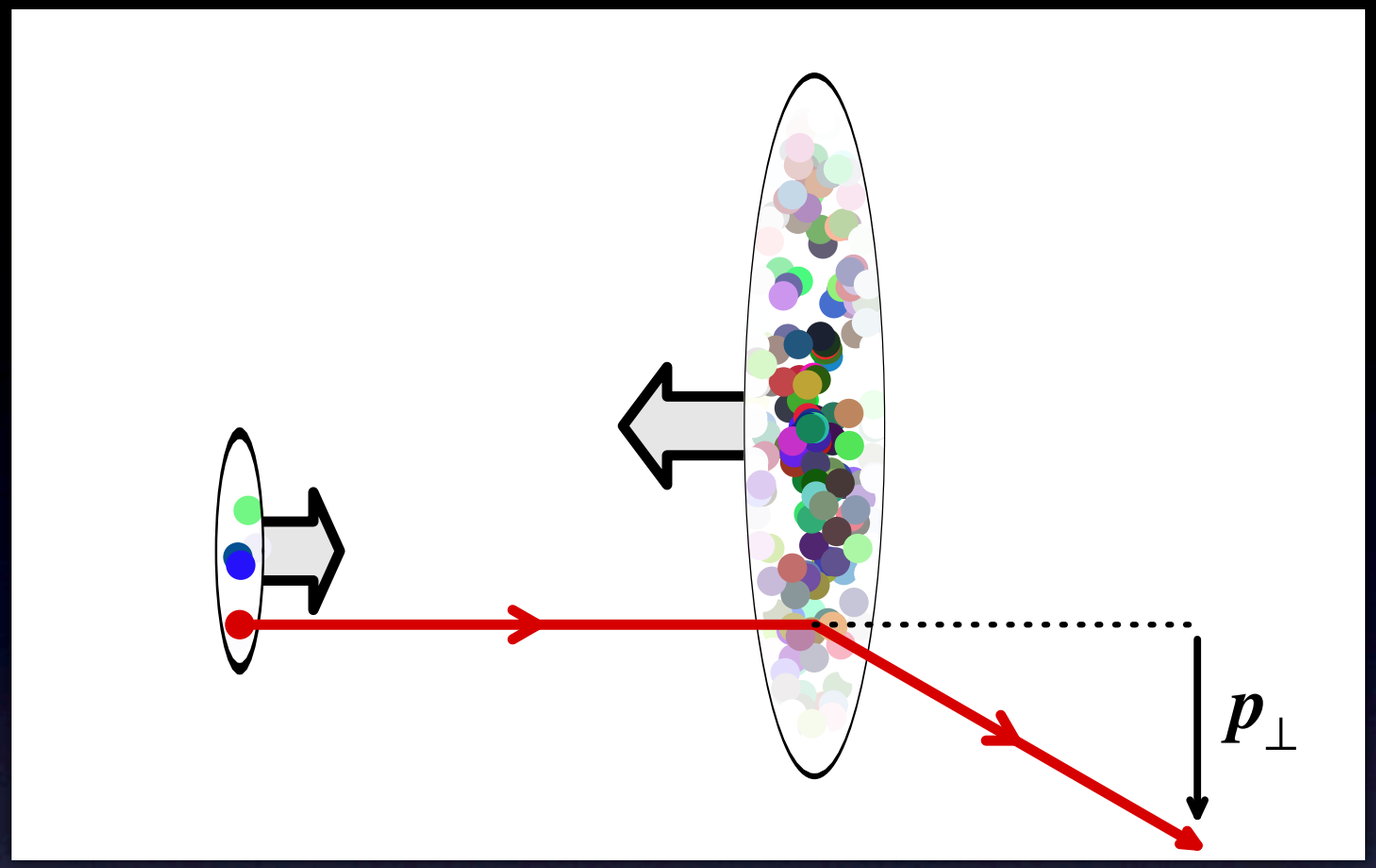

At RHIC energies the d beam can be considered to first order, as a beam of quarks. At mid-rapidity the interactions probe x~0.01 on both beam and target.

At high rapidity the collision is much more skewed; the x of the beam partons is in the range of x~0.1 (valence quarks) and the target is probed at values that can range down to x~0.001

$$x_a = \frac{2M_T}{\sqrt{s}}\cosh(y^*)e^{y_{system}} \qquad x_b = \frac{2M_T}{\sqrt{s}}\cosh(y^*)e^{-y_{system}}$$

$$y_{system} = 1/2(y_1+y_2)$$

$$y^* = 1/2(y_1-y_2)$$

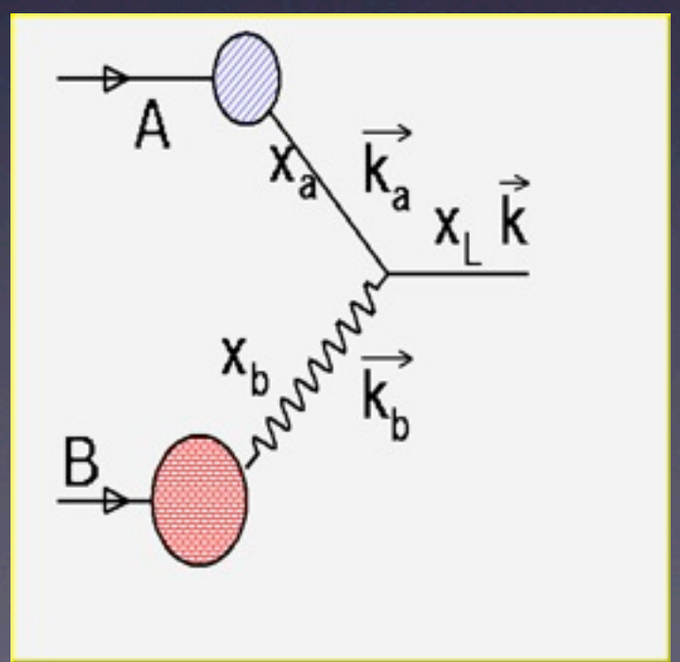

HERA results show the PDFs growing fast as x becomes small. Specially for gluons.

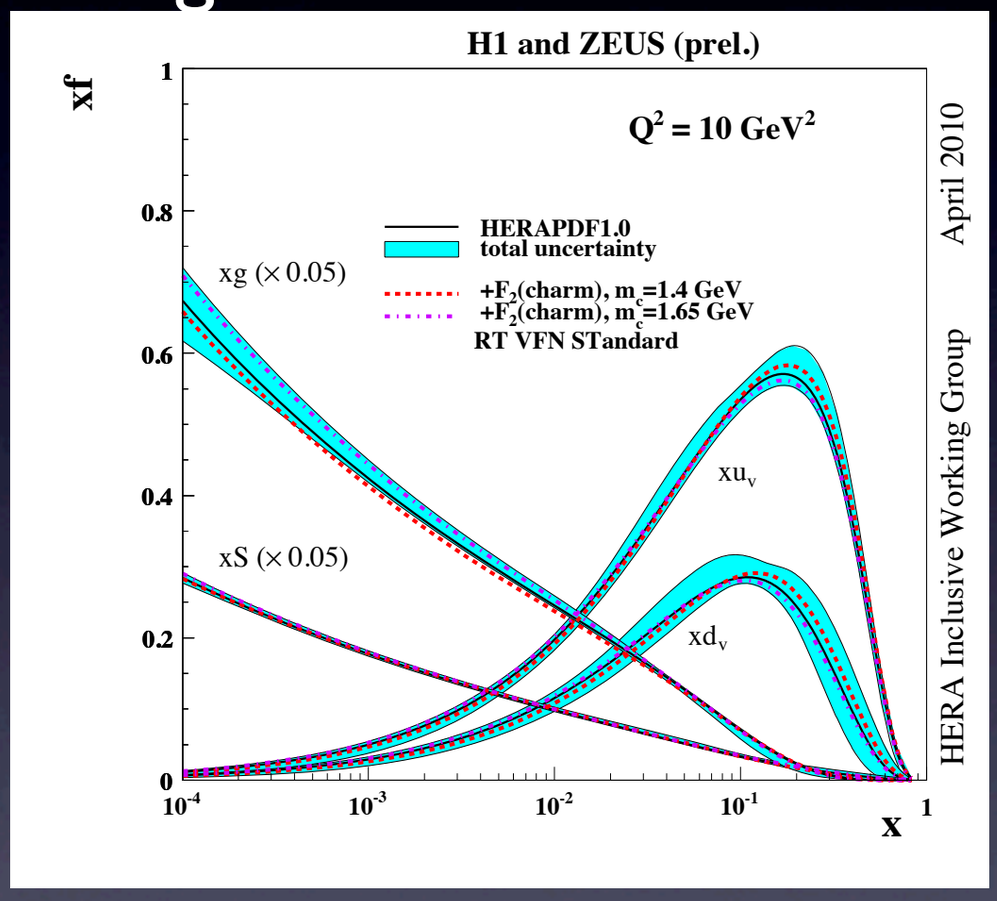

The onset of non-linear effects (gluon fusion) can set at $\sigma n \sim 1$ (probability of interaction with a gluon of the target equal to 1) which with $n=(dN/dy)/\pi R^2$ and $\sigma=\alpha_s N_c/Q^2$ sets the condition on the transverse momentum of the probe:

$$Q^2_s \sim (\alpha_s N_c/\pi R^2) dN/dy$$

the growth of dN/dy with x is set to: $dN/dy \sim 1/x^\lambda$ with λ extracted from HERA data with value ranging from 0.2-0.3

For nuclear targets, the A dependence is introduced with: $Q^2_{sA} = A^{1/3}\, Q^2_s$ which will be written as:

$$Q^2_{sA} = A^{1/3}\, Q^2_0\, (x_0/x)^\lambda = A^{1/3}\, Q^2_0\, x^\lambda_0\, e^{\lambda y}$$

$$Q^2_{sA} = A^{1/3}\, Q^2_0\, (x_0/x)^{\lambda} = A^{1/3}\, Q^2_0\, x^{\lambda}_0\, e^{\lambda y}$$

At RHIC top energy one can "raise" the saturation scale Q_s by increasing the size of the target and/or by measuring at high rapidity.

using $Q_0 \simeq 1$ GeV, $\lambda \simeq 0.3$ and $x_0 \simeq 3.0 \times 10{-}4$ we have:

$Q^2_s(y=0) = 0.49$ GeV^2 and $Q^2_s(y=3) = 1.2$ GeV^2

The impact parameter dependence is added with:

$$Q^2_s(b) = Q^2_s(b=0)\sqrt{1 - (b/R)^2}$$

The Au target leaves a "spray" of mostly pions ~2.5 units of y "behind"

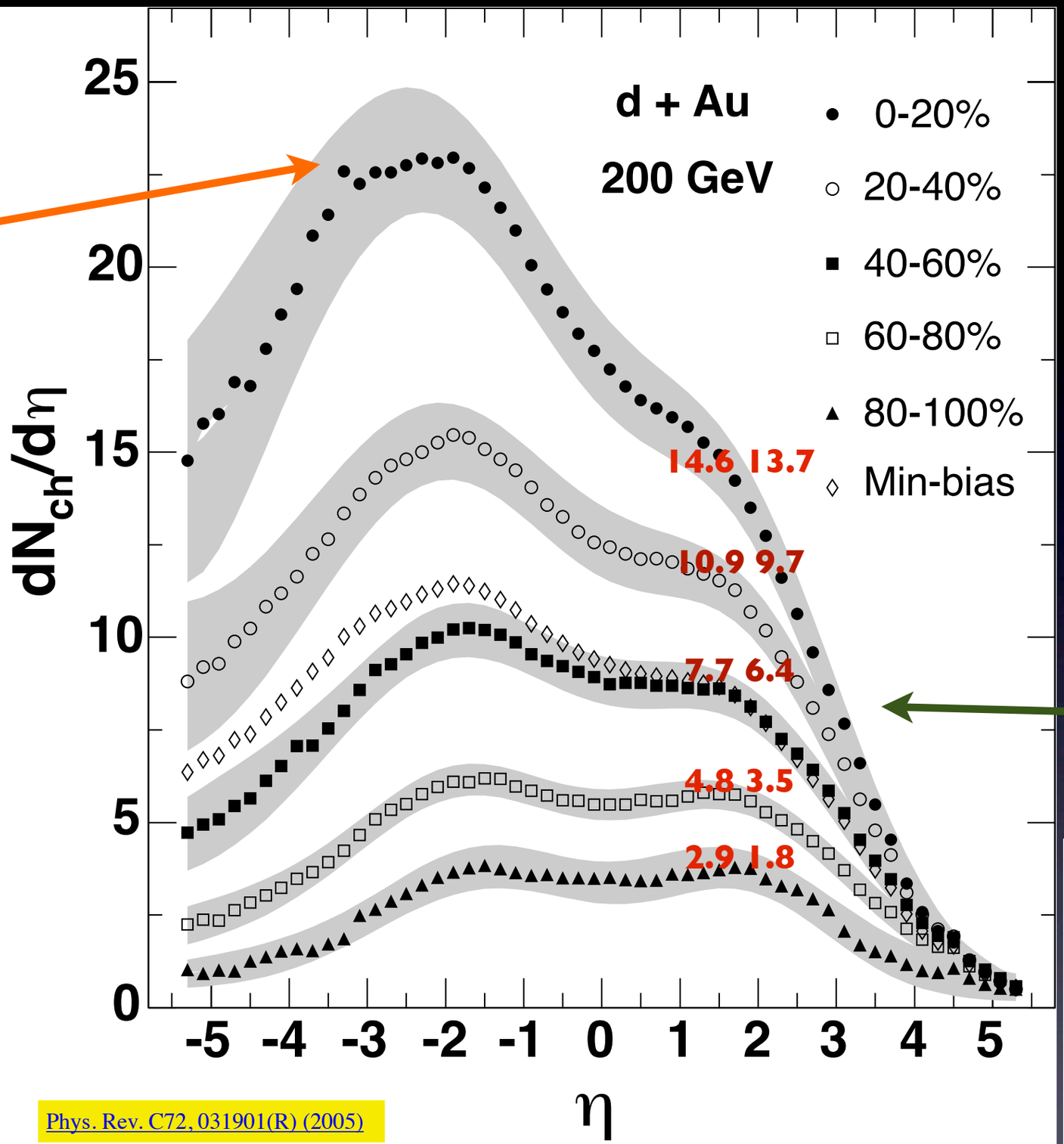

The d beam leaves a "trail" similar to N_{part} or N_{coll} times a proton beam.

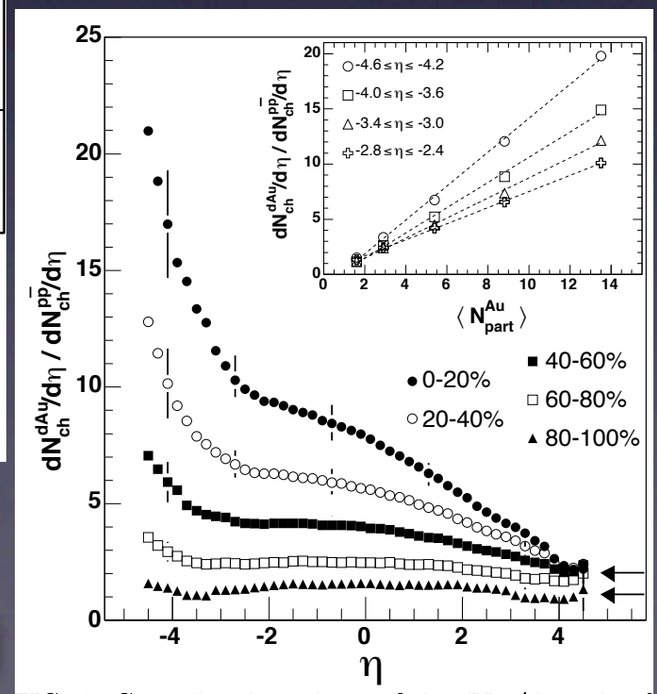

Phys. Rev. C72, 031901(R) (2005)

Triangular distribution

S. J. Brodsky *et al.*, Phys. Rev. Lett., **39**, 1120 (1977).

STAR π^0

BRAHMS FS

PHENIX μ

BRAHMS MRS

PHOBOS

PHENIX STAR π^0

STAR ln rise

PHENIX TOF

STAR TOF

STAR DEDX

PHENIX μ

STAR π^0

BRAHMS mult.

PHOBOS mult.

RAPIDITY

P_T

Particle production in d+Au at 200 GeV and mid-rapidity

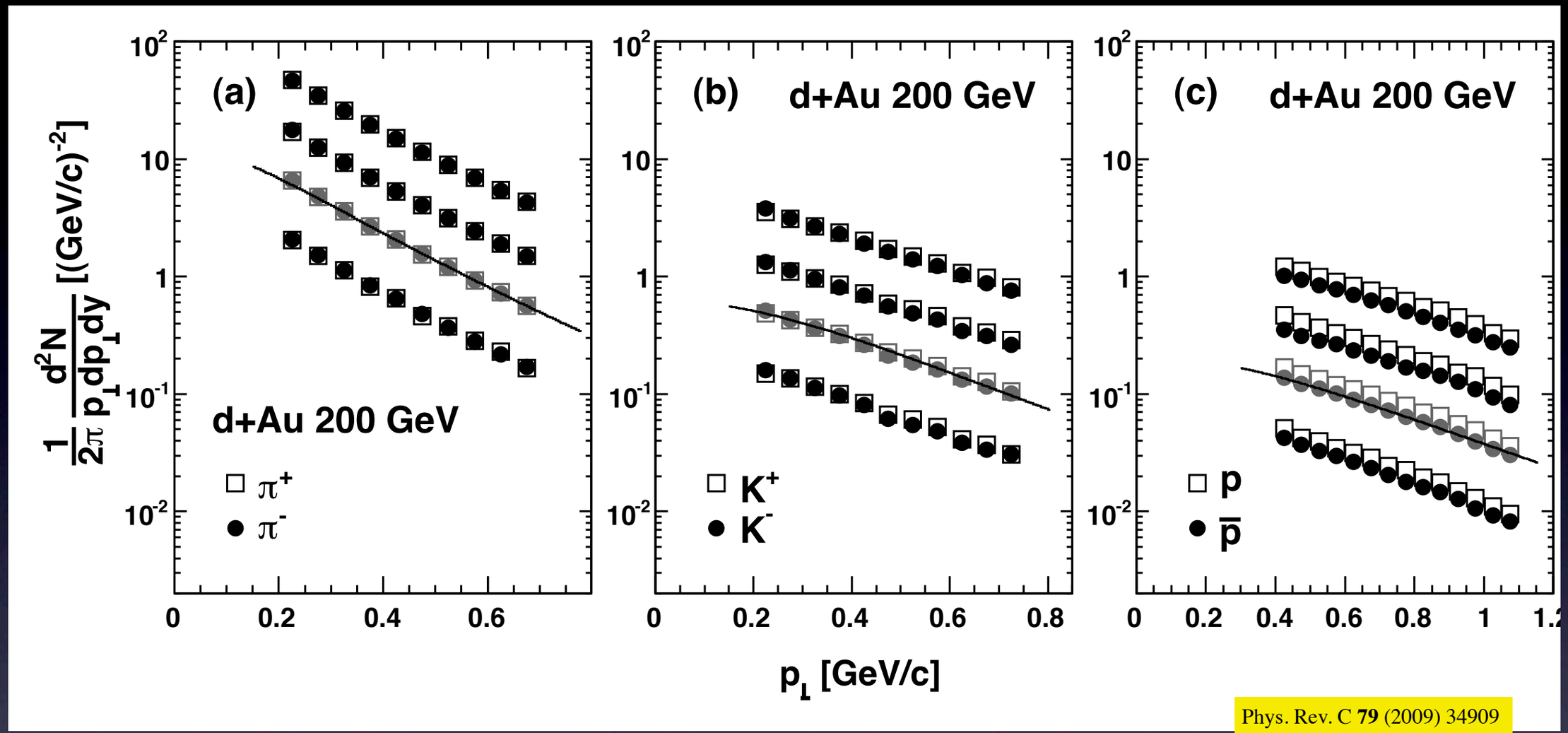

Phys. Rev. C **79** (2009) 34909

STAR TPC measurements at |y|<0.1 Particle identification done with dE/dx. Centrality from top to bottom: 0-20%, 20-40%, MB, 40-80%. Fits to Blast Wave model describe well the data and are used to integrate and extract dn/dy.

System	Centrality	π^-	π^+	K^-	K^+	$\overline{p}$	p	$p-\overline{p}$
pp 200 GeV	min. bias	1.42 ± 0.11	1.44 ± 0.11	0.145 ± 0.013	0.150 ± 0.013	0.113 ± 0.010	0.138 ± 0.012	0.025 ± 0.004
d+Au 200 GeV	min. bias	4.63 ± 0.31	4.62 ± 0.31	0.582 ± 0.052	0.595 ± 0.054	0.412 ± 0.053	0.500 ± 0.069	0.088 ± 0.029
	40-100%	2.89 ± 0.20	2.87 ± 0.21	0.348 ± 0.032	0.356 ± 0.033	0.236 ± 0.030	0.281 ± 0.039	0.045 ± 0.018
	20-40%	6.06 ± 0.41	6.01 ± 0.41	0.783 ± 0.085	0.803 ± 0.087	0.569 ± 0.082	0.72 ± 0.11	0.154 ± 0.050
	0-20%	8.42 ± 0.57	8.49 ± 0.58	1.09 ± 0.09	1.11 ± 0.10	0.793 ± 0.087	0.95 ± 0.11	0.159 ± 0.049

Centrality defined with tracks in Au side FTPC -3.8<η<-2.8

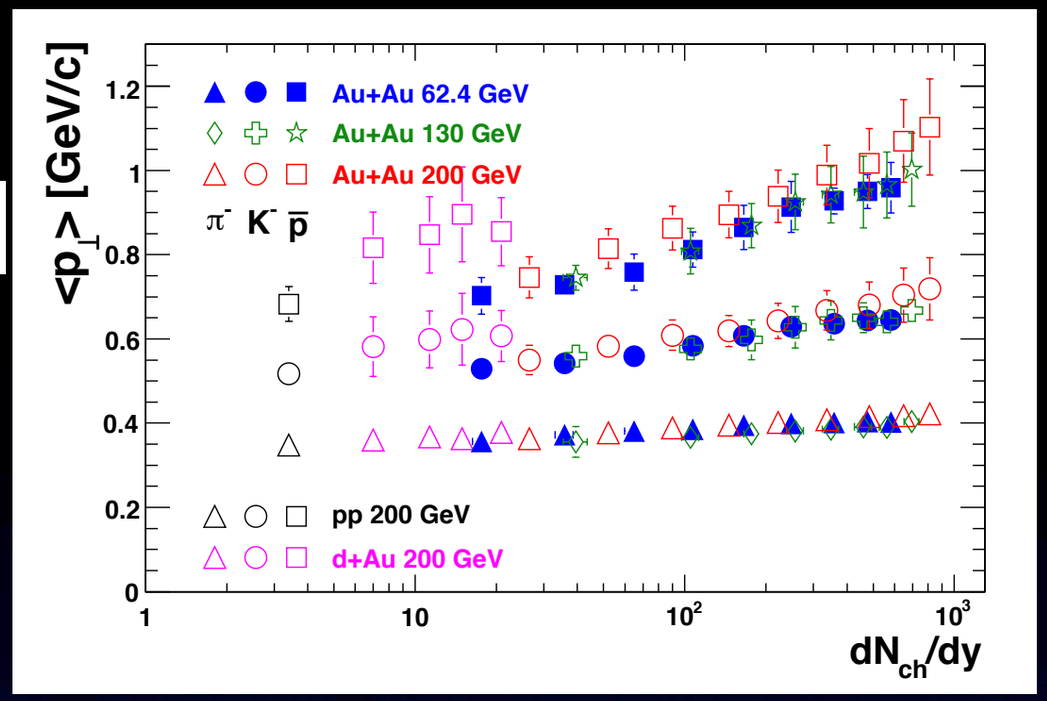

Even though no radial flow is expected if d+Au, Blast wave fits from p+p to A+A provide a common tool to characterize all those systems. In particular the $\langle p_T \rangle$ for K and p do not follow the trend from A+A to p+p.

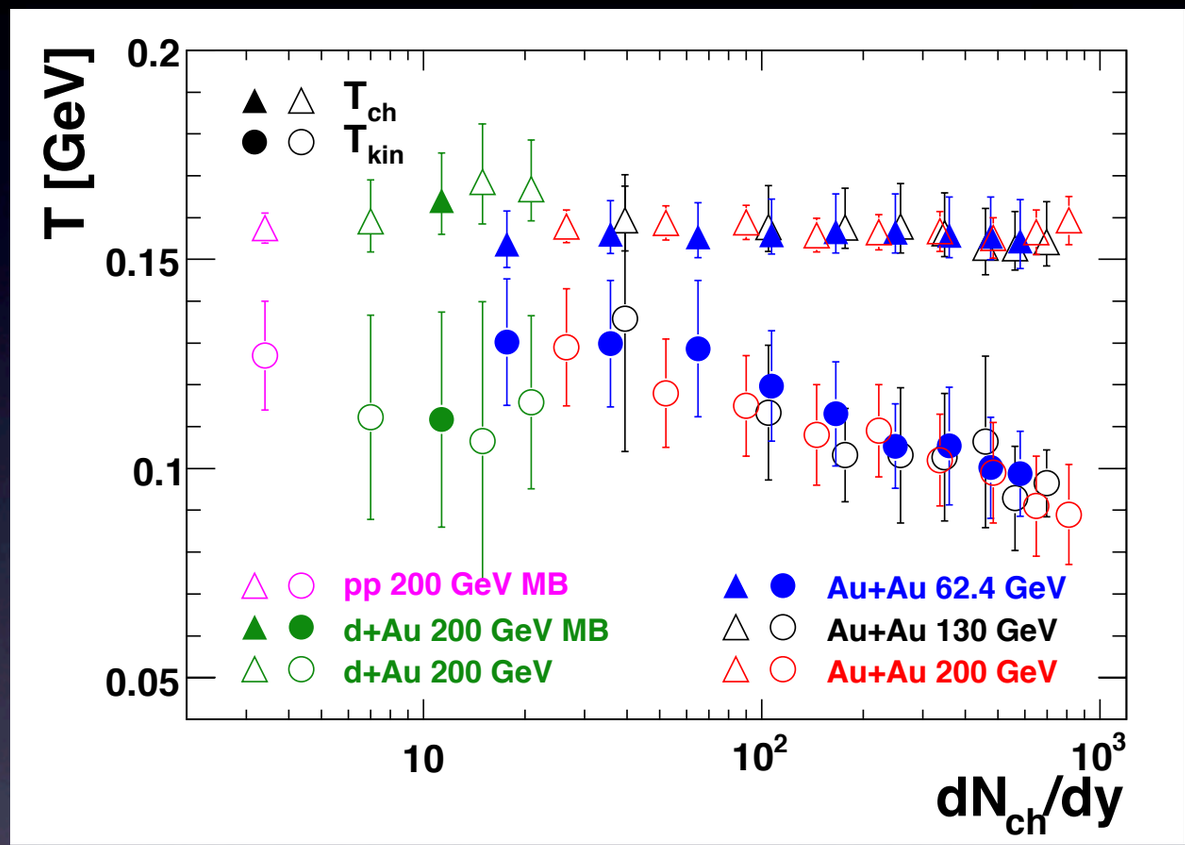

Chemical freeze-out temperature extracted from fits to particle ratios.
Kinetic freeze-out temperature T_{kin} is a parameter in the blast-wave model. Within errors, T_{ch} is constant for all systems. T_{kin} appears constant in pp and dAu and only drops in the expanding A+A systems.

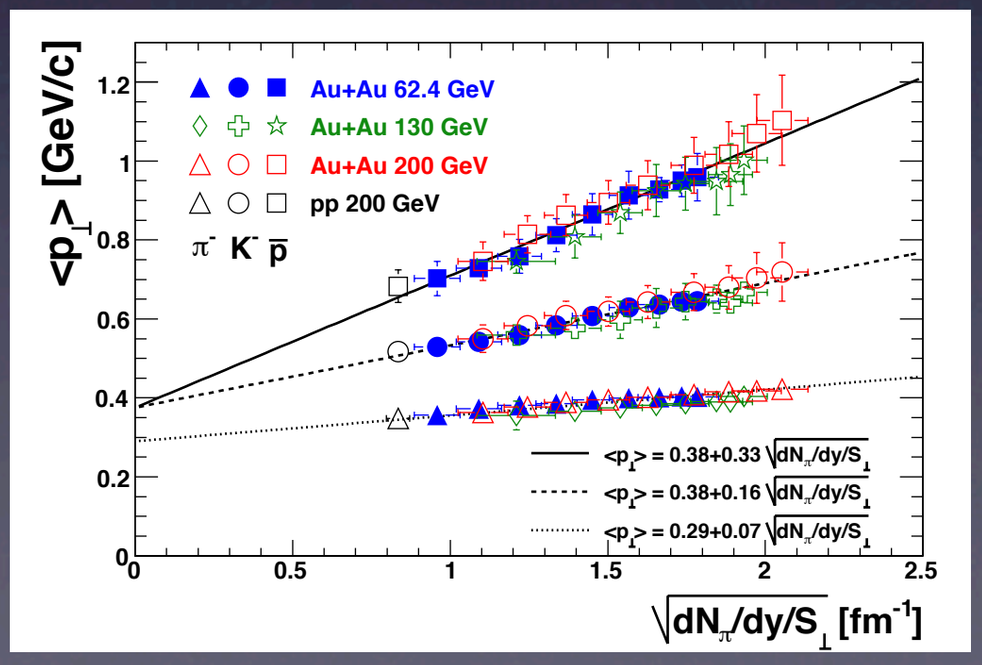

Q_s the only scale in CGC can be related to the pion yield (parton-hadron duality) and the transverse size of the overlap $S_\perp$

Phys. Rev. C **79** (2009) 34909

Pseudo-rapidity Asymmetry and Centrality Dependence of Charged Hadron Spectra

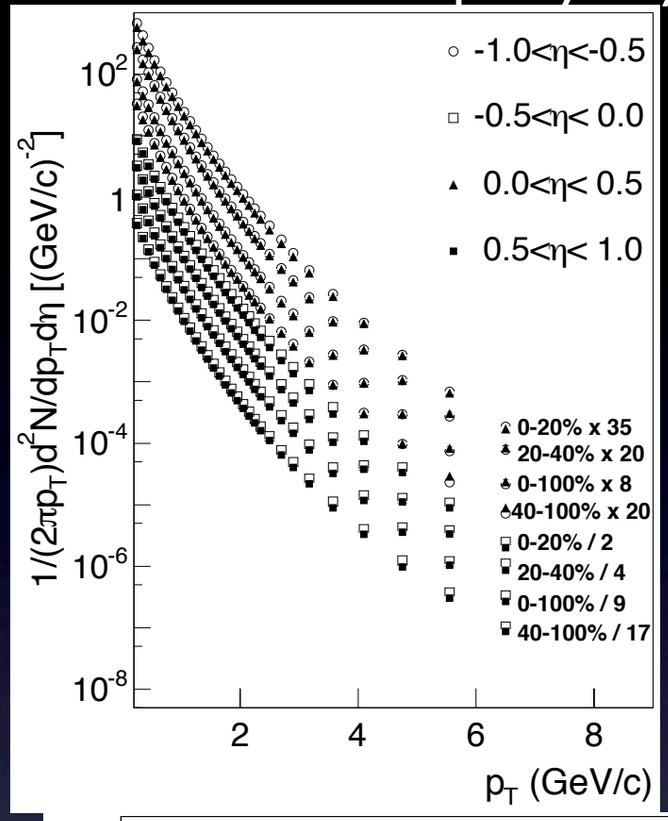

Contrasting beam and target fragmentation regions close to mid-rapidity

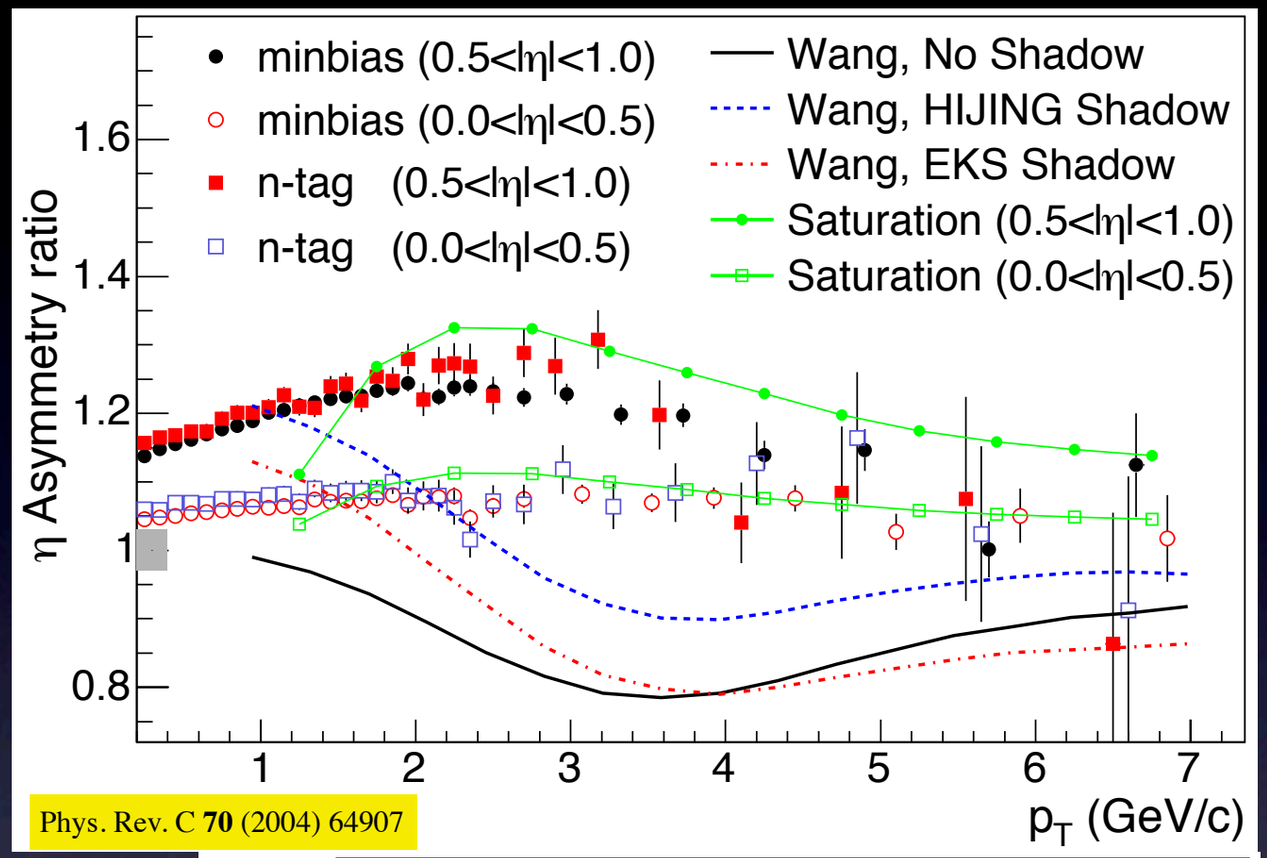

Phys. Rev. C **70** (2004) 64907

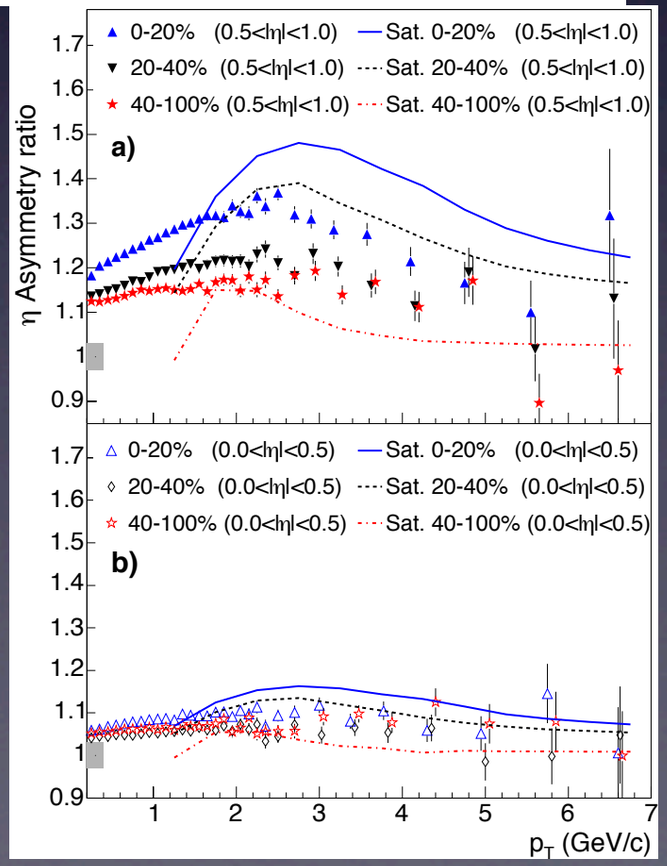

The centrality dependence is stronger at the high η bins.

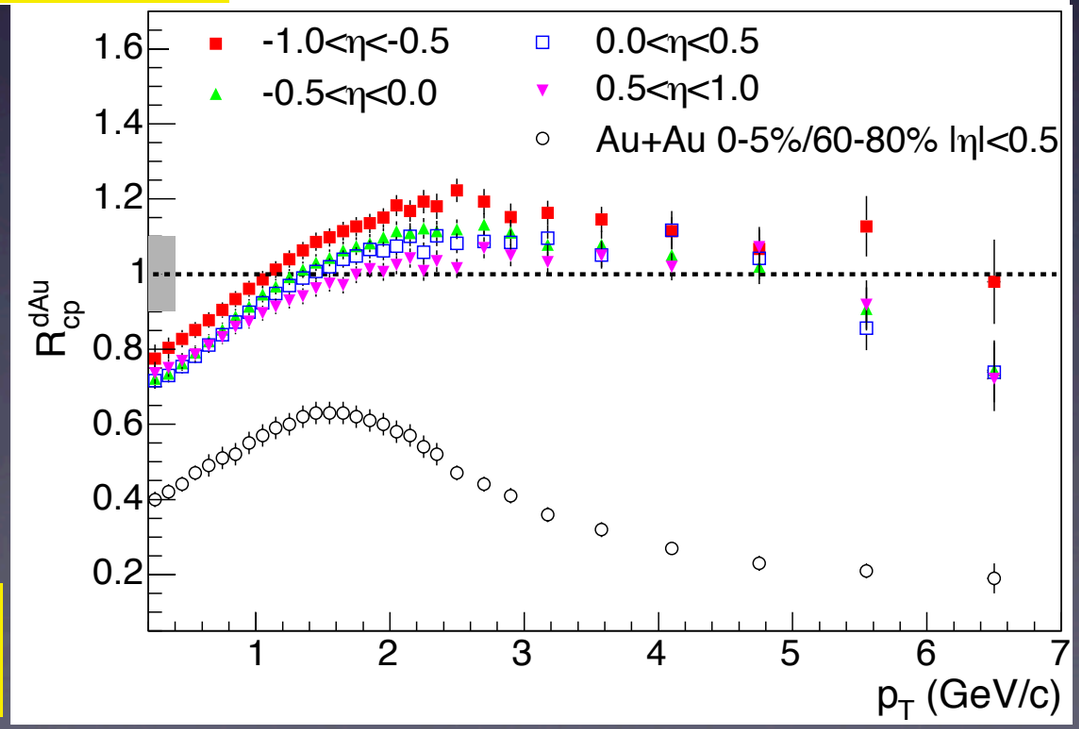

Wang: Phys.Lett. B565, 116 (2003)

Sat. : D. Kharzeev, Y. Kovchegov and K. Tuchin, Phys. Rev. D 68, 094013 (2003).

Similar measurement with pions

STAR TPC, pid with logarithmic rise. The STAR acceptance has been divided in four rapidity bins.

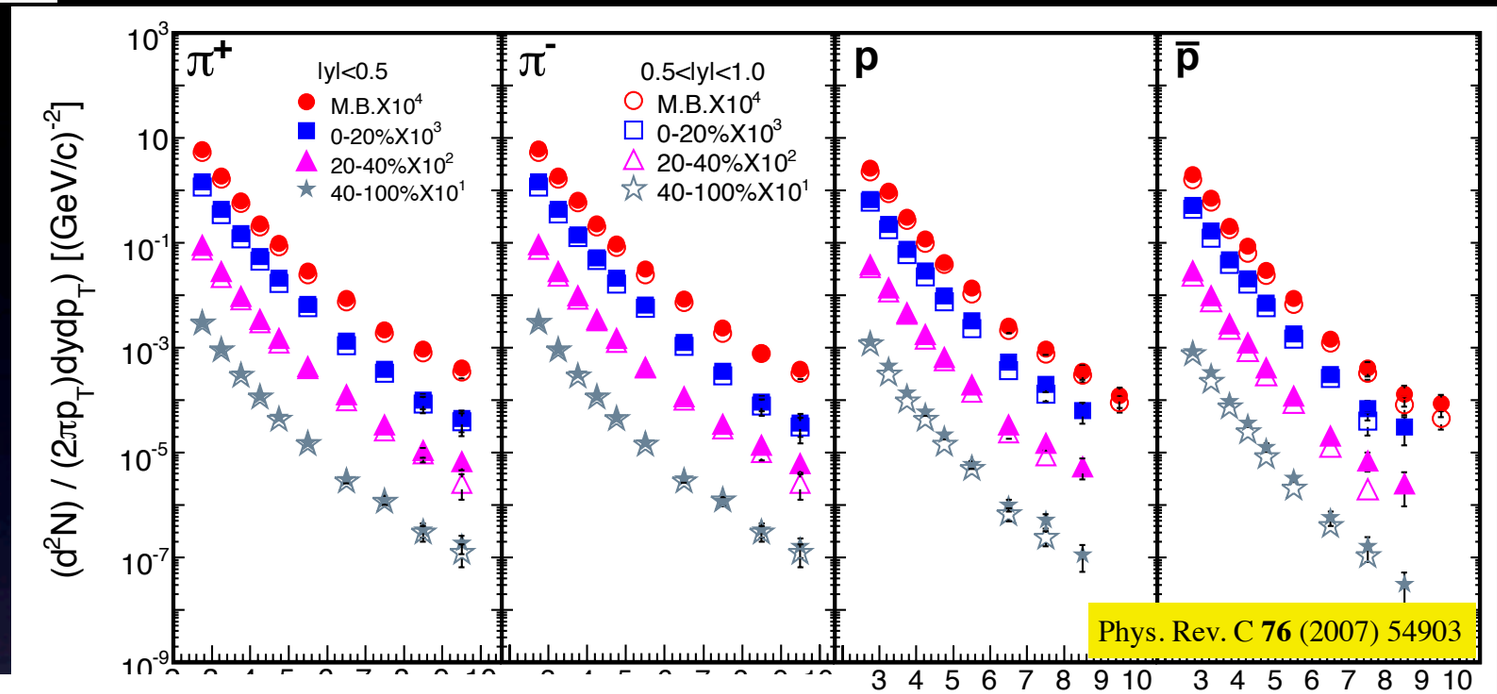

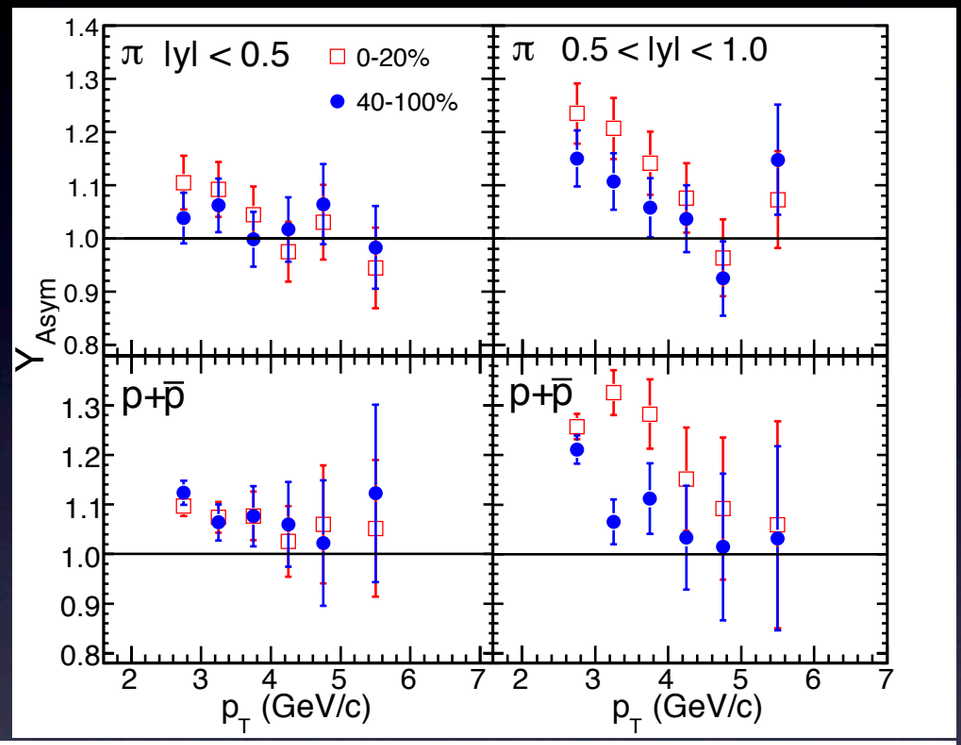

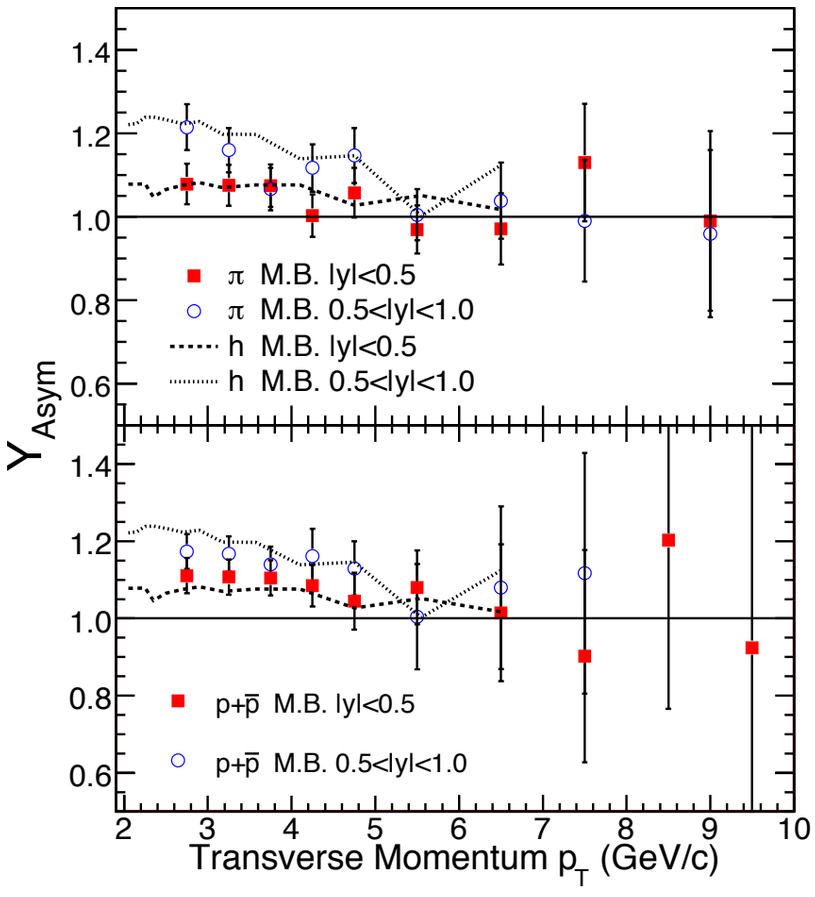

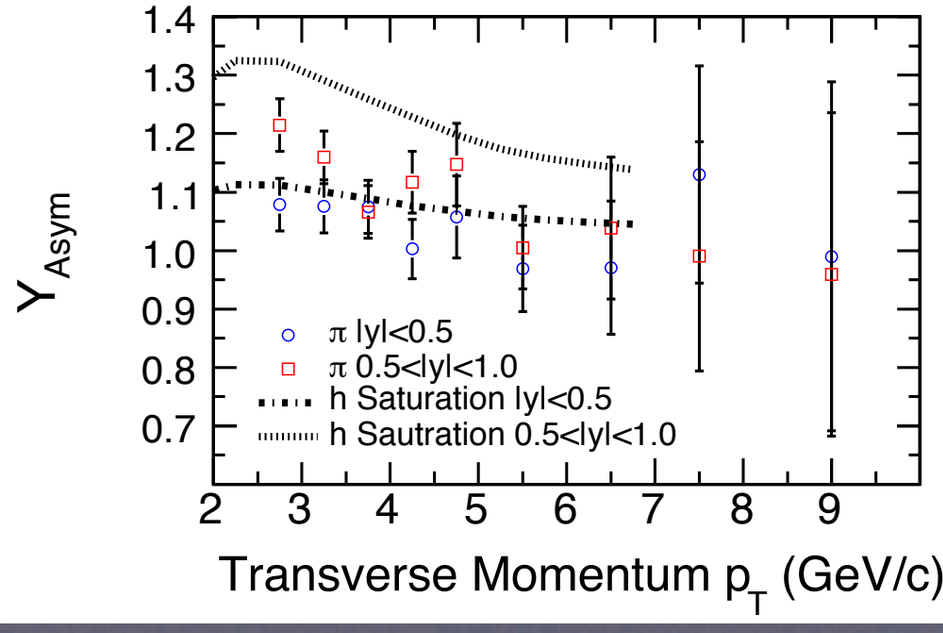

Nuclear modification factor for different particles

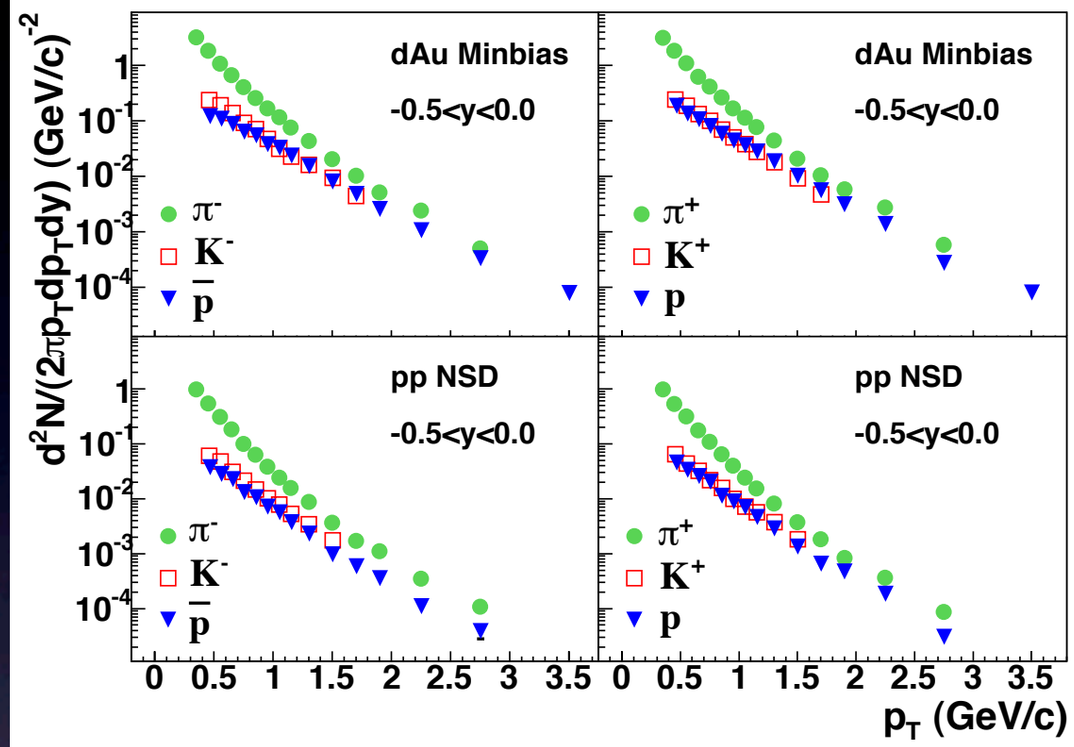

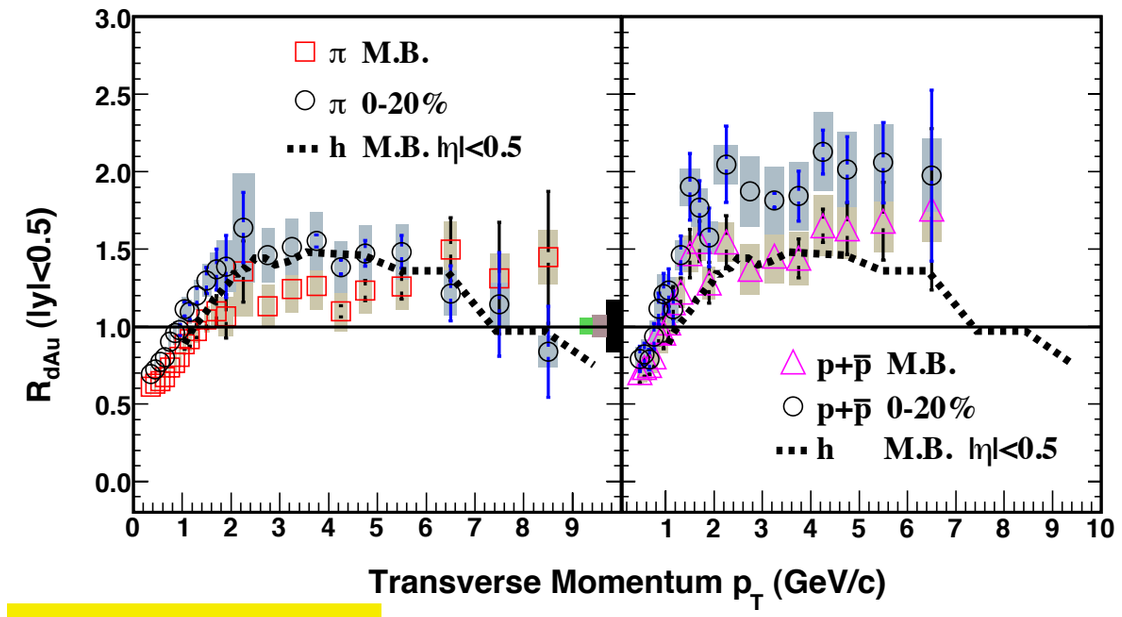

Phys. Lett. B **637** (2006) 161

Protons have stronger Cronin, K and pi behave similarly

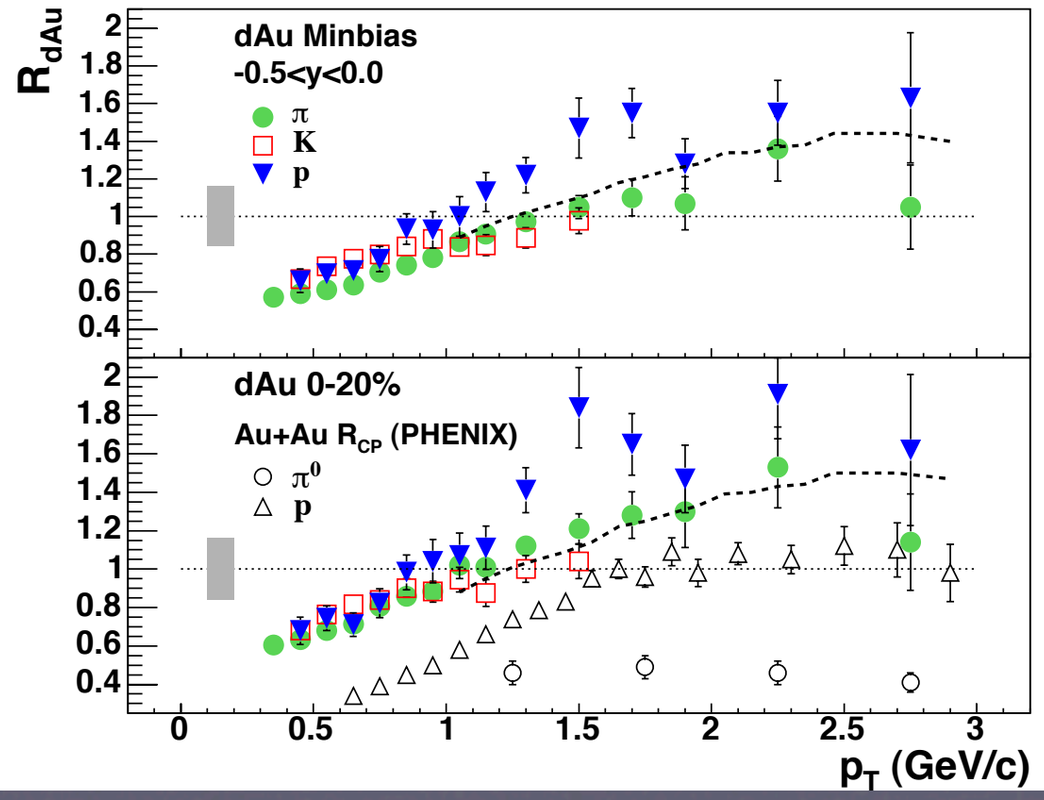

Phys. Lett. B **616** (2005) 8

NMF for charged hadrons in d+Au and nucleon+Au

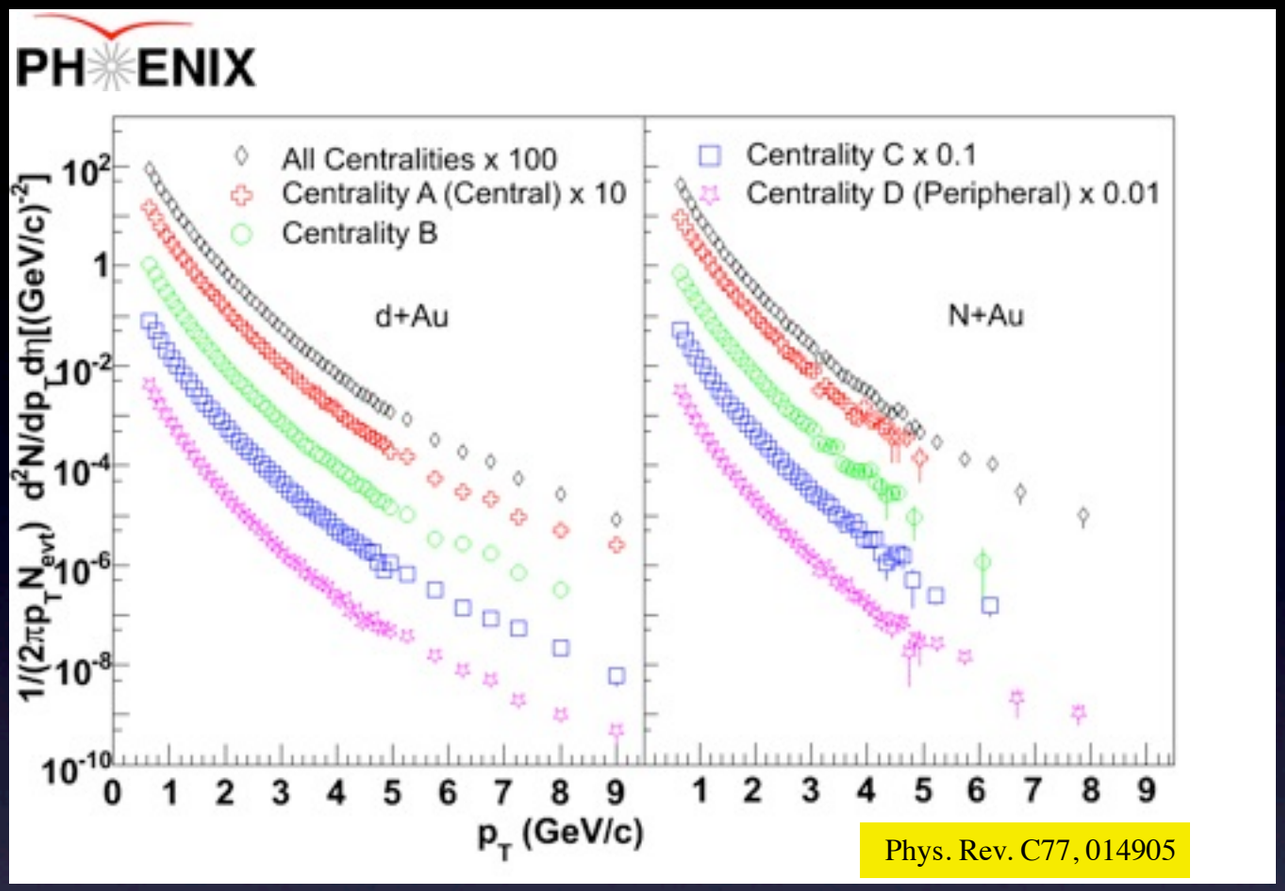

Phys. Rev. C77, 014905

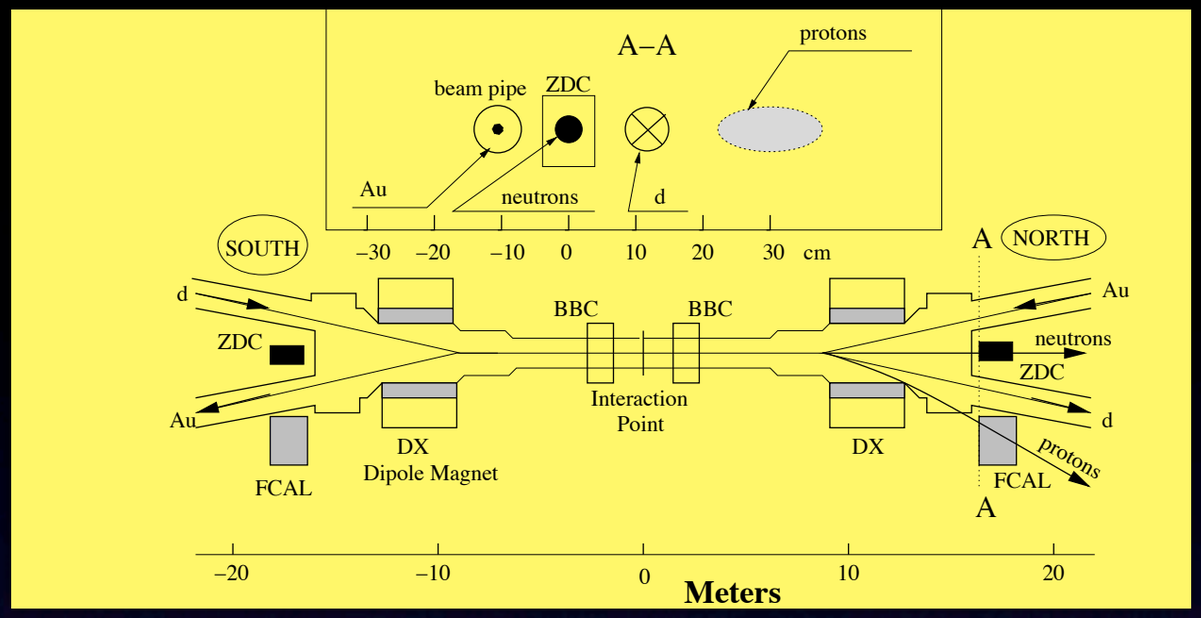

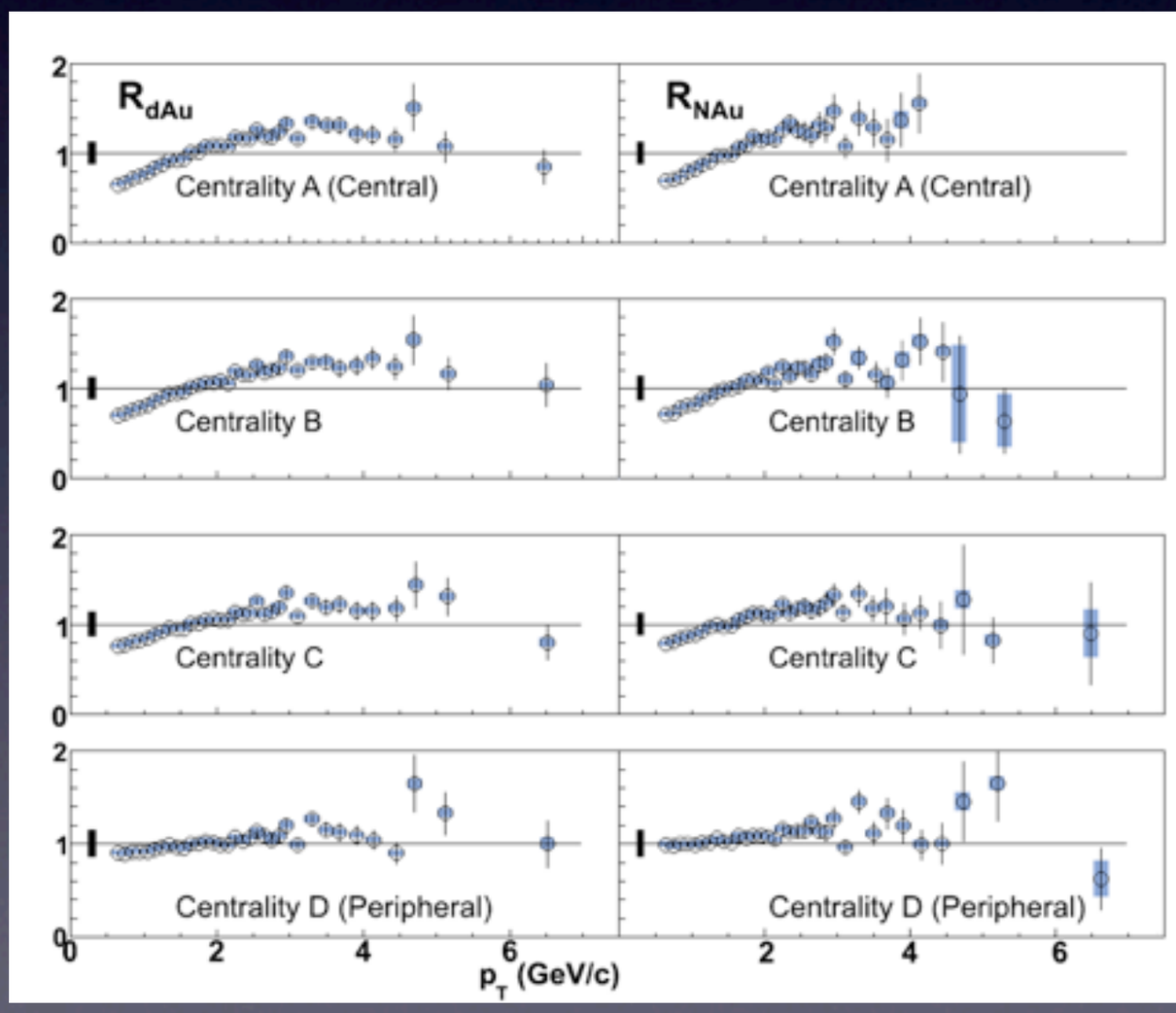

Charged hadron spectra at different centralities for d+Au and nucleon+Au defined with ZDC and FCAL information.

Centrality defined with cuts on the BBC multiplicity corresponding to the following fraction of cross section:

A: 0-20% B: 20-40% C: 40-60% D: 60-80%

nucleon+Au tagged events are biased towards peripheral collisions but same BBC cuts are used.

Cronin effect studied in d+Au at mid-rapidity

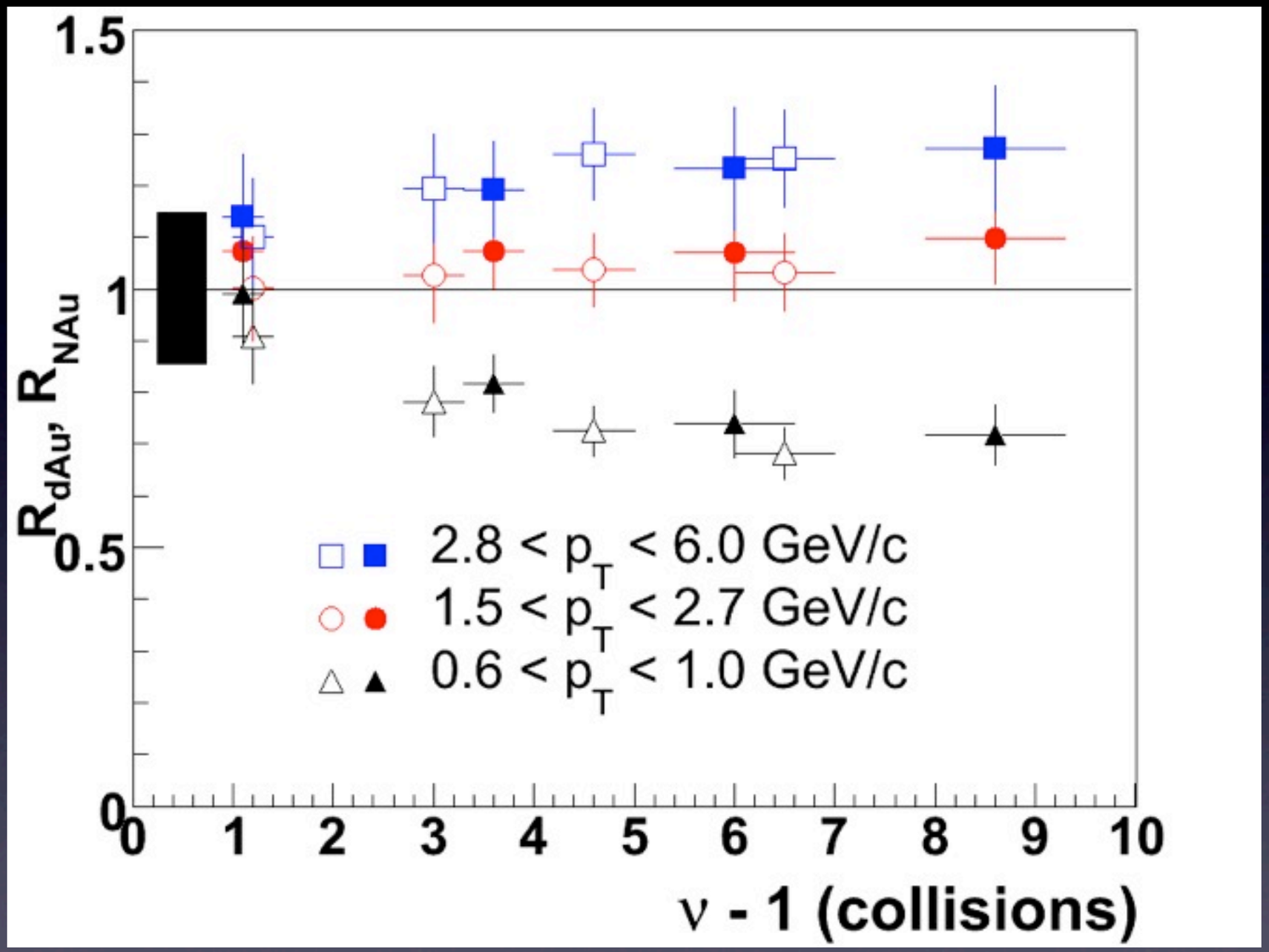

The Cronin effect is expected to be the result of soft interactions before the main hard collisions, each adding a "kick" <k_T>:

$$\langle k_T^2 \rangle_A(b) = H(\nu(b) - 1),$$

Within errors, Cronin enhancement is present above 2.8 GeV/c but remains constant as the projectile undergoes further collisions.

Open markers: d+Au Filled markers: nucleon+Au

Cronin at y=0 as function of centrality

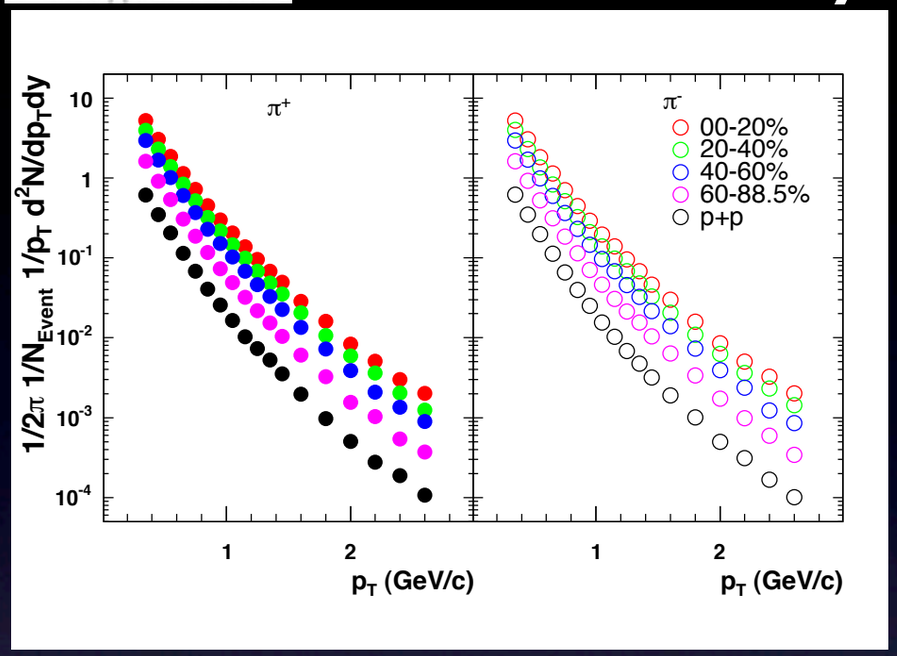

Calculations using a pQCD model of multiple semi-hard collisions and taking geometrical shadowing into account describe well the pion R_{dAu}

A. Accardi and M. Gyulassy, Phys. Lett. B586, 244 (2004).

PID done with high resolution TOF, which covers $-0.35 \leq \eta \leq 0.35$ and $\Delta\varphi = \pi/8$

The proton and antiproton spectra are corrected for feed-down from weak decays via a Monte Carlo simulation using as input experimental data on Λ production.

The enhancement for protons is stronger, by approximately 30%-50% in the most central collisions

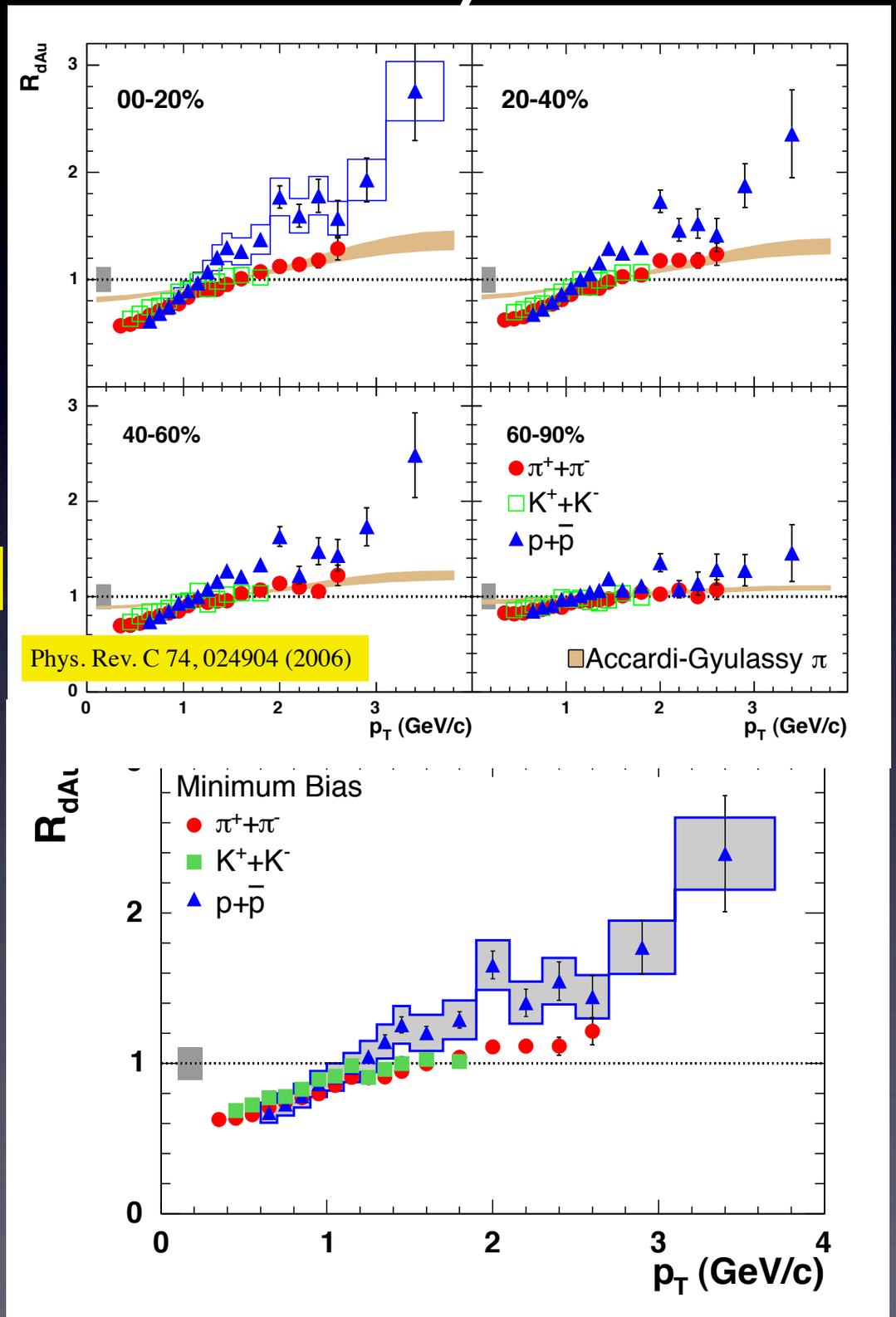

Phys. Rev. C 74, 024904 (2006)

Comparison to Cronin effect at lower energies

The figure shows the NMF as per beam-nucleon cross section ratios in order to compare it to lower energy p+A measurements. D. Antreasyan et al., Phys. Rev. D19, 764

The differences between the two energy regimes, both for protons and pions is clear. This could be "evidence for a different production mechanism for high p_T hadrons at RHIC". At high energy, coherent gluon radiation from different target nucleons, may produce suppression.

B.Z. Kopeliovich, J. Nemchik, A. Schafer and A.V. Tarasov, Phys. Rev. Lett. 88, 232303 (2002).

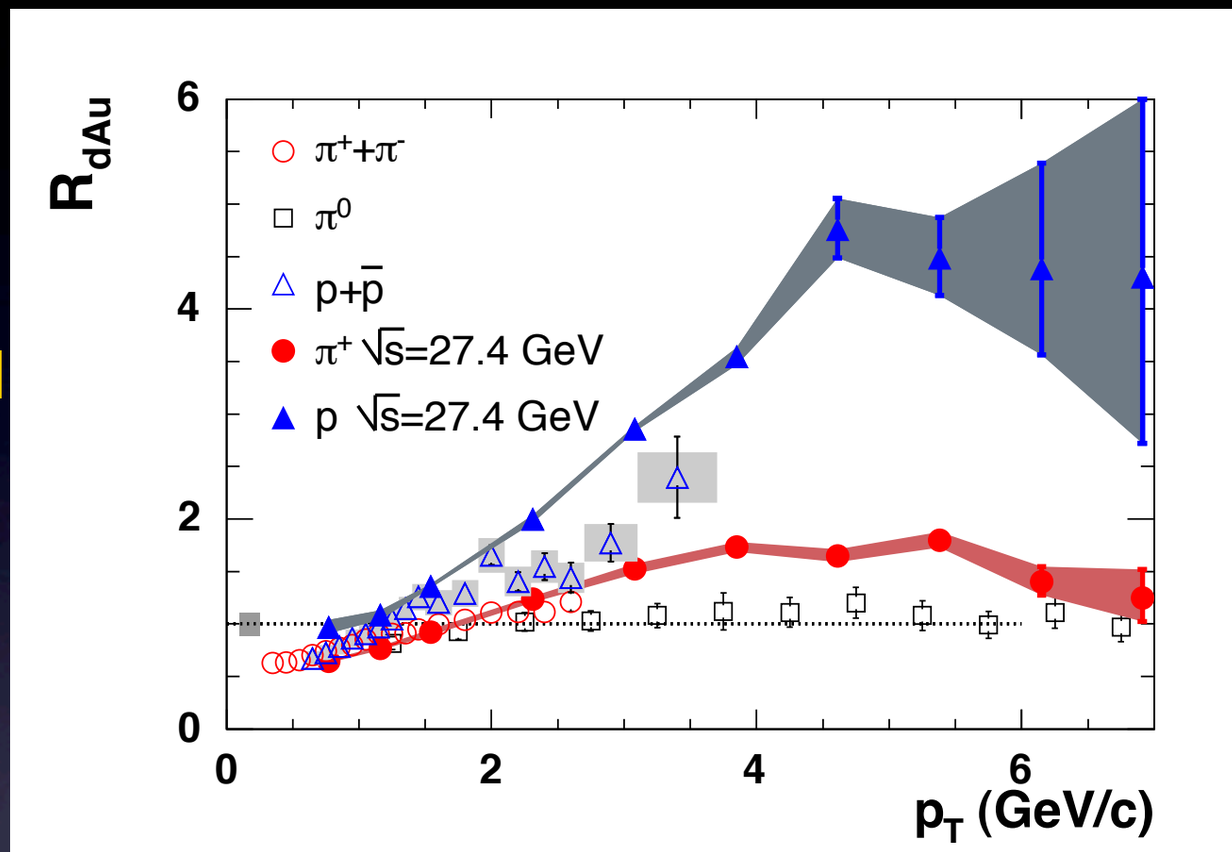

Investigating mass effects in the Cronin effect

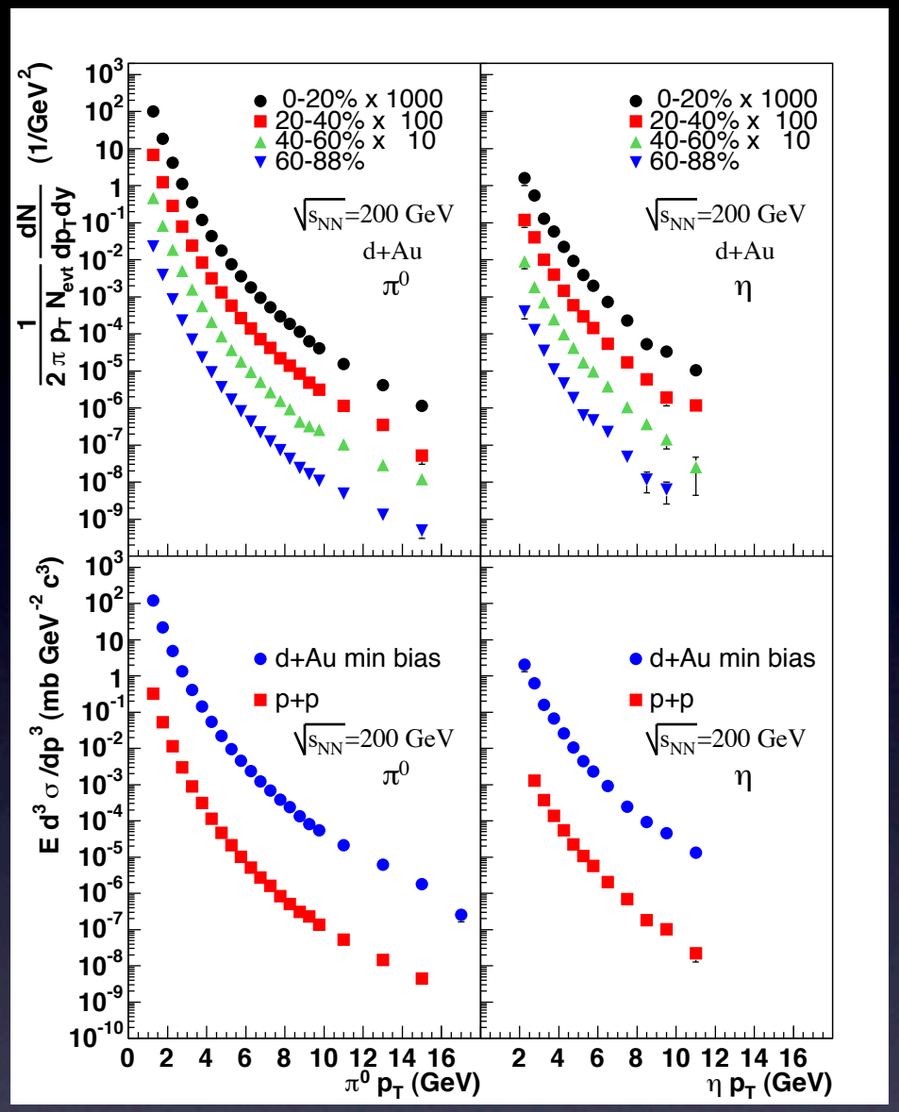

Even though the η meson is more massive than a pion, it produces a very similar R_{dAu} The centrality dependence of the small Cronin enhancement is weak for both pions and η.

Centrality defined with multiplicity in the Au side BBC -3.9<η<-3.0

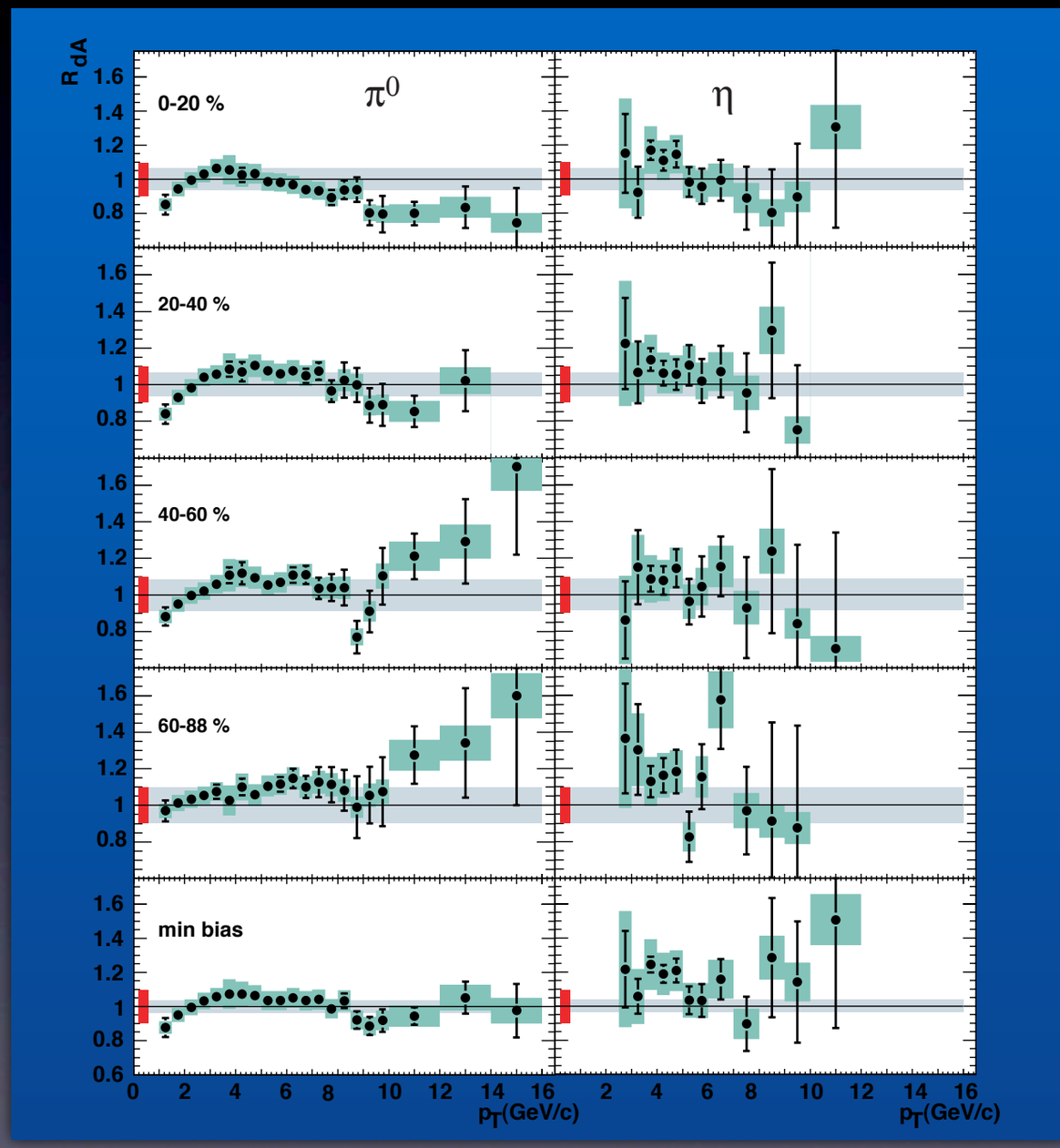

The π0 and η measured with the PHENIX (EMCal) via the $\pi_0 \rightarrow \gamma\gamma$ and $\eta \rightarrow \gamma\gamma$ decay. The EMCal consists of six lead scintillator (PbSc) and two lead glass (PbGl) sectors, at a radial distance of ~ 5 m from the beam axis. covering $|\eta| \leq 0.35$ and $\Delta\varphi = \pi$.

The uncertainty on the energy scale is 1.2%.

Neutral pion and η production at y=0

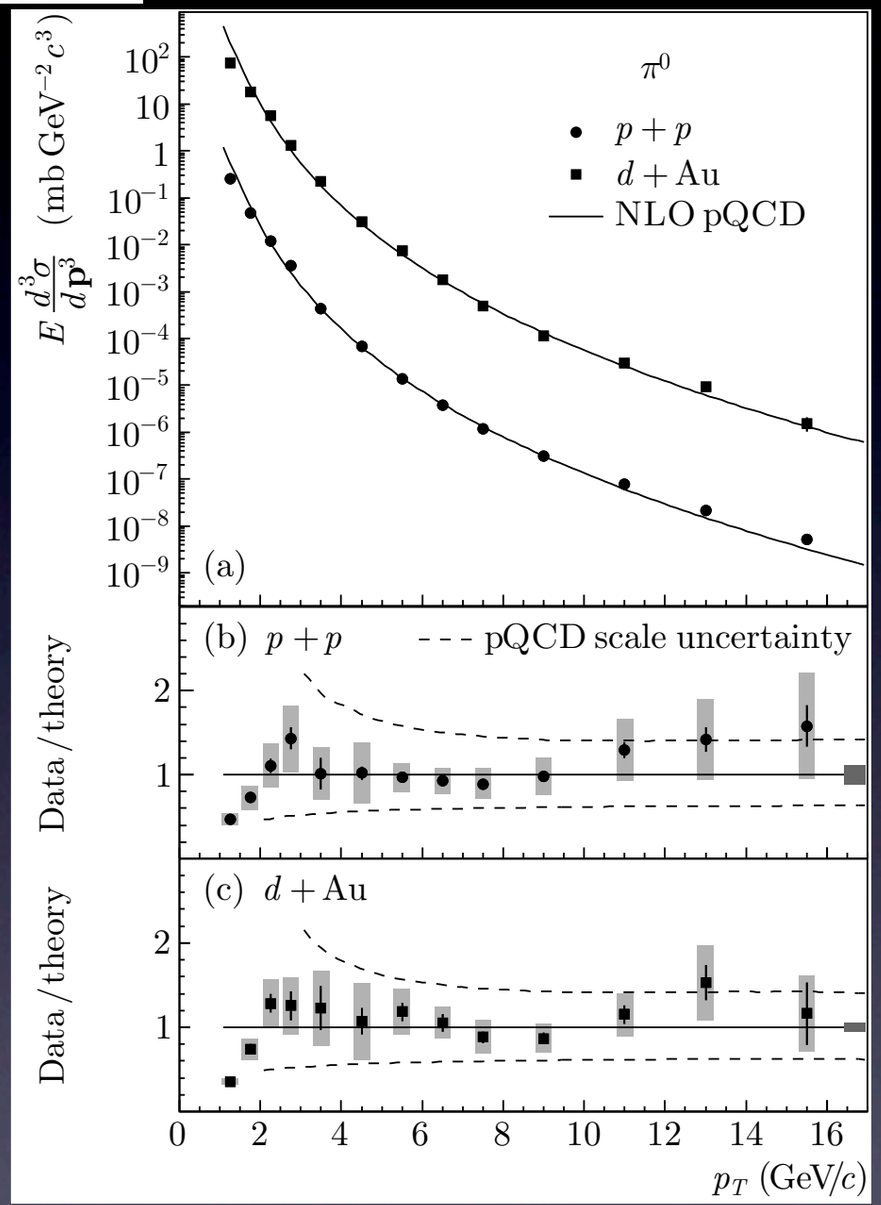

The STAR Barrel Electromagnetic Calorimeter BEMC was used to detect statistically high-p_T π_0 and η mesons via their γγ decays. 0<η<1 d+Au: at least 1 neutron on Au side ZDC. p+p: BBC coincidence. Centrality defined with Au side FTPC multiplicity. Energy scale calibration done with e measured with TPC with 5% uncertainty.

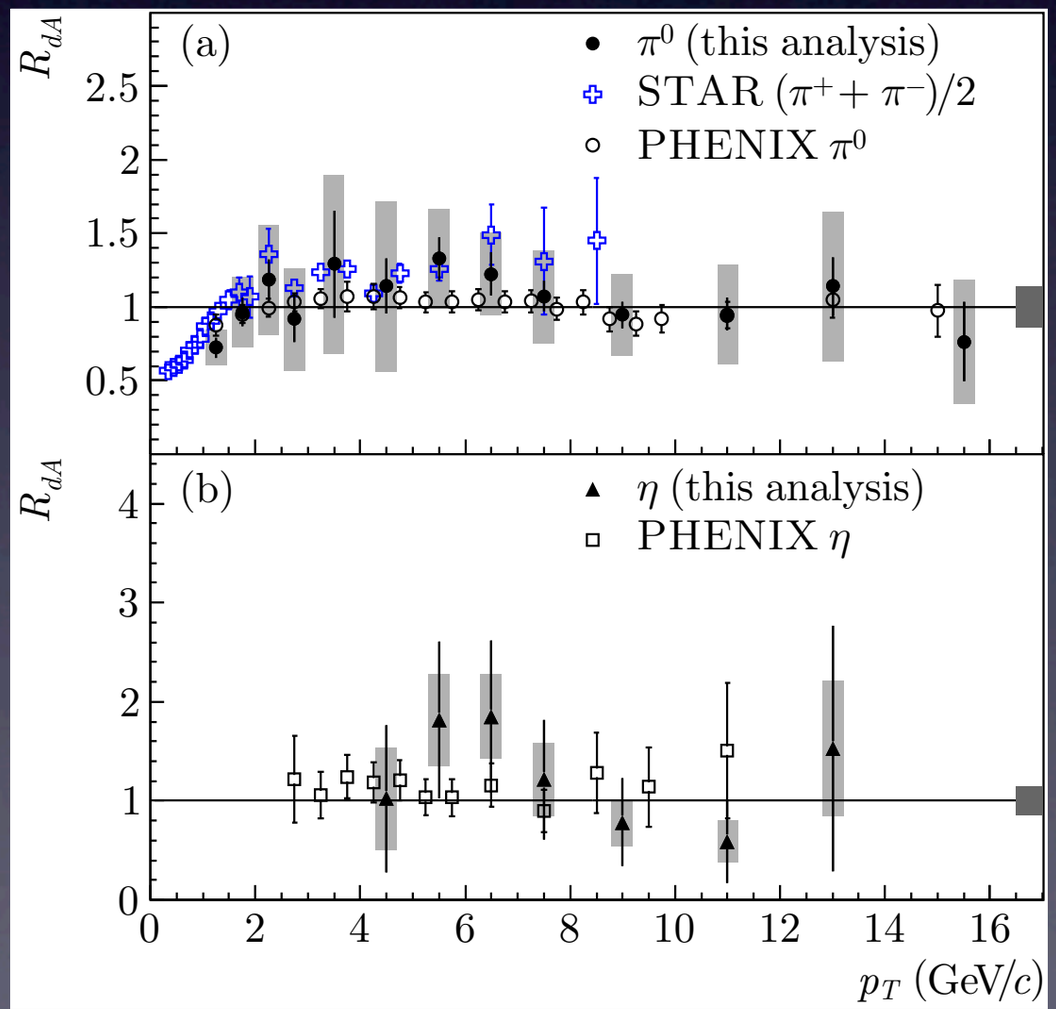

NLO pQCD calculations reproduce well the measurements. The pp calc. uses CTEQ6M PDF and KKP FFsf The d+Au calculation used Au nuclear parton distributions.

L. Frankfurt, V. Guzey, and M. Strikman, Phys. Rev. D 71, 054001 (2005).

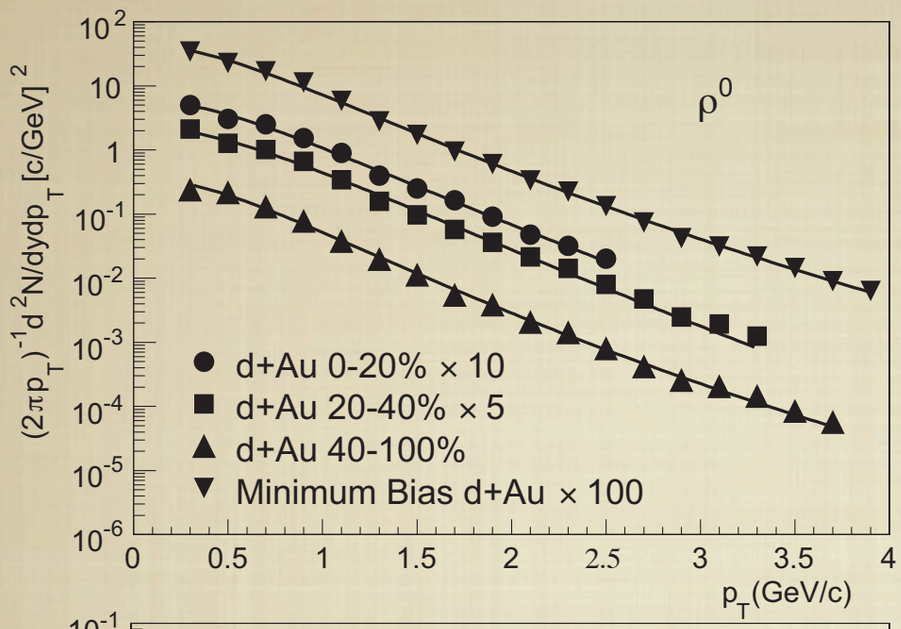

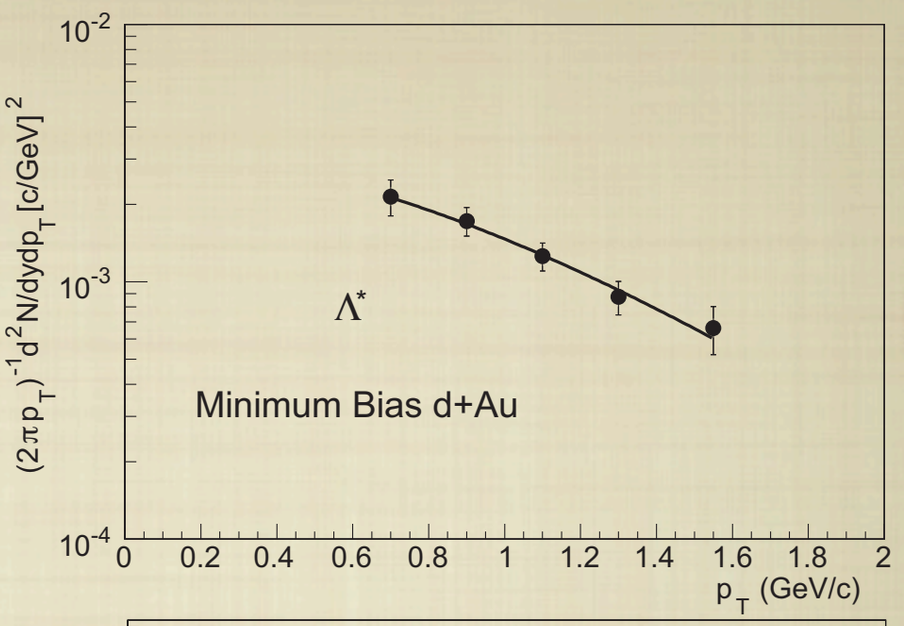

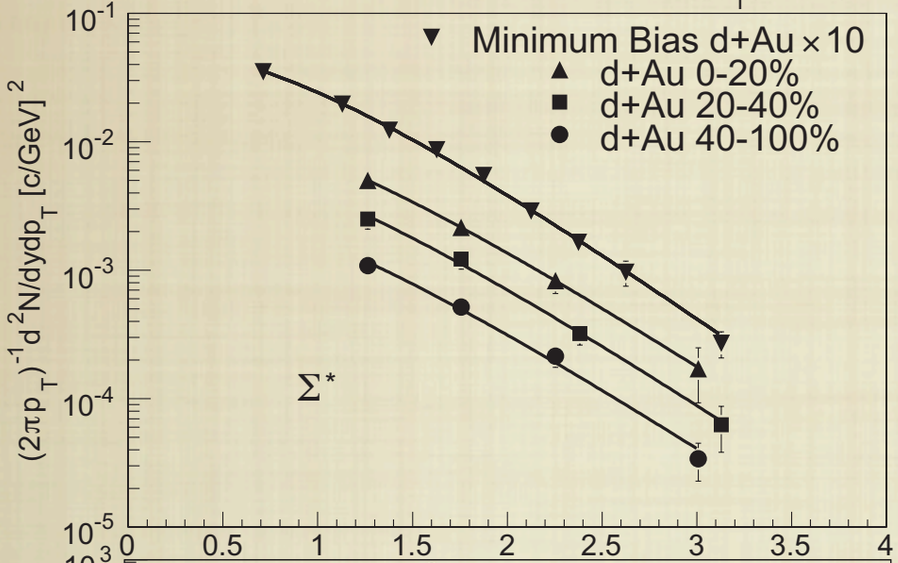

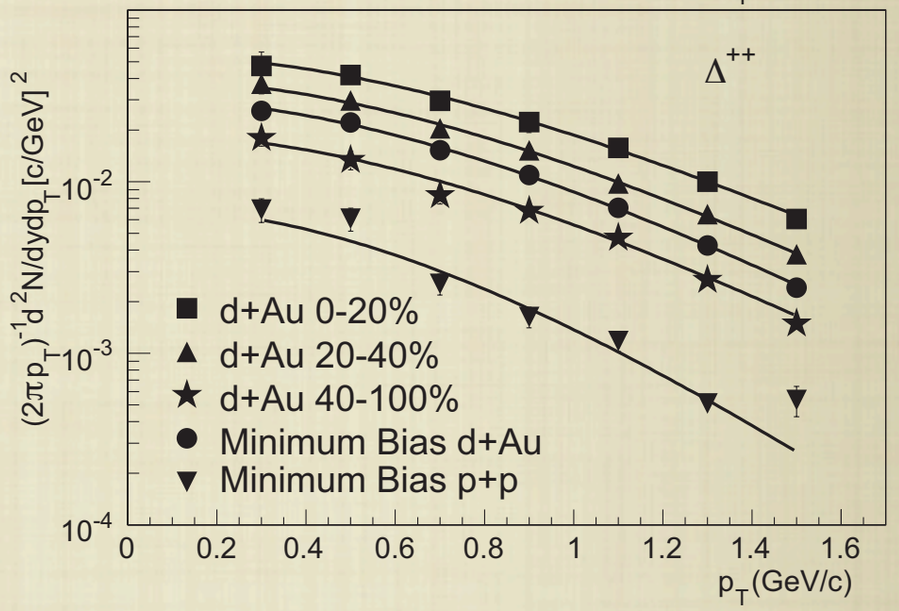

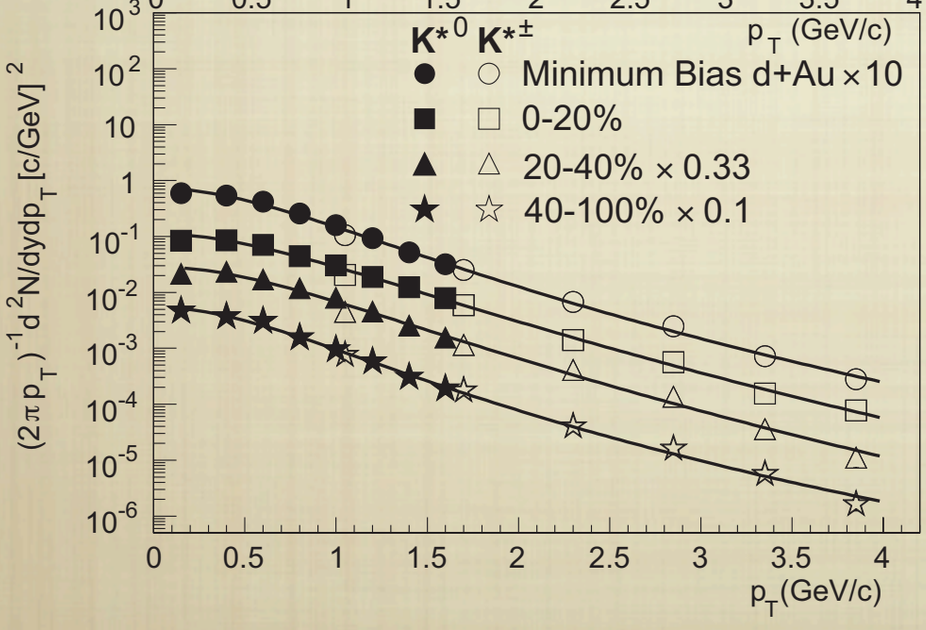

Resonances reconstructed via their hadronic decays within the STAR TPC.

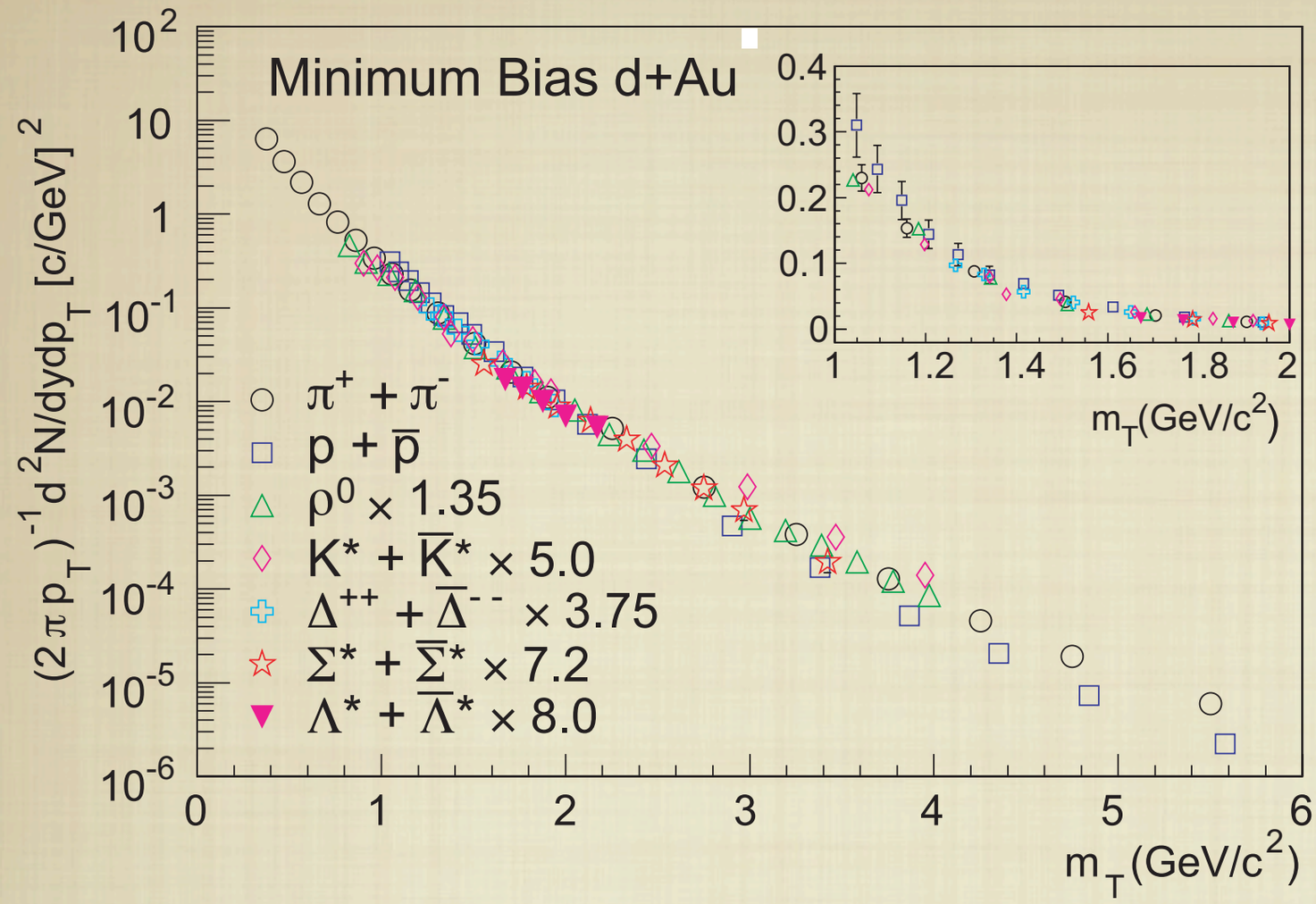

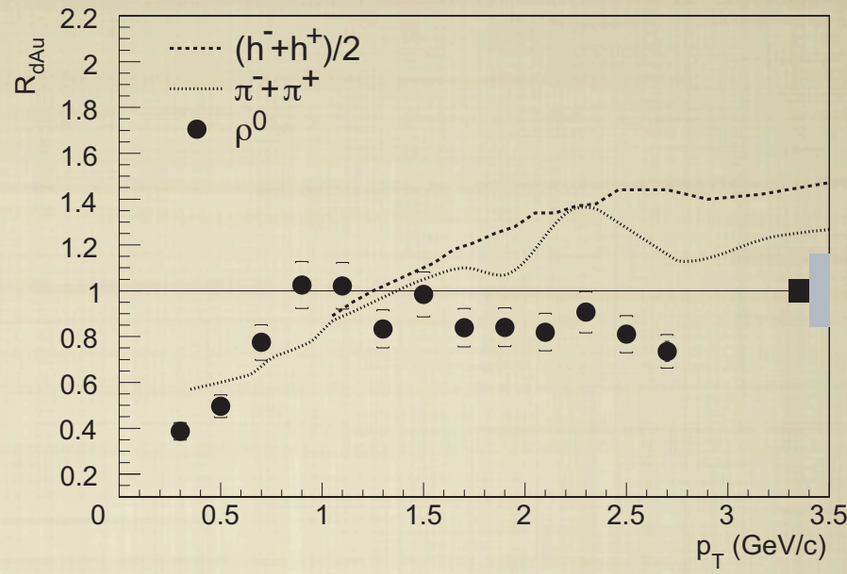

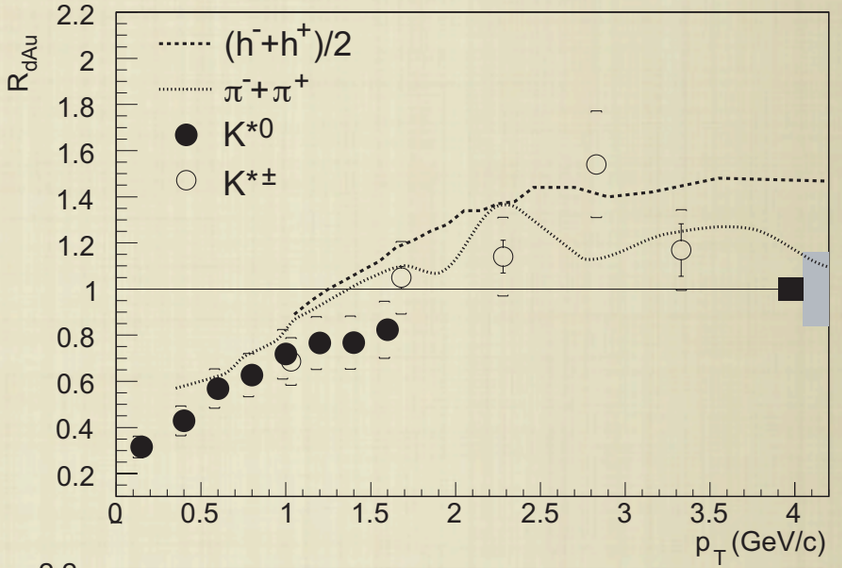

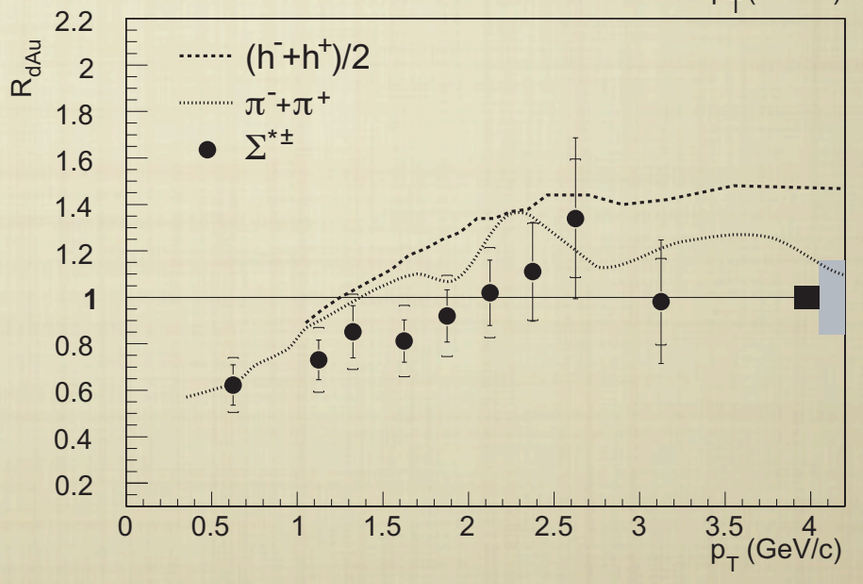

All resonances display m_T scaling and have similar R_{dAu} (consistent with pion's)

Production of Φ mesons at mid-rapidity

The Φ meson was measured thru its decays into a kaon pair, no PID on tracks, combinatorial background estimated using event-mixing technique. Yields: Breit-Wigner+gauss (mass. res.) and polynomial for remaining background.

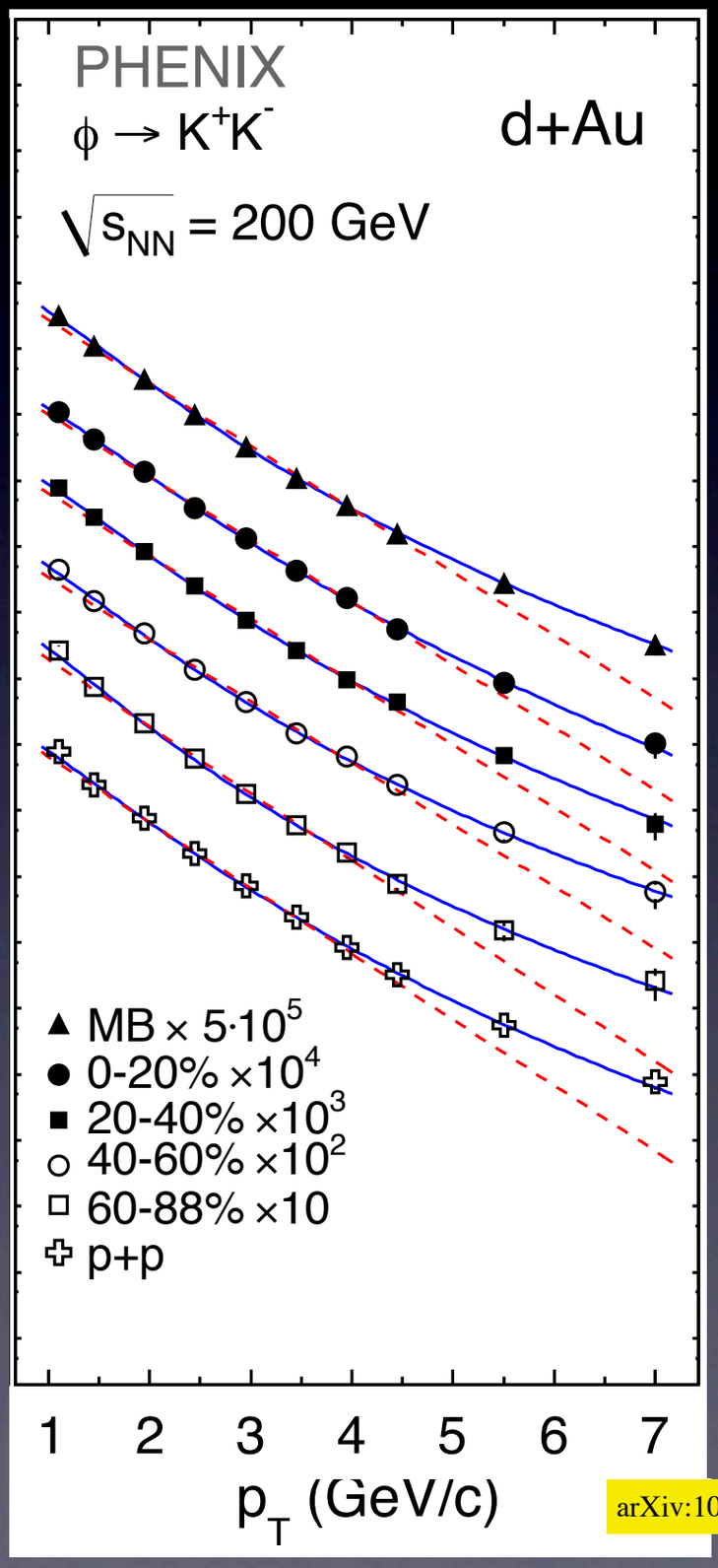

For both centralities, the RdA for ϕ and π_0 are similar indicating that cold nuclear effects are not responsible for the differences between ϕ and π_0 seen in Au+Au and Cu+Cu collisions.

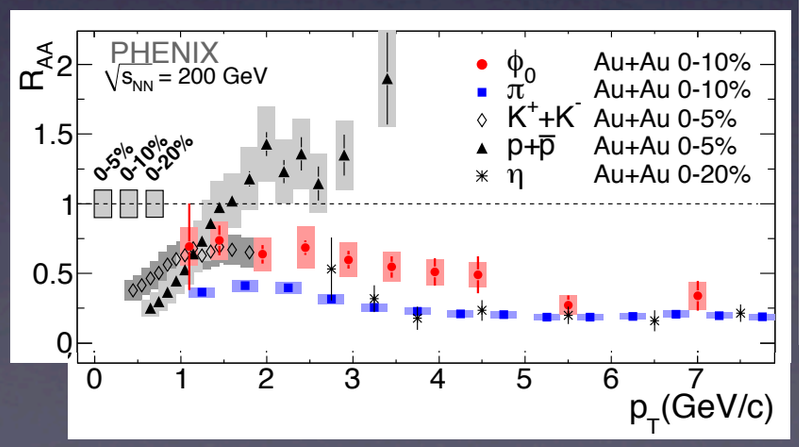

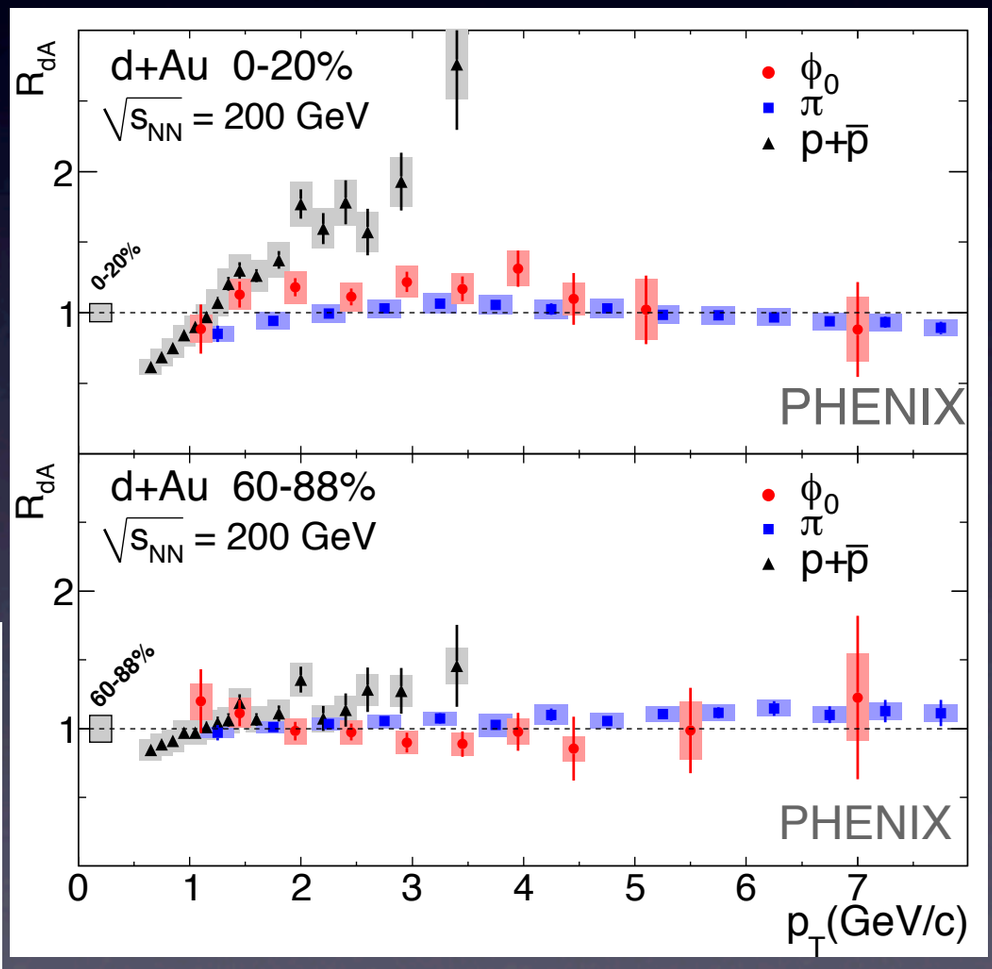

arXiv:1004.3532

Production of ω at mid-rapidity (spin dep.)

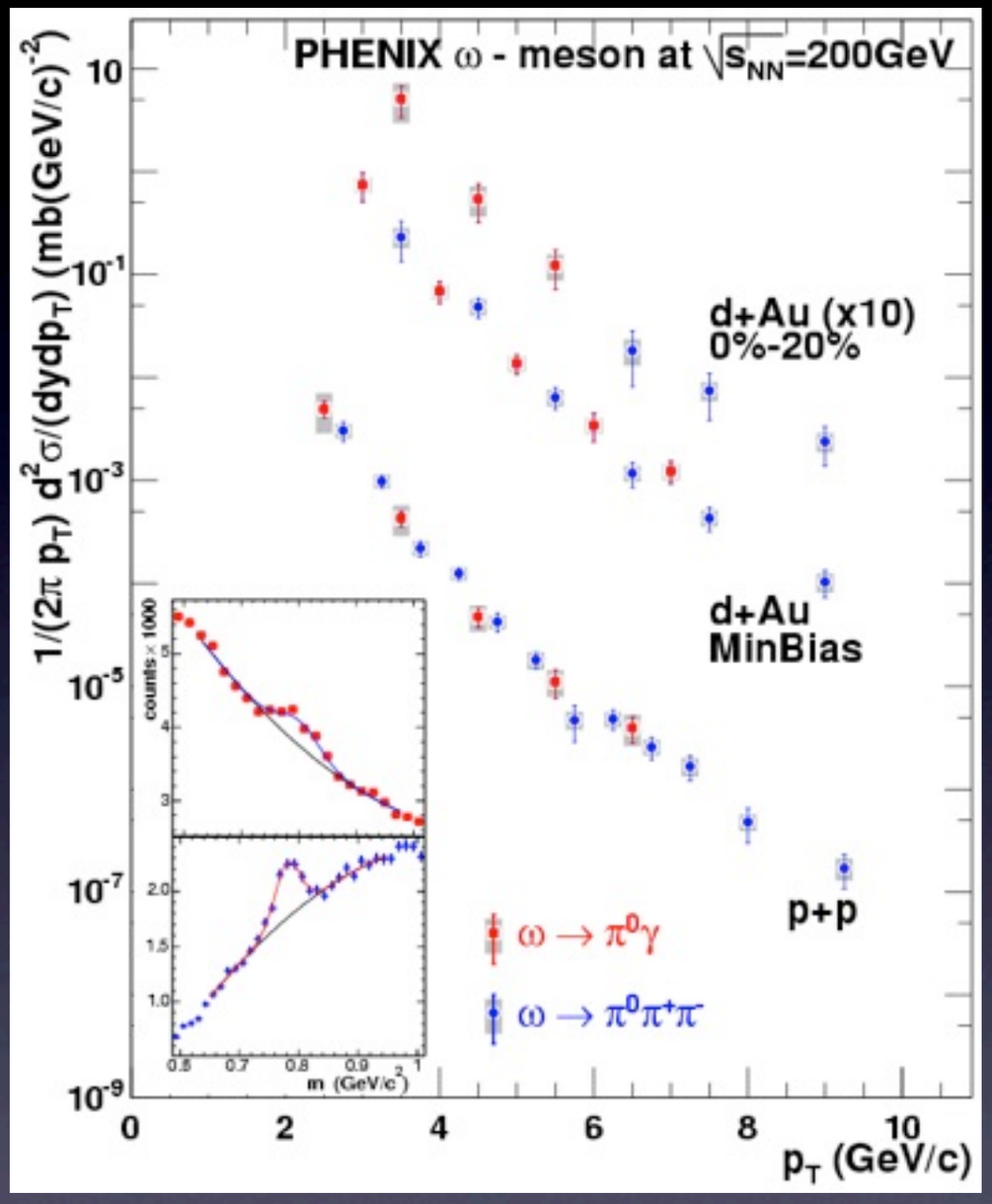

Measured statistically thru their decays $\omega \rightarrow \pi^0 \pi^+ \pi^-$, $\omega \rightarrow \pi^0 \gamma \rightarrow 3\gamma$ with EMCal and tracking.

The nuclear modification factor for ω production in d +Au collisions is consistent with 1 and p_T independent for $p_T > 2$ GeV/c similar to other meson measurements.

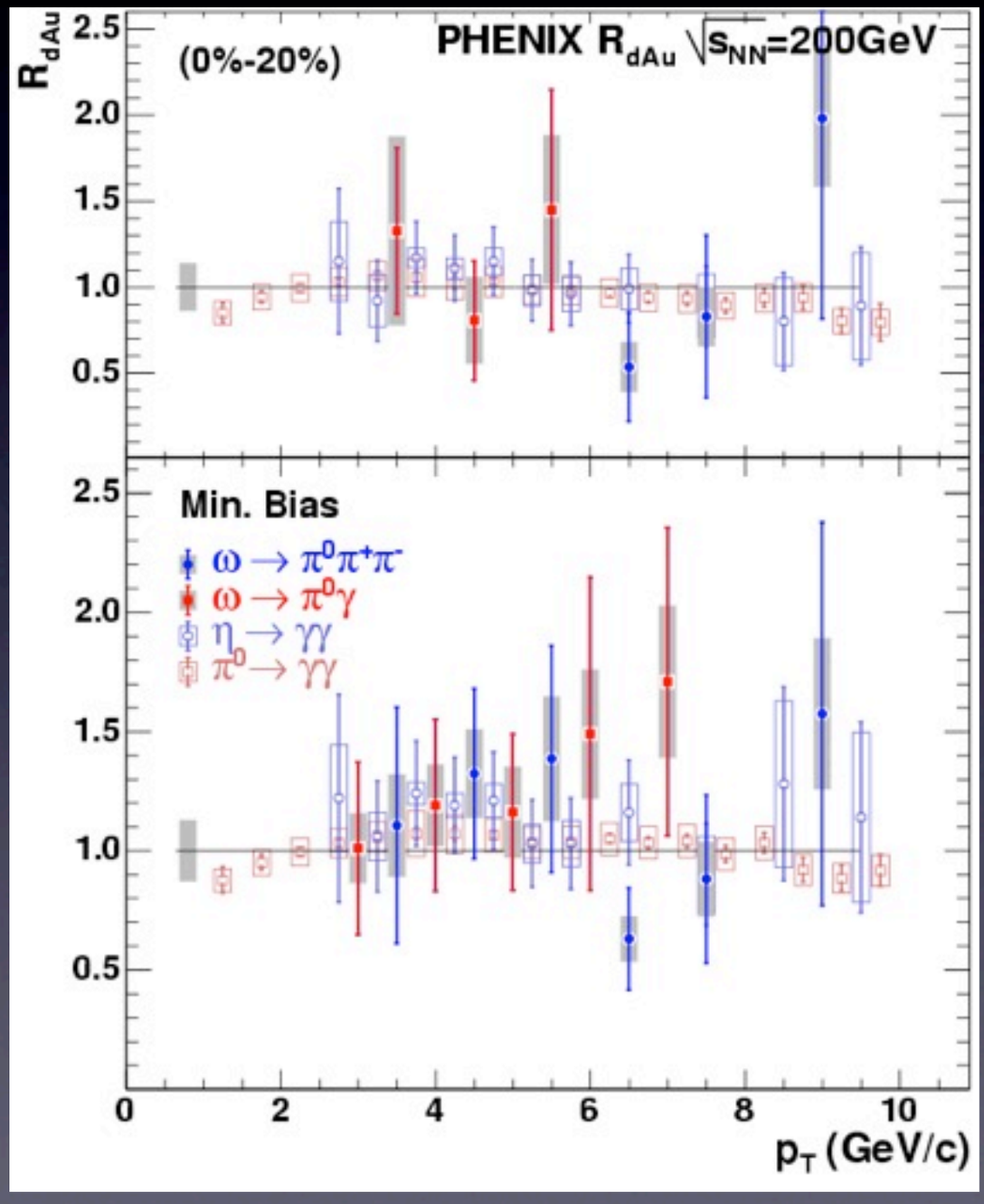

Mass resolution (20-25 MeV) for the mixed neutral-charged particle decay mode.

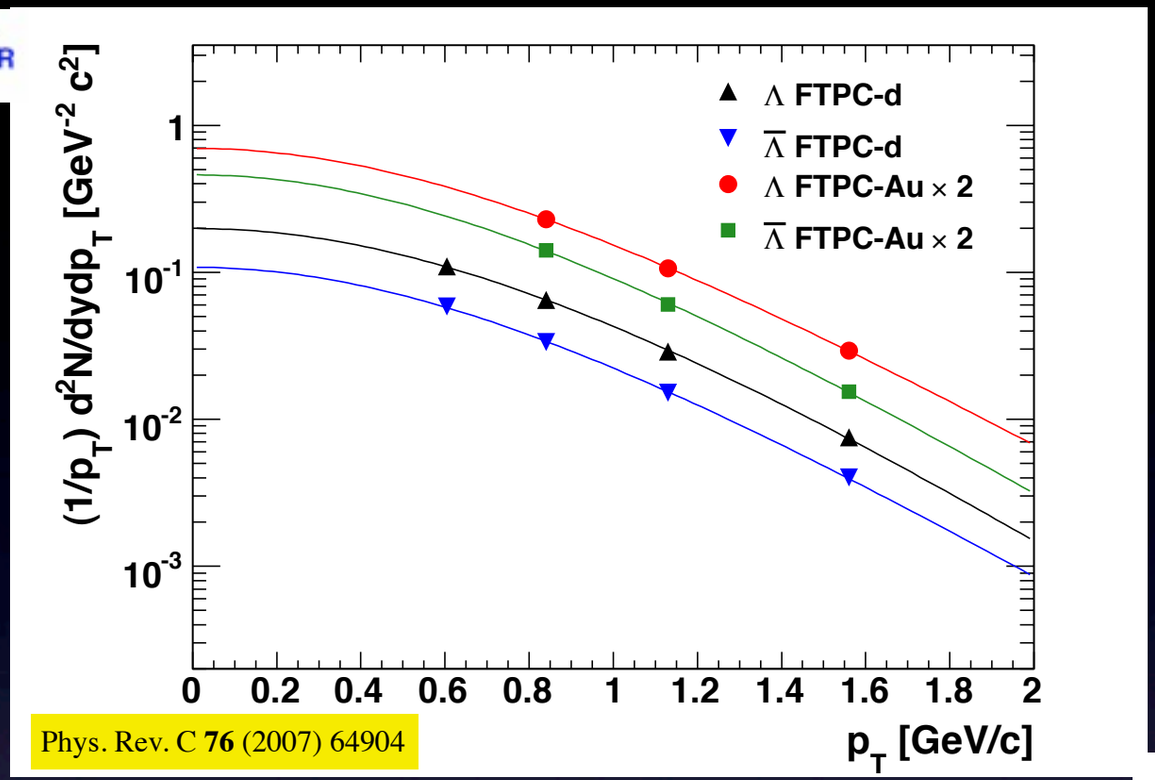

Phys. Rev. C **76** (2007) 64904

Λ and $\overline{\Lambda}$ detected in the STAR FTPCs used to deduce stopping power in d+Au at 200 GeV/c

$$\delta y = (n_{coll} - 1)/\alpha + 1,$$

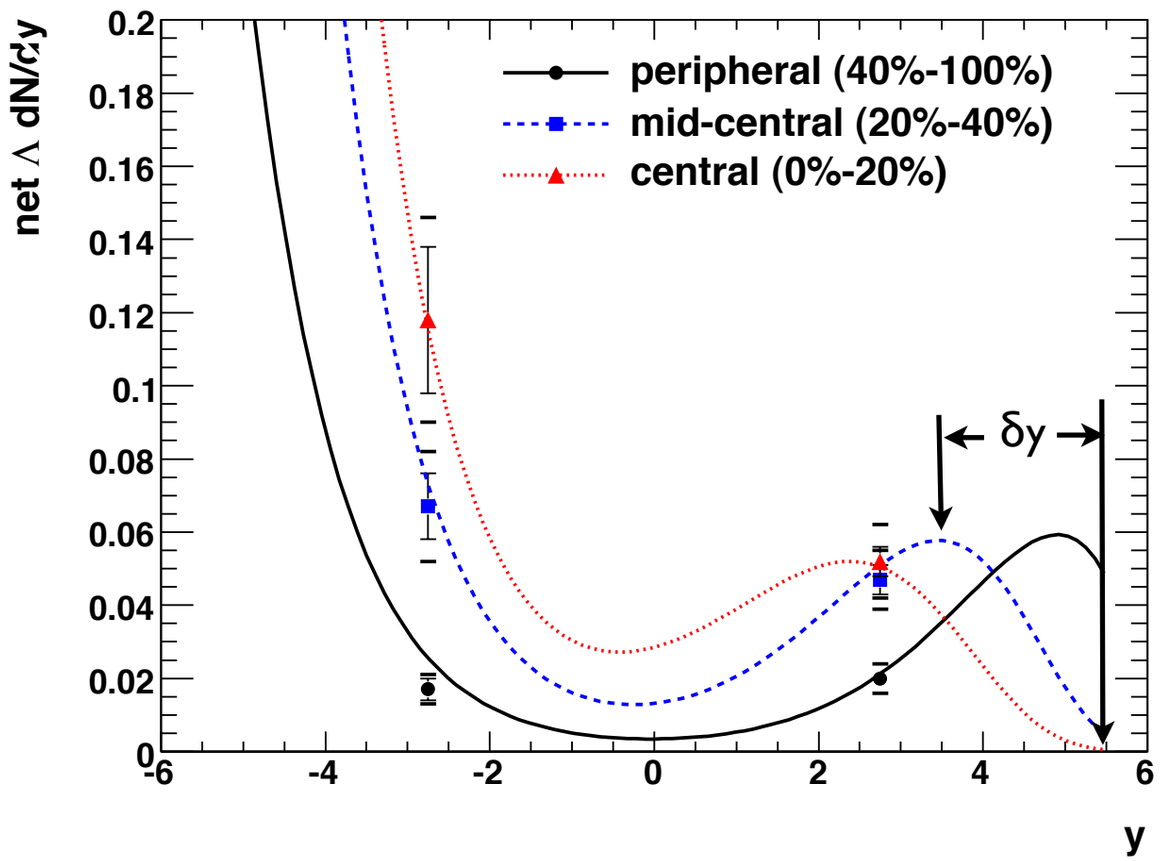

Curves are based on the Multi-Chain-Model (S. Date, M. Gyulassy, and H. Sumiyoshi, Phys. Rev. D32, 619) set α=2.9±0.5 The model consistently describes stopping in fixed target at 100 GeV (α = 3±1) this may indicate that stopping in d+A is independent of cm energy and is mainly driven by the number of collisions.

Baryons measured close to beam y probed the saturated target at small x. CGC based calculations of stopping have been performed.

Phys.Rev.C80:054905,2009

Open charm with non-photonic electrons

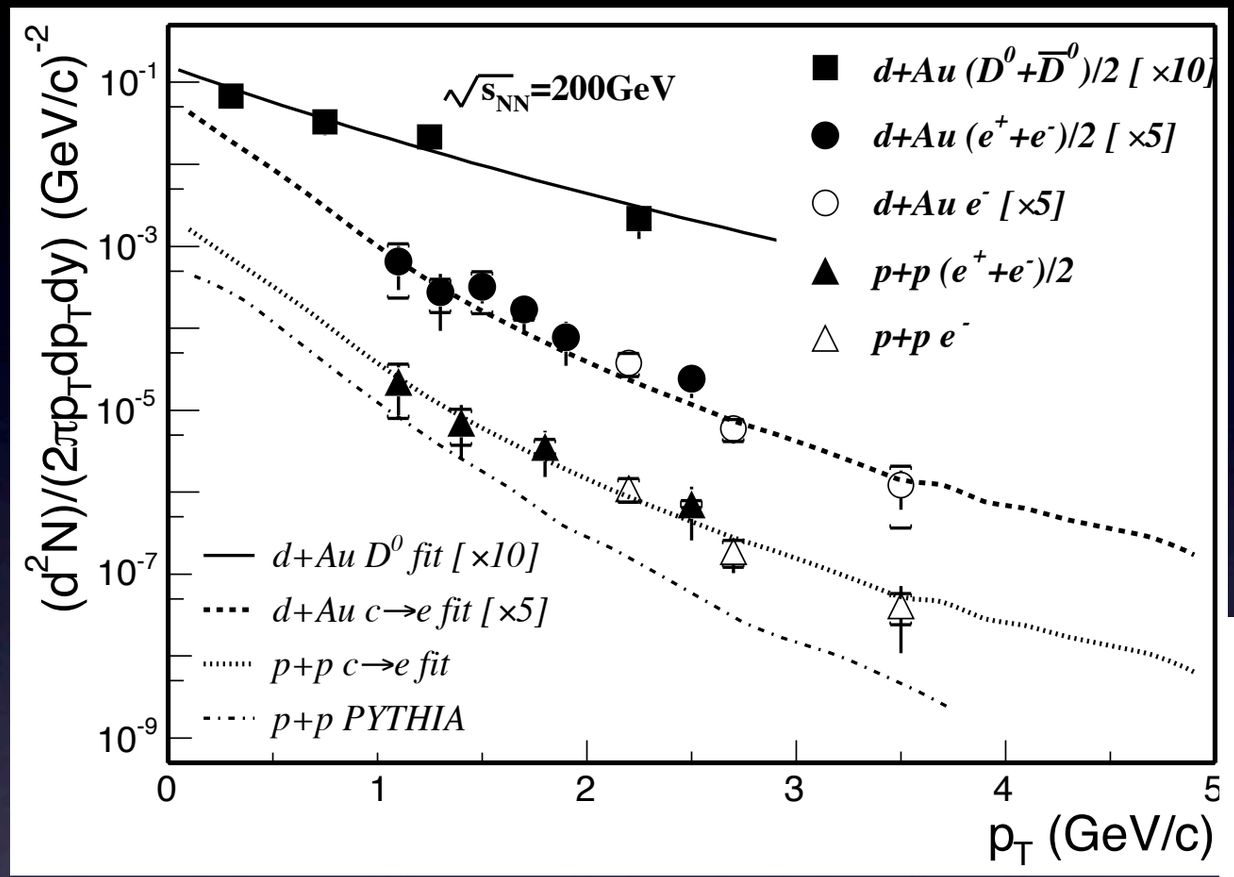

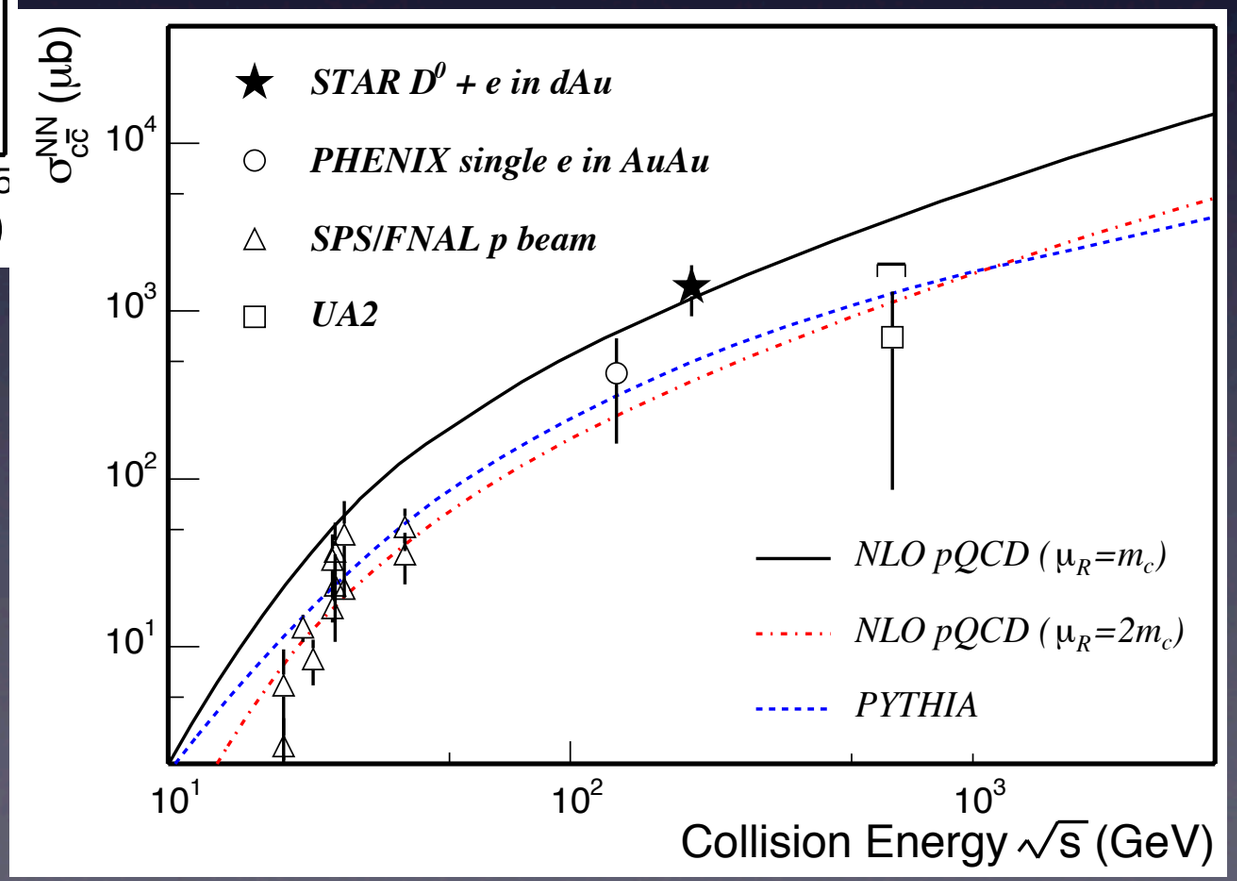

Comparison of pion spectra measured at RHIC at y=0

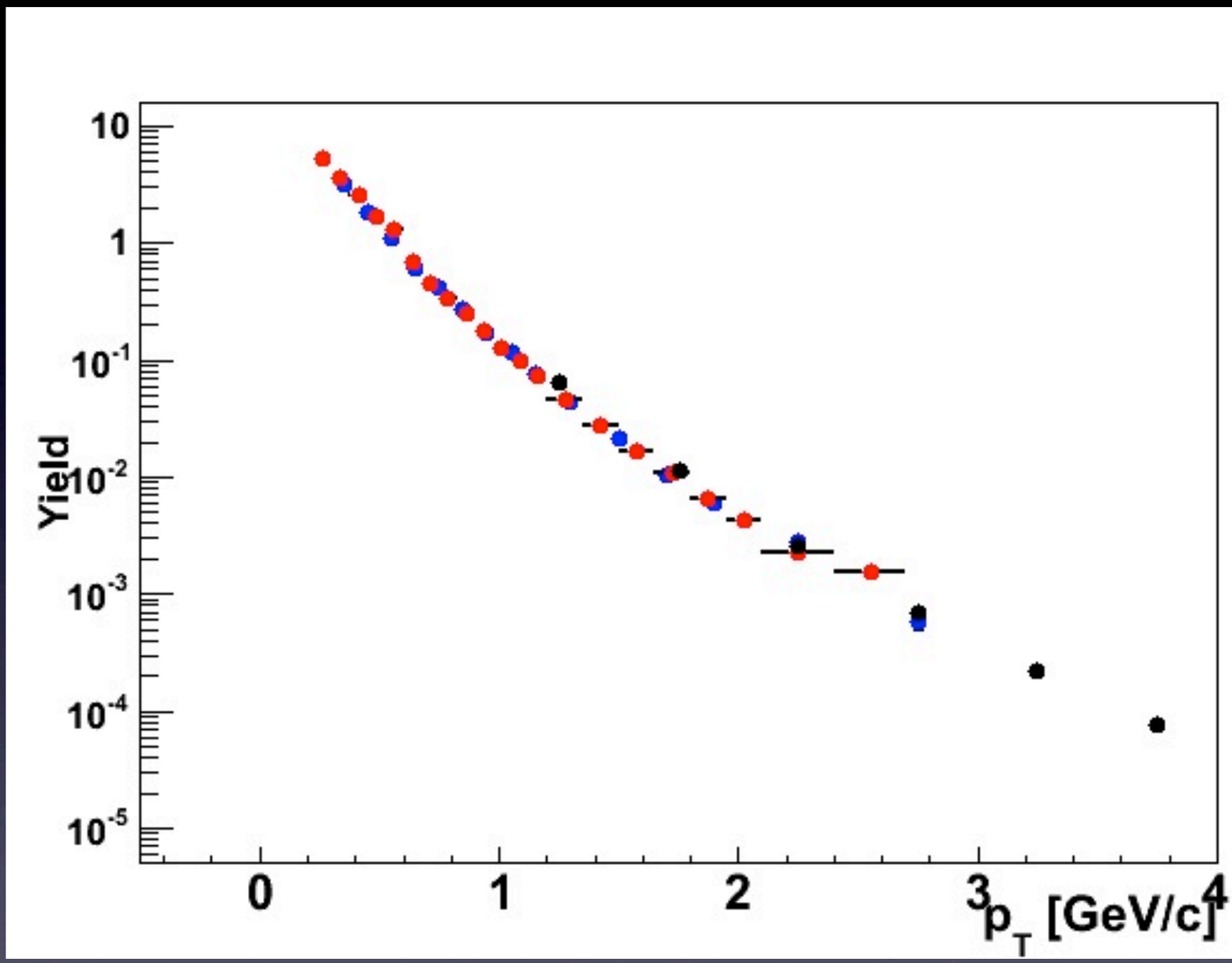

Red: BRAHMS π^+

Blue: STAR π^+

Black: PHENIX π^0

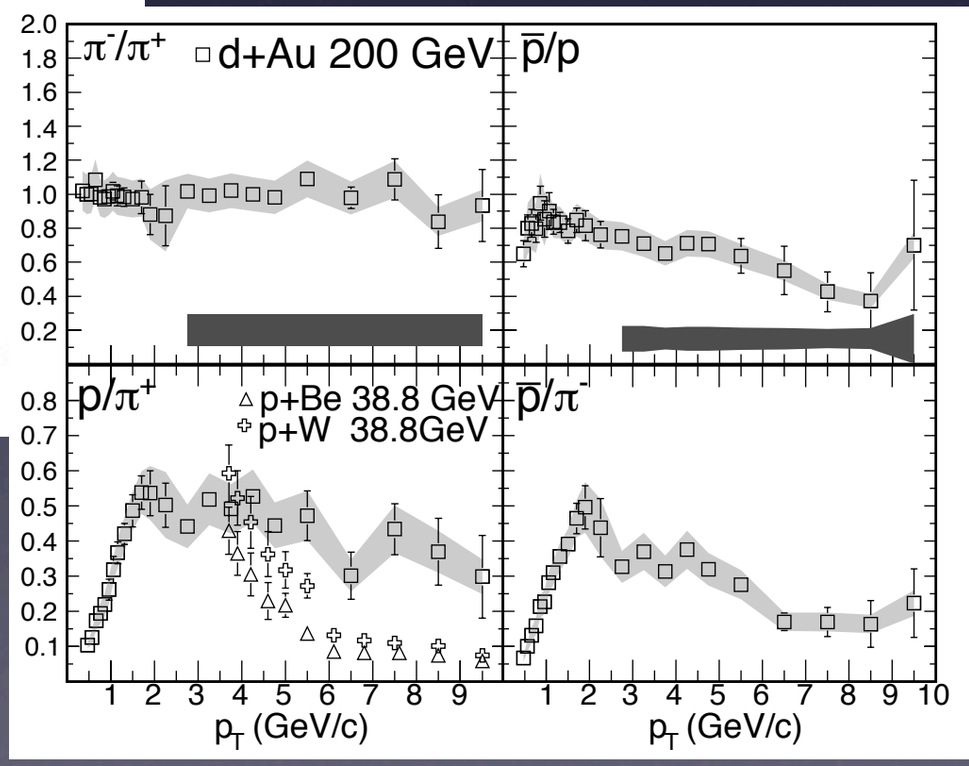

Good agreement between all three experiments.

Rapidity dependence

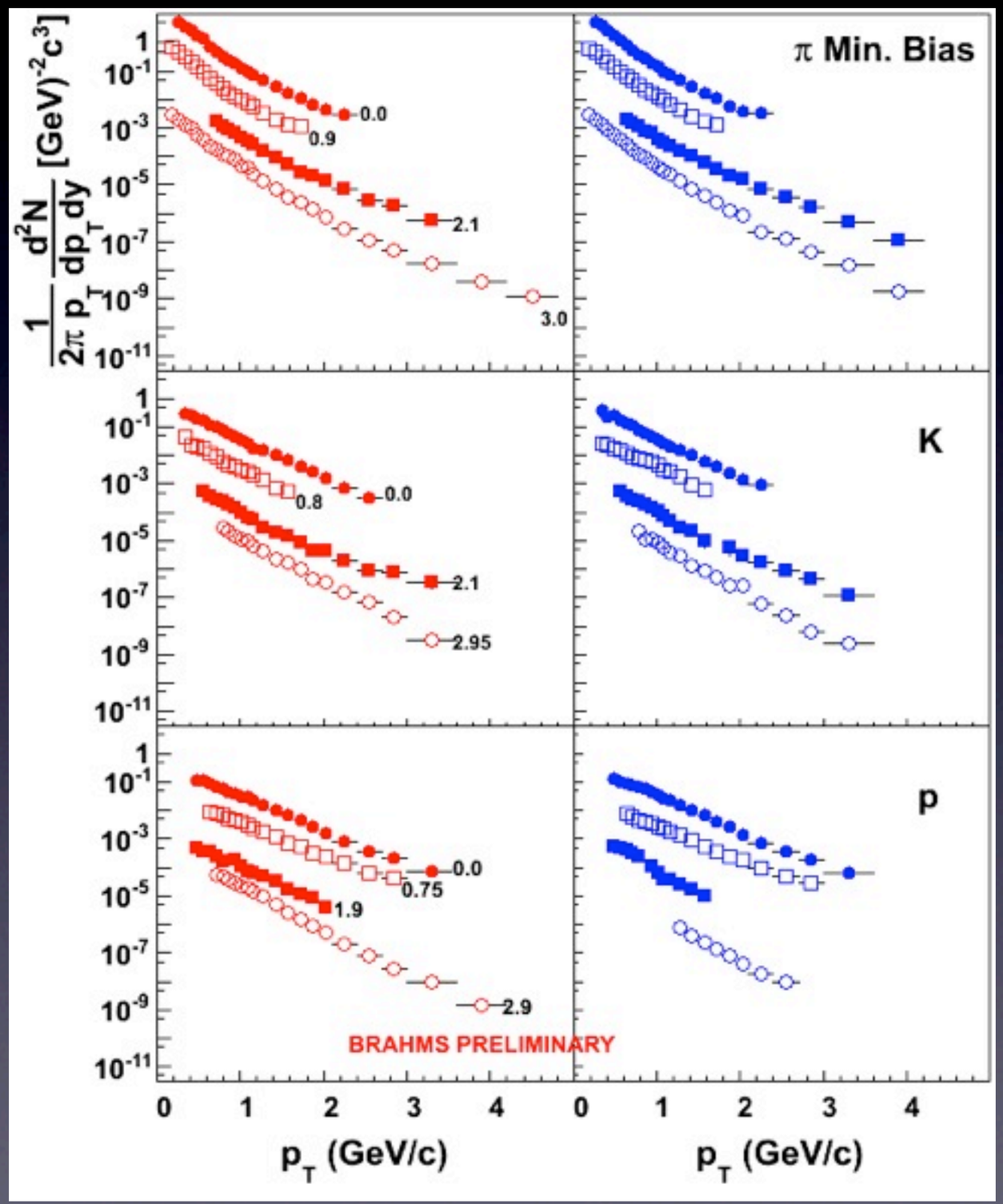

Fully corrected spectra for identified particles (TOF at MRS and RHIC at FS) in narrow rapidity windows. Positive particles are shown in red and negative ones with blue.
No feed down corrections applied to p spectra.

These rapidity values were selected because they provide us with the highest p_T coverage.

The center of the rapidity window for each spectra is shown at the end-point of the positive charge distributions.
For clarity, each spectra is divide by powers of10.

Only statistical error are displayed, the identification of systematic uncertainties is in progress.

Centrality defined with multiplicity measurements in $-2<\eta<2$ We use three centrality data samples 0-30%, 30-60% and 60-80%

R_{dAu} for pions in central collisions (0-30%)

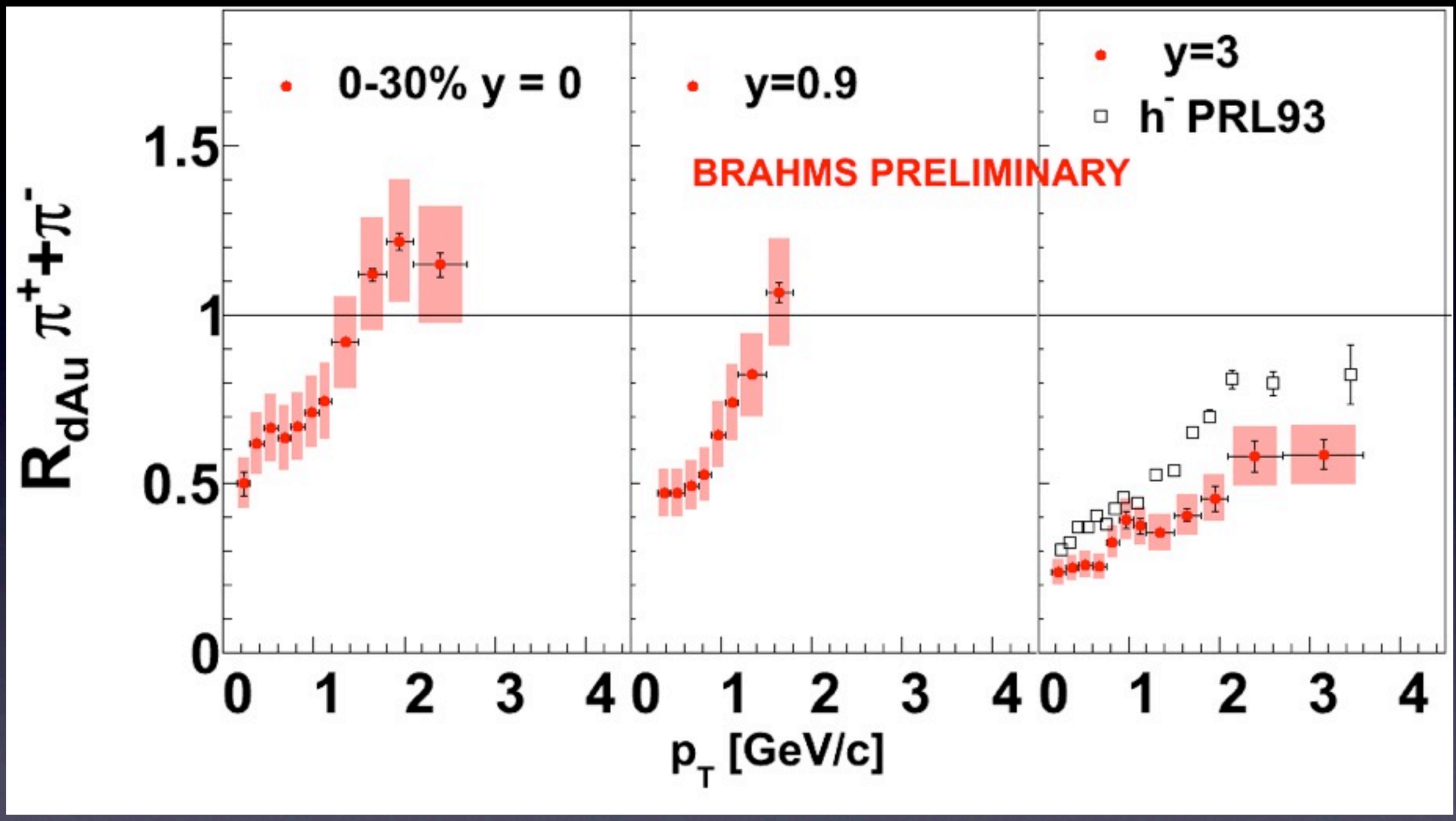

As the rapidity of the measurements increases, the growth of the cross section in the numerator slows down because of its proximity to the saturated regime (non-linear effects in quantum-evolution). Meanwhile, the cross section of the denominator (dilute p+p system) continues to increase.

R_{dAu} for pions in semi-central collisions (30-60%)

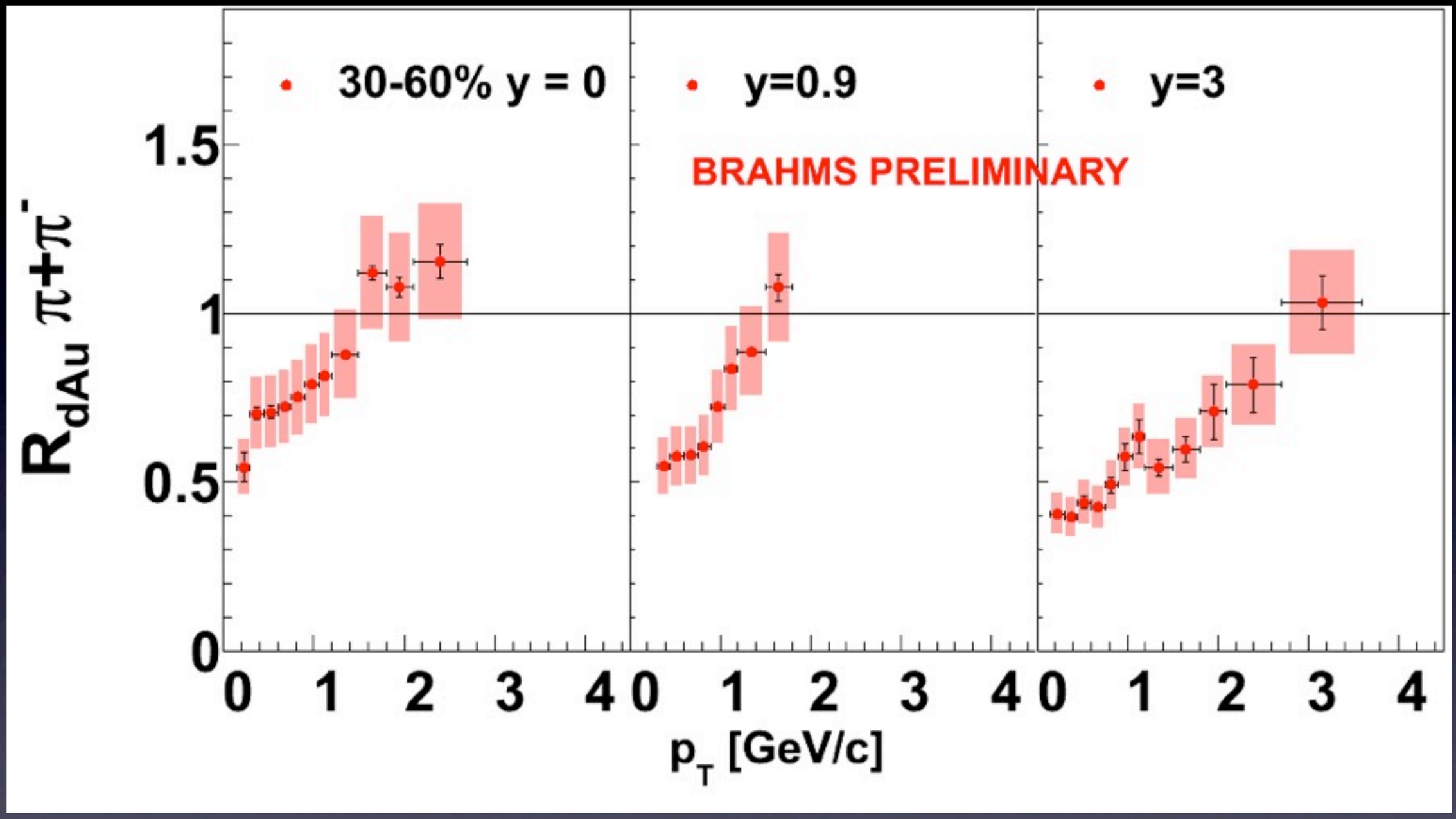

As mentioned in the introduction, the saturation scale grows with the number of participant nucleons in the target. As we study the RdAu in semi-central collisions, the change of the ratio as rapidity increases is less pronounced.

RdAu for Kaons in central collisions (0-30%)

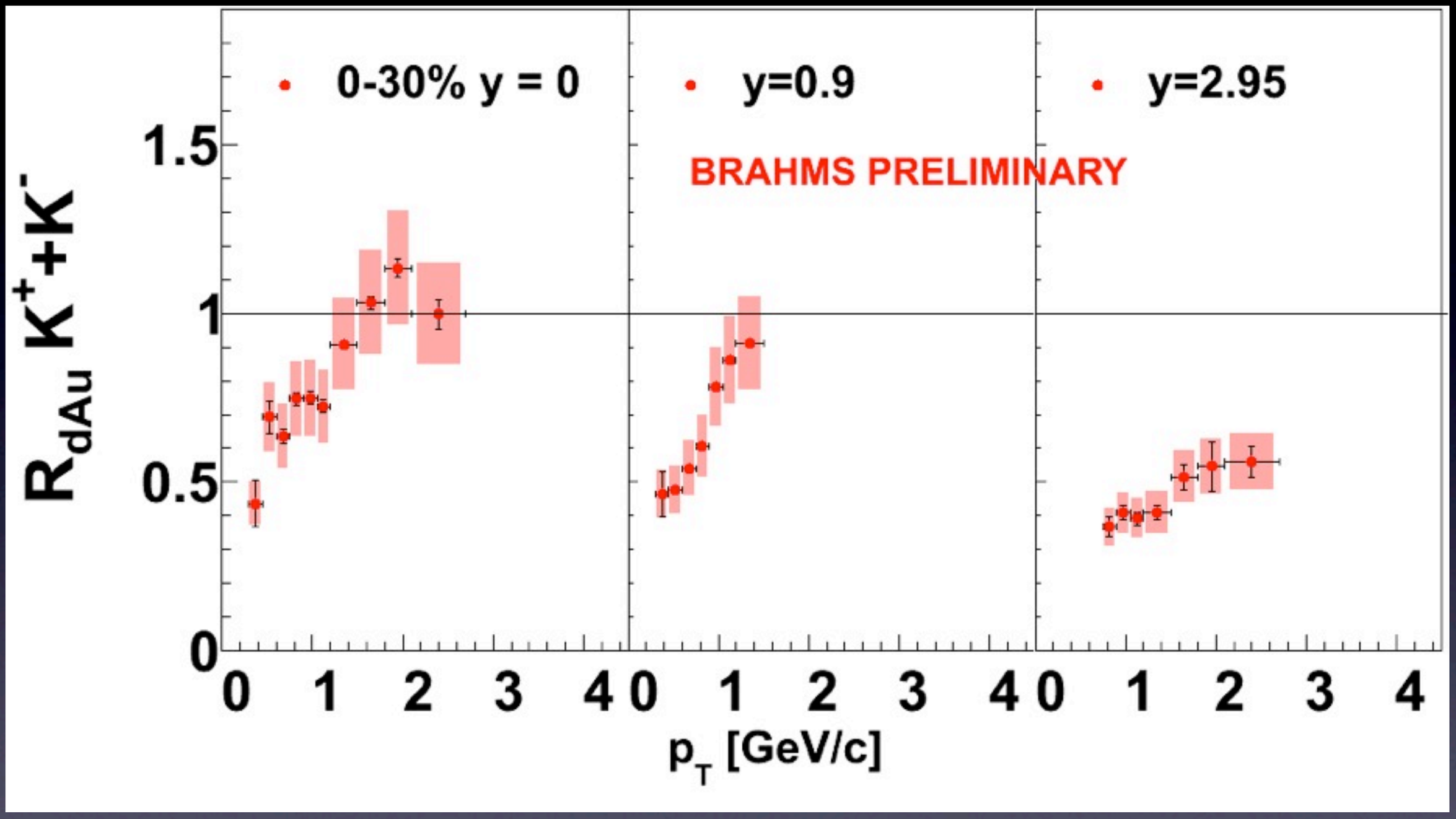

The kaons have a rapidity and centrality dependence that is very similar to the one found in pions.

RdAu for protons in central collisions (0-30%)

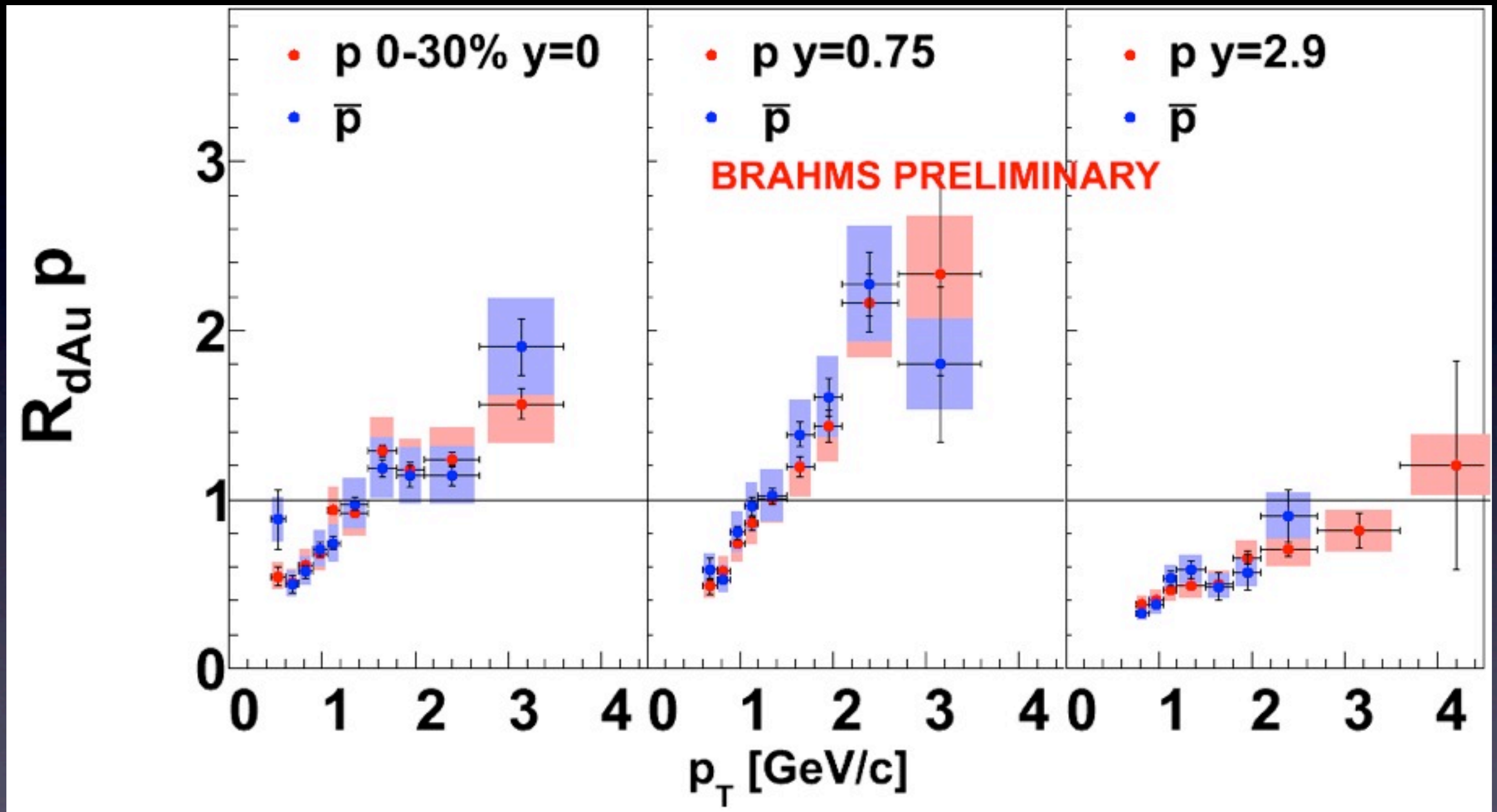

Protons have a more pronounced Cronin "peak" near mid-rapidity and they show similar behavior at high rapidity. There appears to be a shift of the peak towards higher values of transverse momentum.

R_{dAu} for all species in central collisions (0-30%)

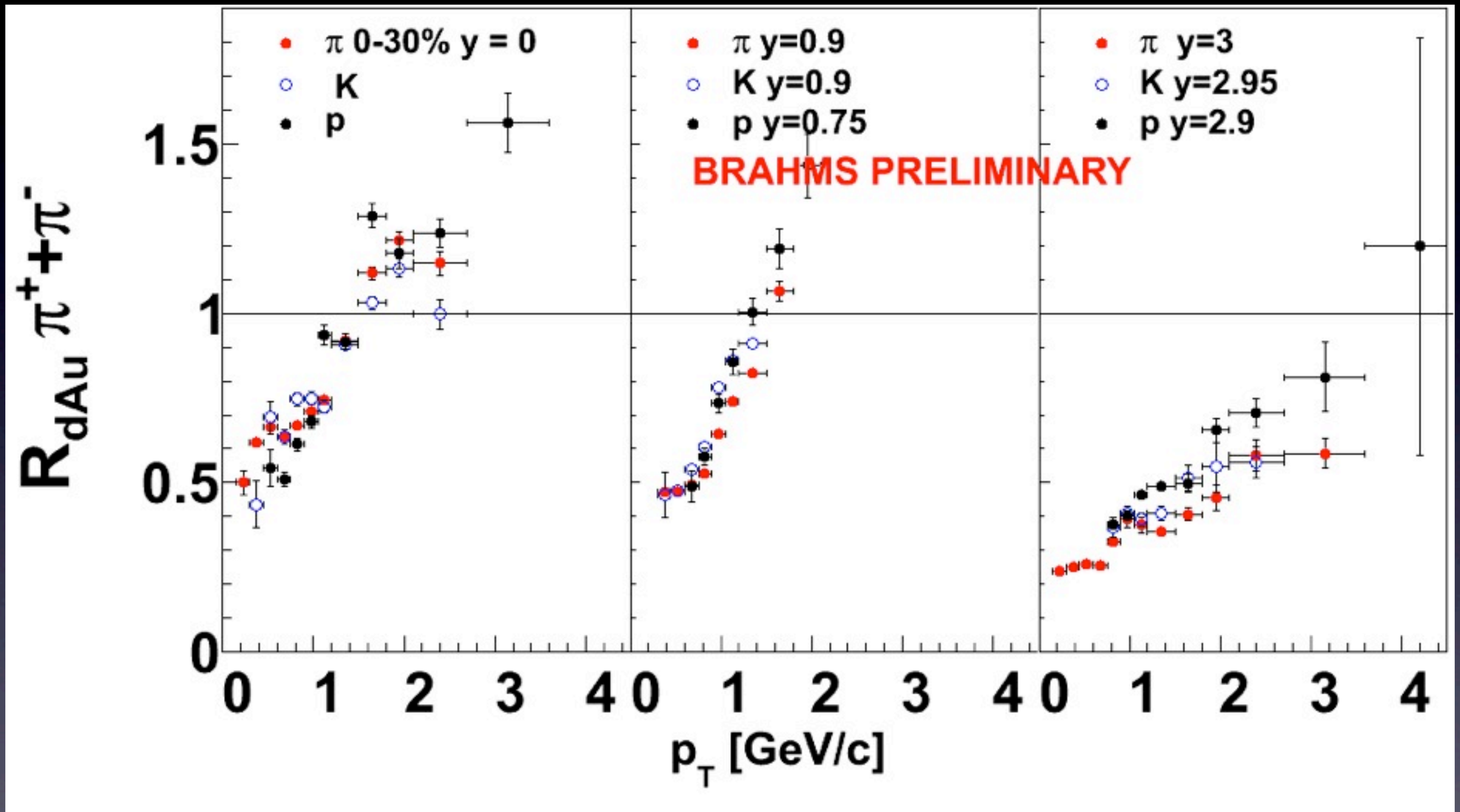

R_{cp} for pions in the most central collisions (0-30%)

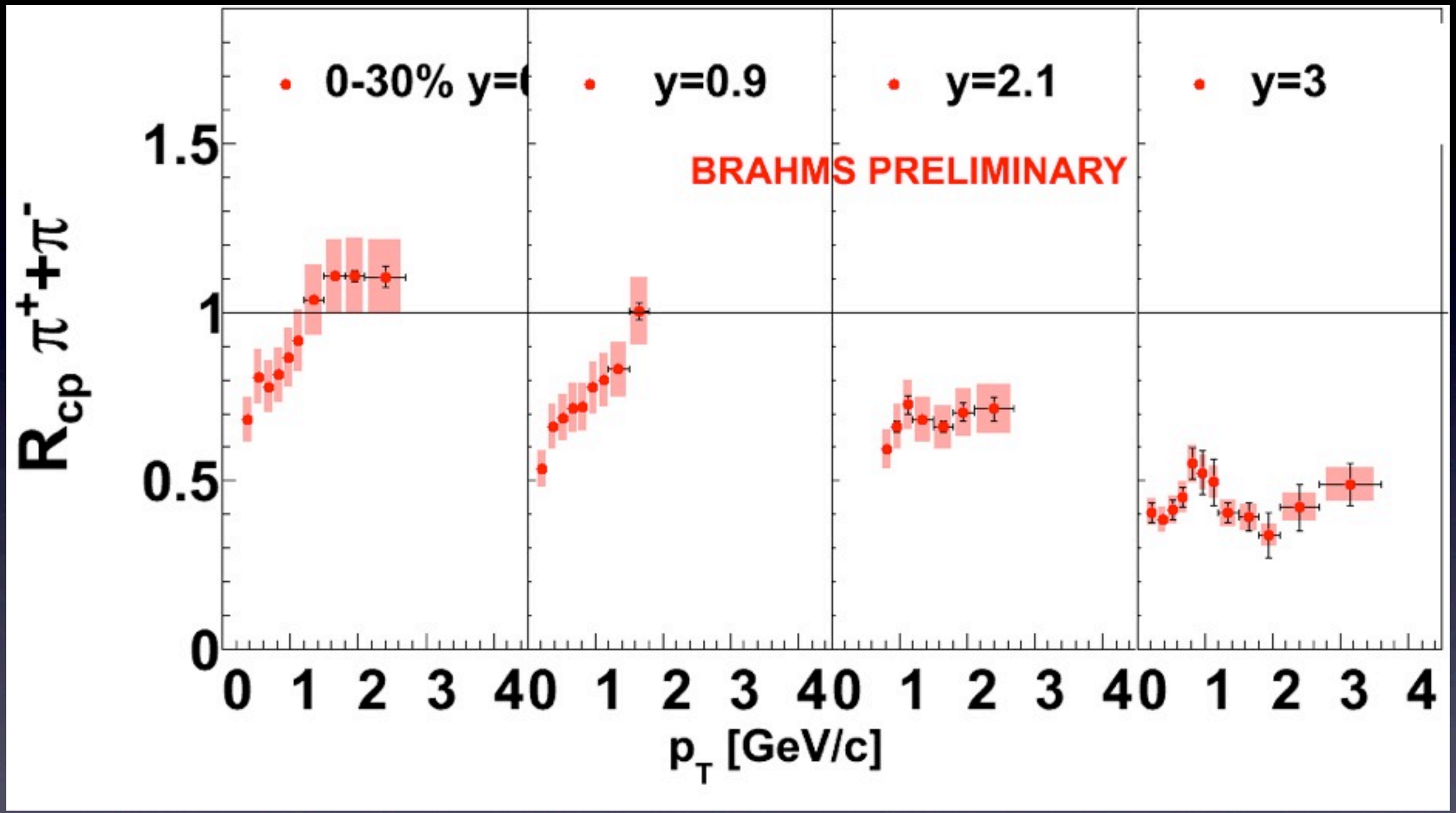

The onset of suppression appears close to y=0

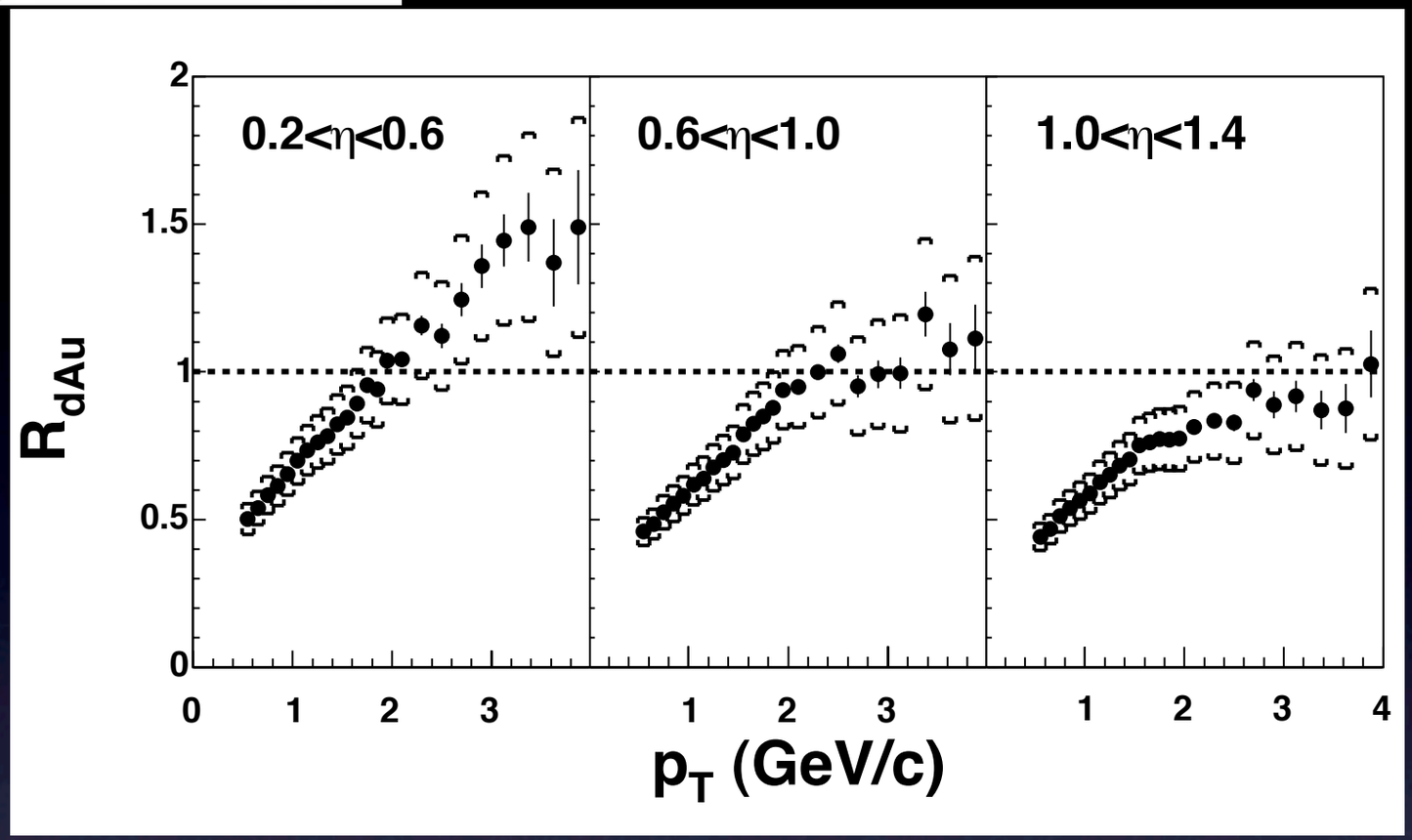

PHOBOS charged hadron yields in a Min. Bias sample compared to scaled UA1 p+anti-p distribution.

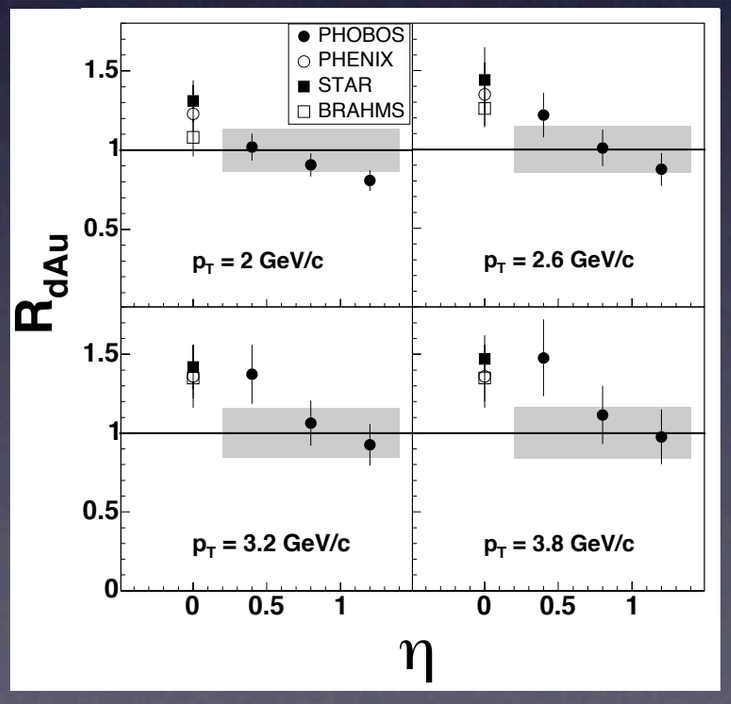

R_{dAu} constructed with ratio of fits to d+Au yields and the UA1 reference, calculated at four p_T values greater than 2 GeV/c, and plotted as function of η. The shaded bands show the systematic uncertainty of the scale.

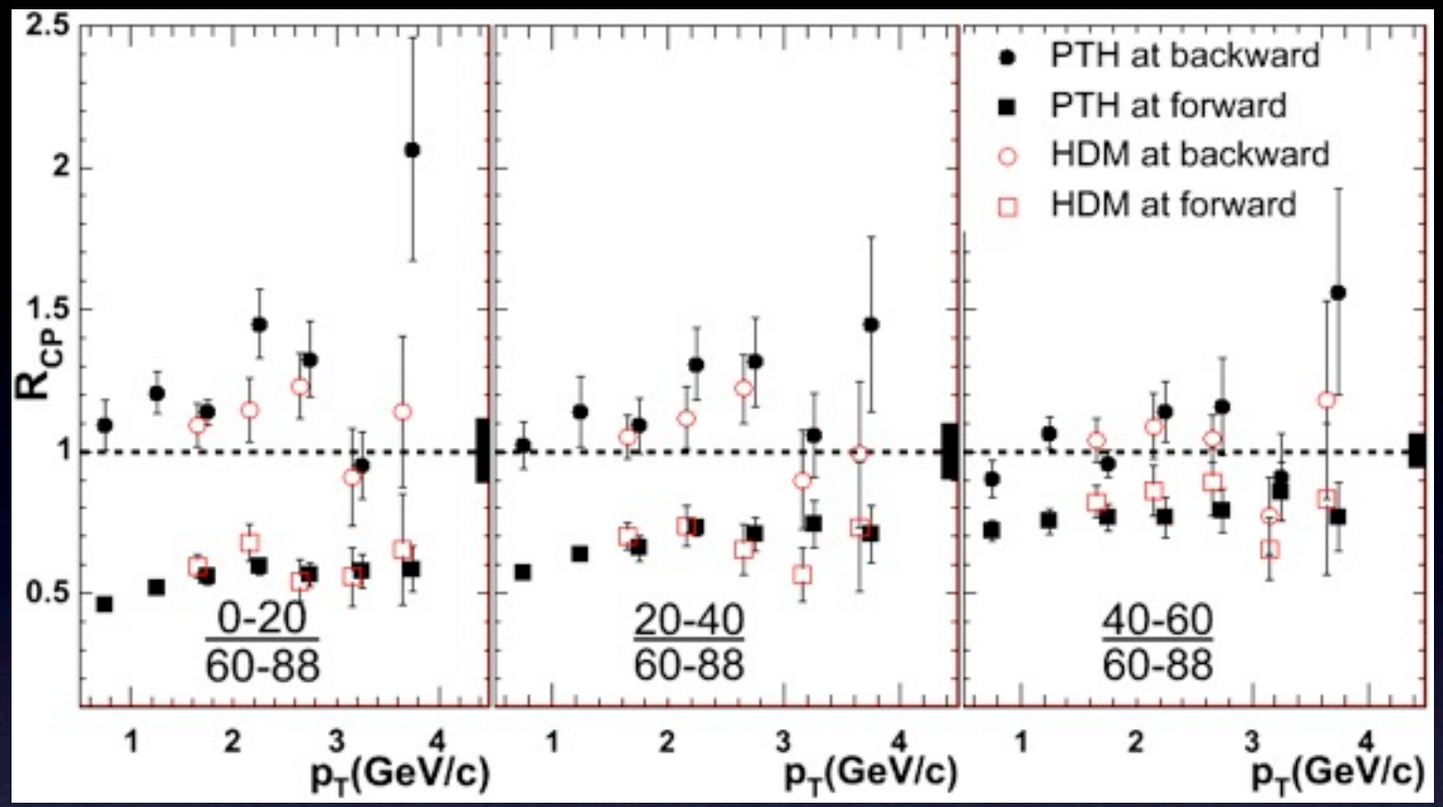

Charged hadron production in d+Au reactions at 200 GeV measured in the d-direction (forward): $1.4 < \eta < 2.2$, and in the gold-direction $-2.0 < \eta < -1.4$, (backward) with MuID detectors.

PTH: punch thru hadrons reach part way the MuID
HDM: identified muons from decay of hadrons.

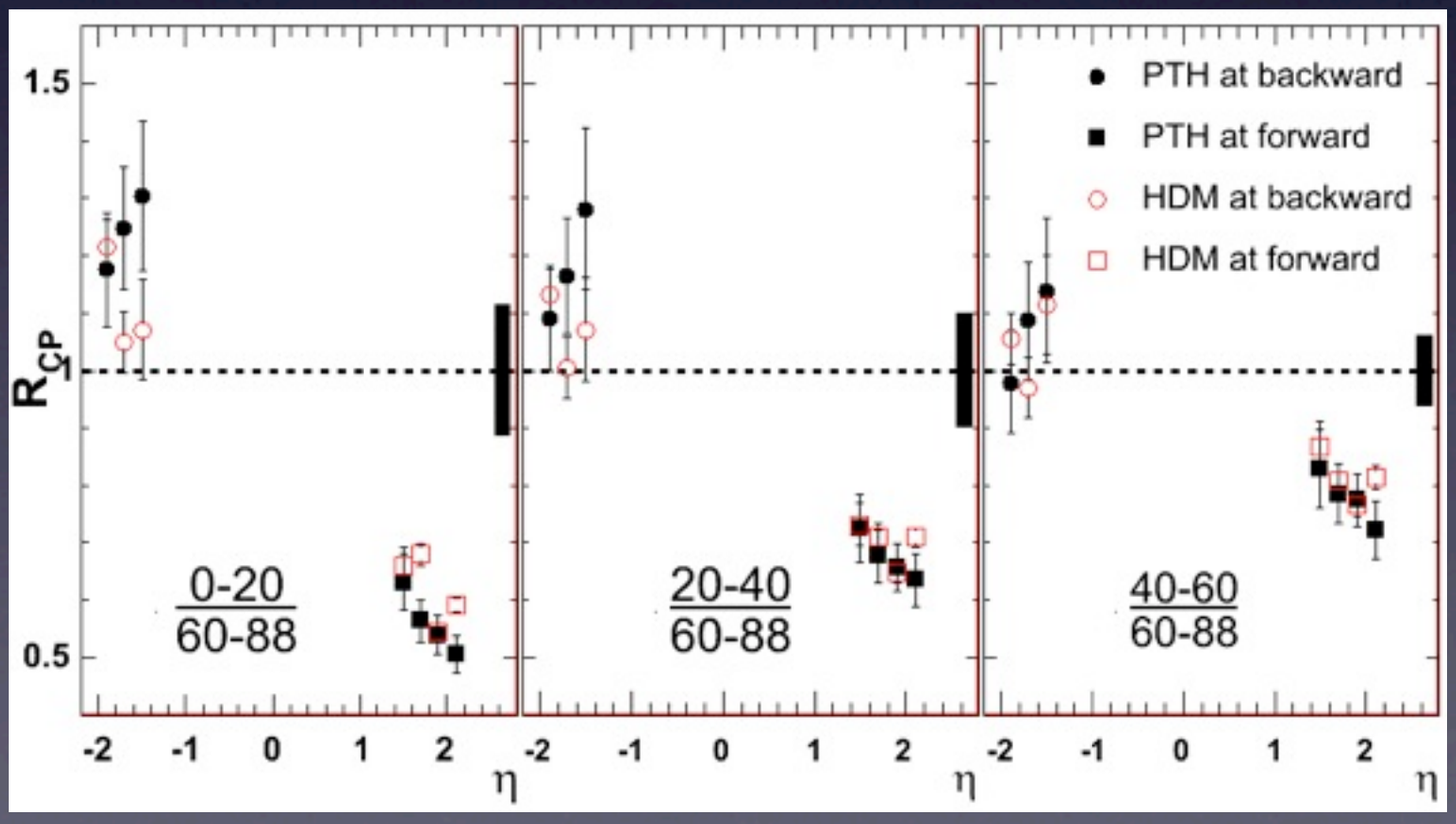

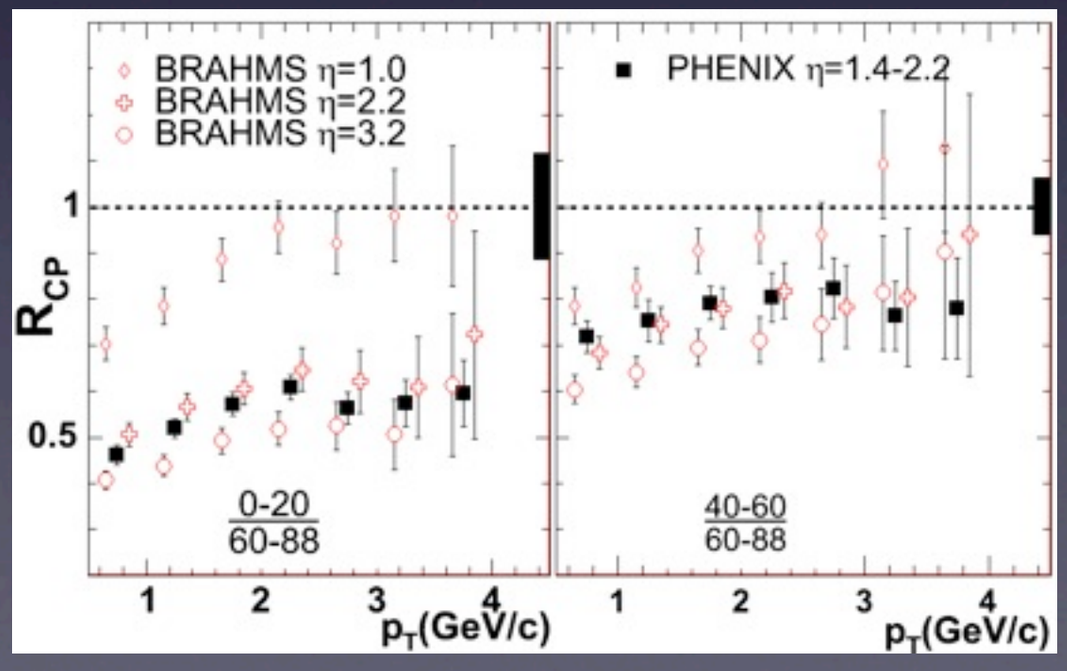

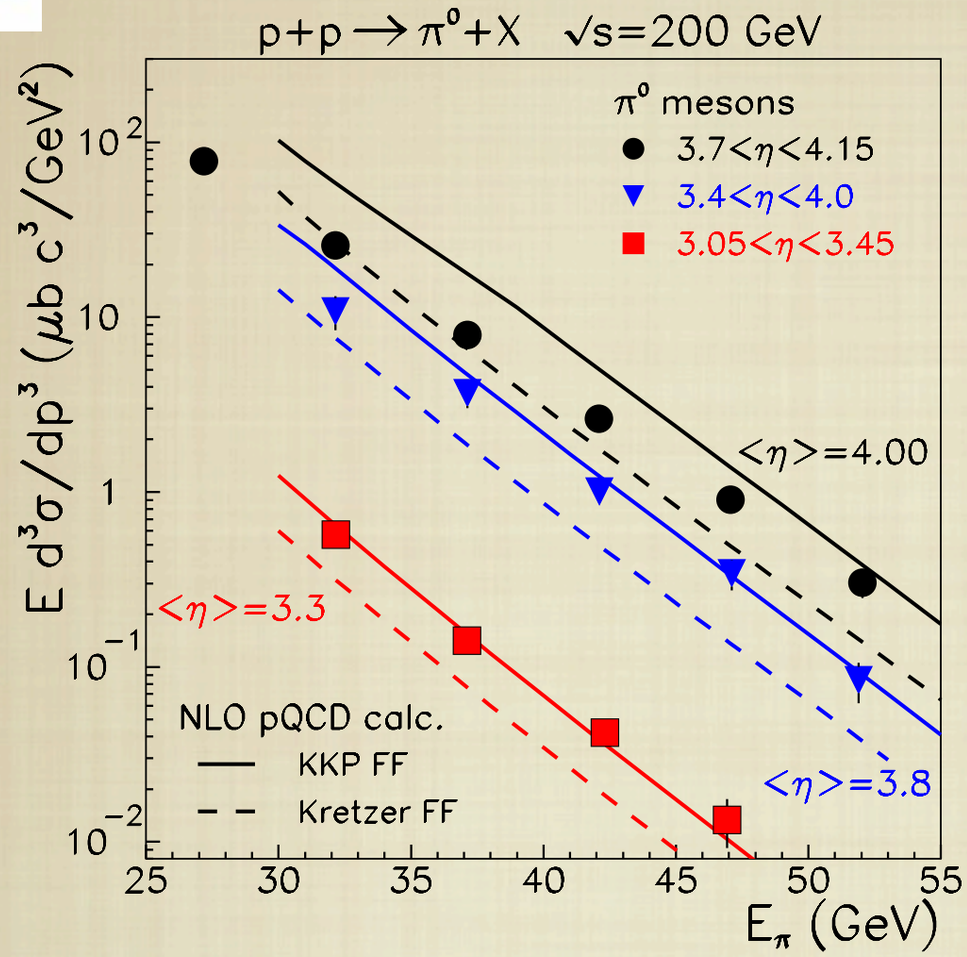

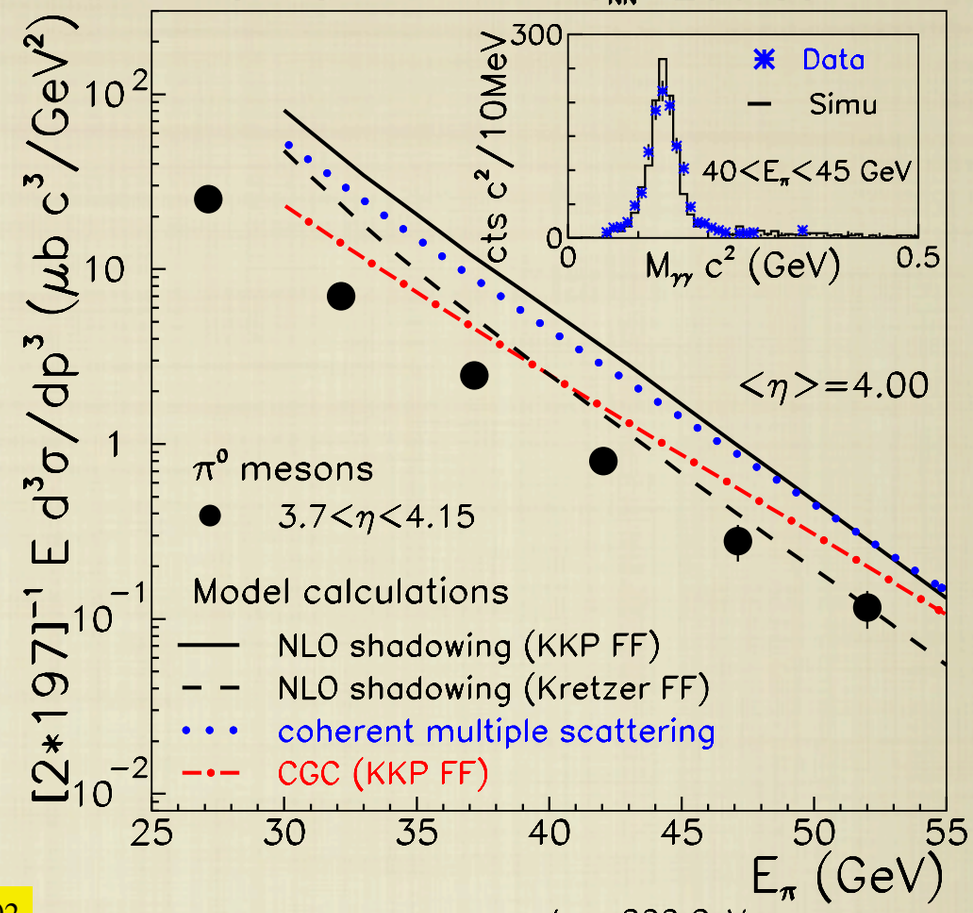

Phys. Rev. Lett. **97** (2006) 152302

Yields of high energy π^0 ($25 < E\pi < 55$GeV) at forward rapidities ($3.0 \sim< \eta \sim< 4.2$) from p+p and d+Au measured with the STAR FPD

R_{dAu} for π^0 at $\langle\eta\rangle = 4.00$ together with h− BRAHMS data at smaller. Systematic errors from p+p and d+Au are added in quadrature. The curves in inset are the NLO calc. shown above.

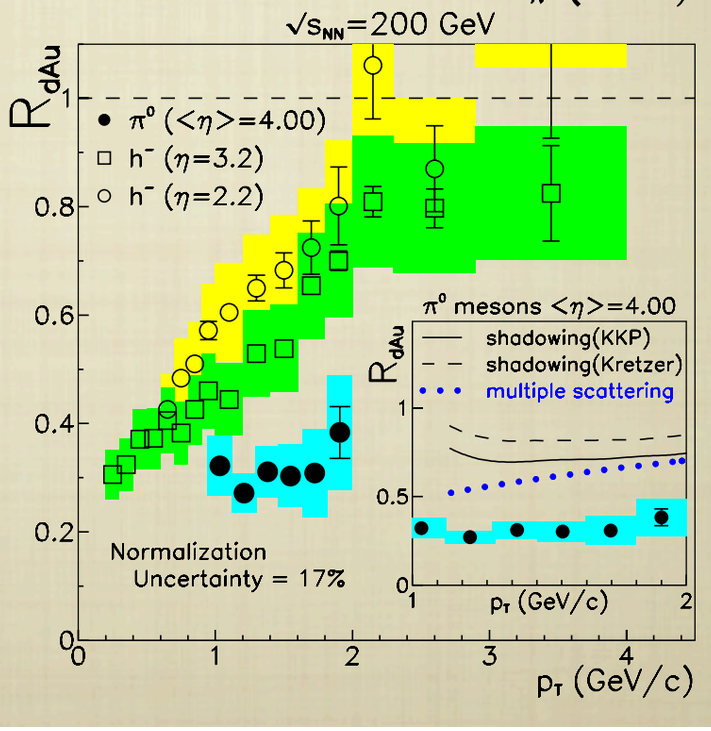

Descriptions of the high rapidity measurements

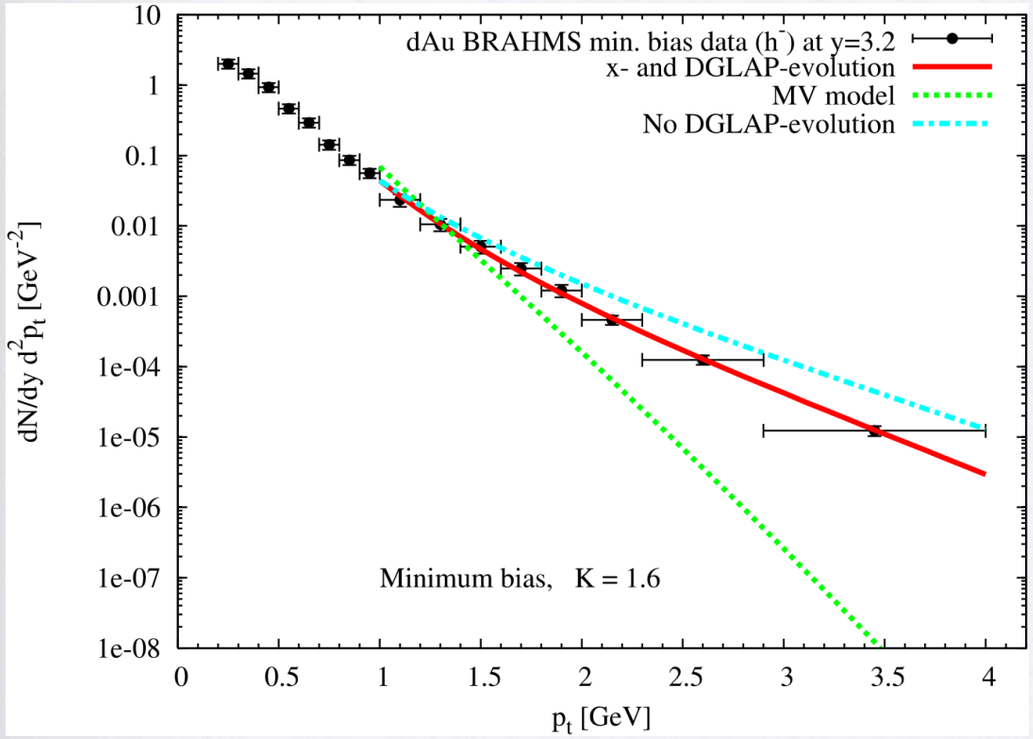

Fig. 5. Importance of DGLAP evolution of the proton/hadron distribution/fragmentation functions and of the anomalous dimension of the target gluon distribution.

A. Dumitru, A. Hayashigaki and J. Jalilian-Marian, Nucl. Phys. A 765, 464 (2006).

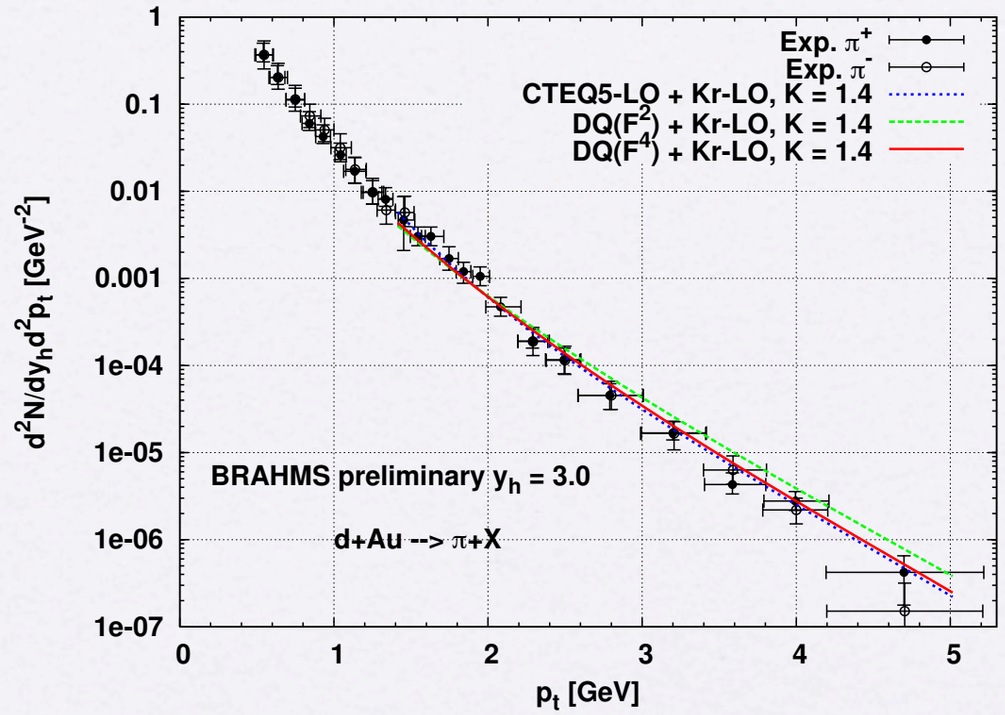

Figure 2: p_t spectra of π^+ and π^- from d+Au collisions compared to BRAHMS preliminary minimum bias data ($y_h = 3.0$). The lines show the CGC results with the LO Kretzer FFs and $K = 1.4$, where either the LO CTEQ5 or diquark PDFs are used.

A. Hayashigaki Nucl.Phys.A775:51-68,2006.

Includes recoil correction from gluon radiation by projectile quarks. As well as DGLAP evolution of quark and gluon PDF in projectile.

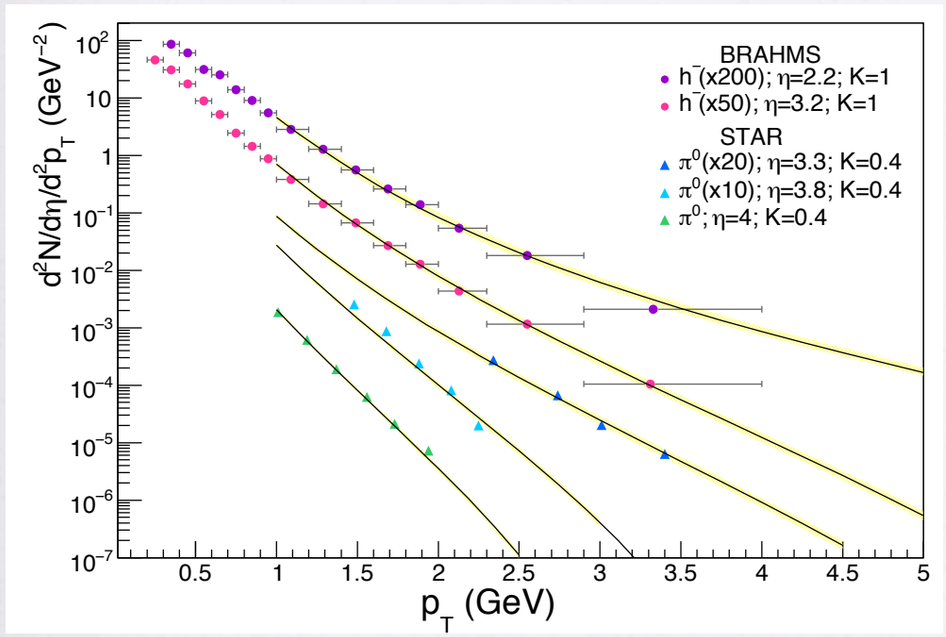

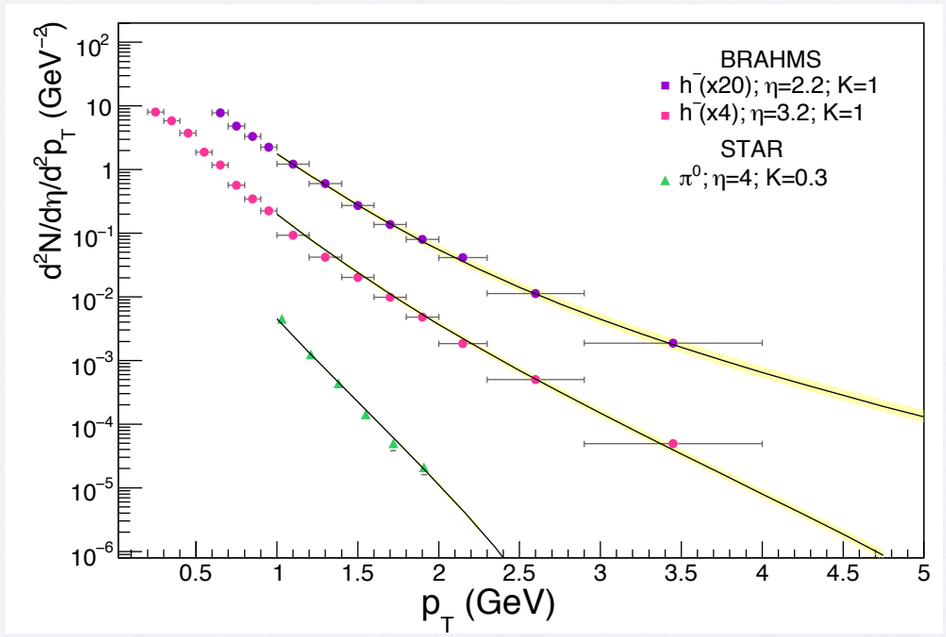

Figure 1: Negatively charged hadron and π^0 yields in proton-proton (at pseudo-rapidities (2.2, 3.2) and (3.3, 3.8 and 4)) and deuteron-gold (at pseudo-rapidities (2.2, 3.2) and 4) collisions at $\sqrt{s_{NN}} = 200$ GeV. Data by the BRAHMS and STAR collaborations.

Javier L. Albacete, Cyrille Marquet, (Saclay, SPhT) . Jan 2010. 12pp.
Published in **Phys.Lett.B687:174-179,2010**.

$$\frac{dN_h}{dy_h\, d^2p_t} = \frac{K}{(2\pi)^2} \sum_q \int_{x_F}^1 \frac{dz}{z^2} \left[x_1 f_{q/p}(x_1, p_t^2)\, \tilde{N}_F\left(x_2, \frac{p_t}{z}\right) D_{h/q}(z, p_t^2) + x_1 f_{g/p}(x_1, p_t^2)\, \tilde{N}_A\left(x_2, \frac{p_t}{z}\right) D_{h/g}(z, p_t^2) \right] ,$$

where N_F and N_A are numerical solutions of the BK equation with running coupling.

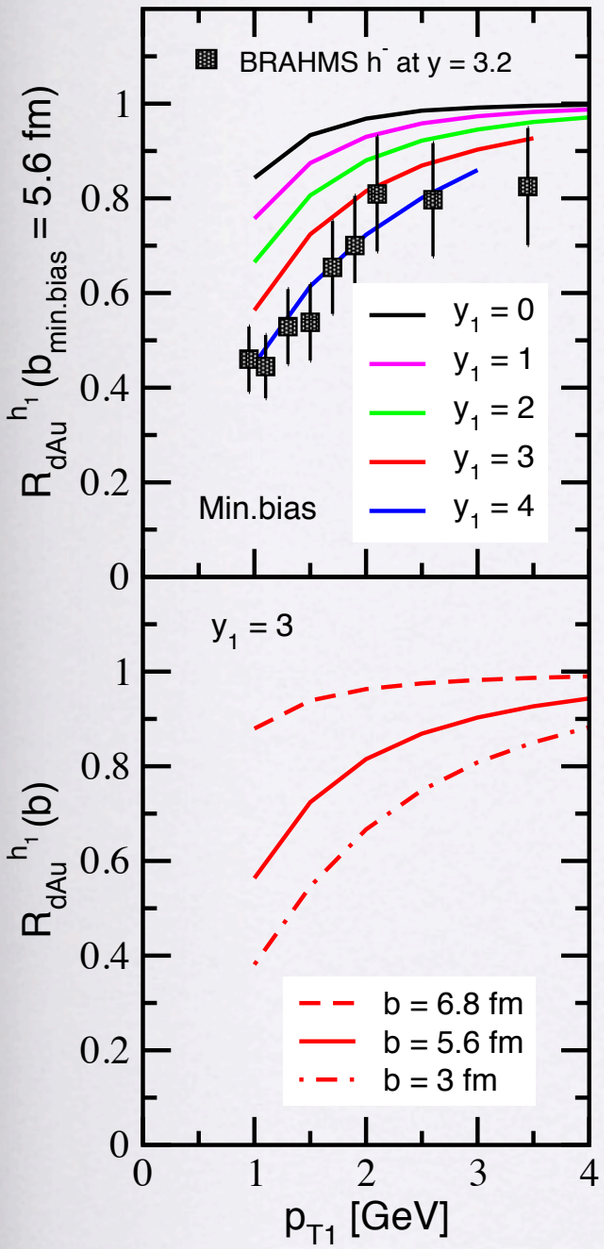

Jian-wei Qiu, Ivan Vitev Phys.Lett.B632:507-511,2006.

Coherent multiple parton scattering with several nucleons in lepton-nucleus and hadron-nucleus collisions leads to shadowing.

BDR in central pA collisions: Leading partons in the proton, x_1, interact with a dense medium of small x_2 – gluons in the nucleus (shaded area), loosing fraction of its momentum and acquiring a large transverse momentum, > $p_{t\ BDR}$

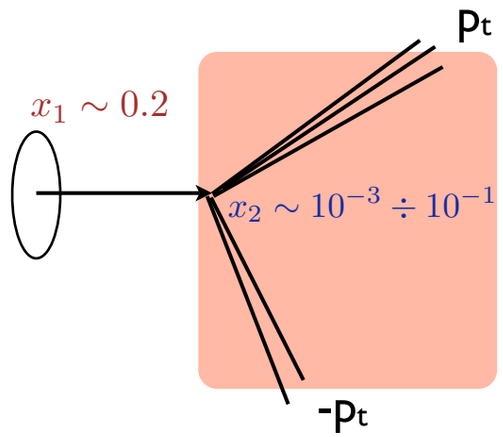

L. Frankfurt, (Tel Aviv U.) , M. Strikman, (Penn State U.) . May 2007

Hamburg 2007, Blois07, Forward physics and QCD* 327-335

Phys.Lett.B645:412-421,2007.

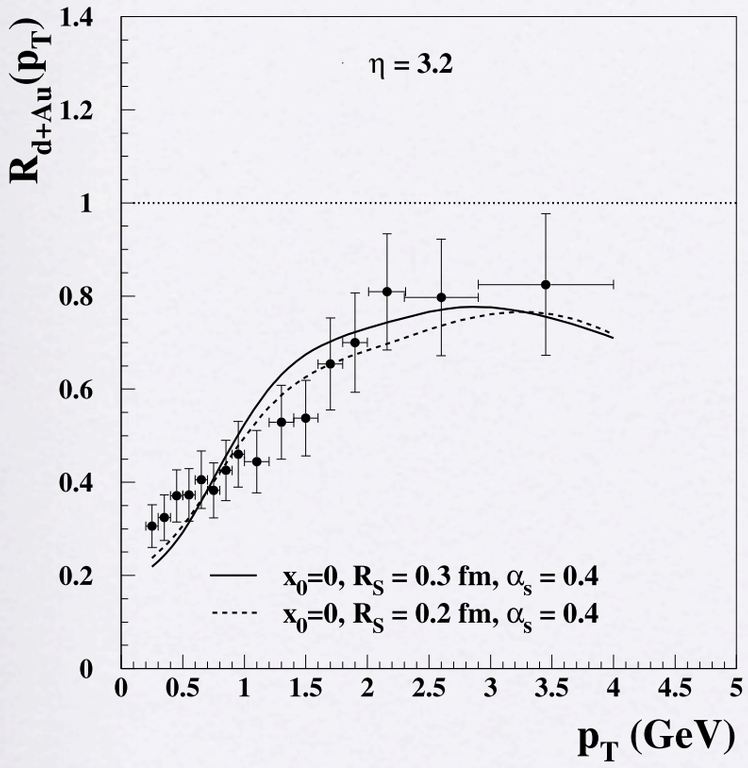

$$I_i(p_T, A) = I_i(p_T, 1) \cdot A^{\alpha_i(p_T)}$$

FIG. 3: Ratio of negative particle production rates in $d - Au$ and pp collisions as function of p_T. Data are from [1], solid and dashed curves correspond to calculations with the diquark size 0.3 fm and 0.4 fm respectively.

B. Z. Kopeliovich, J. Nemchik, I. K. Potashnikova, M. B. Johnson, I. Schmidt, Break- down of QCD factorization at large Feynman x, Phys. Rev. C72 (2005) 054606.

Energy conservation implies large rapidity gaps when particles are detected at $x_F \rightarrow 1$ which imply suppression.

R. Baier et al. / Nuclear Physics A 764 (2006) 515–527

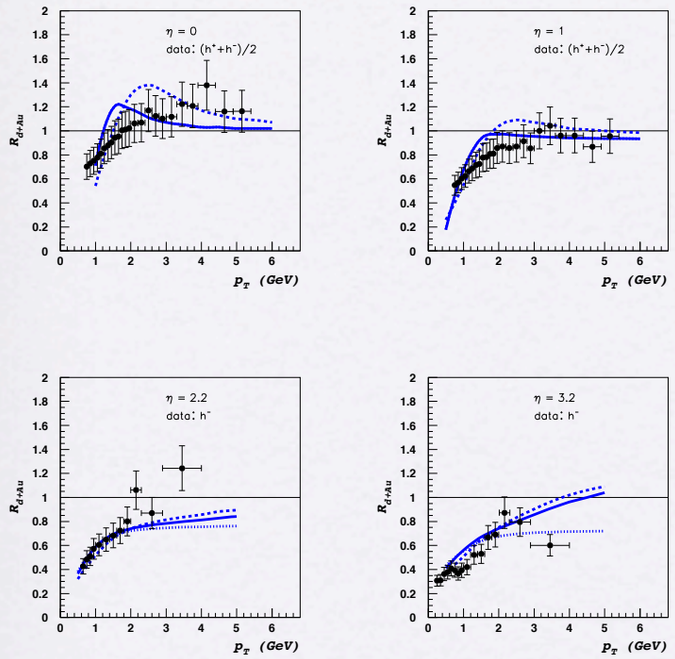

FIG. 2: Nuclear modification factor R_{dAu} of charged particles for different rapidities. In the top two figures, corresponding to $\eta = 0, 1$, the solid line corresponds to $(h^- + h^+)/2$ contribution calculated with $\kappa = 0$ in the isospin-independent approximation, while the dashed line gives the same $(h^- + h^+)/2$ contribution but with $\kappa = 1$ GeV. In the lower two plots, corresponding to $\eta = 2.2, 3.2$, the solid line gives the h^- contribution calculated in the constituent quark model with $\kappa = 0$, the dashed line gives the same h^- contribution for $\kappa = 1$ GeV, while the dotted line at $\eta = 2.2, 3.2$ gives the $(h^+ + h^-)/2$ contribution with $\kappa = 0$. Data is from [2].

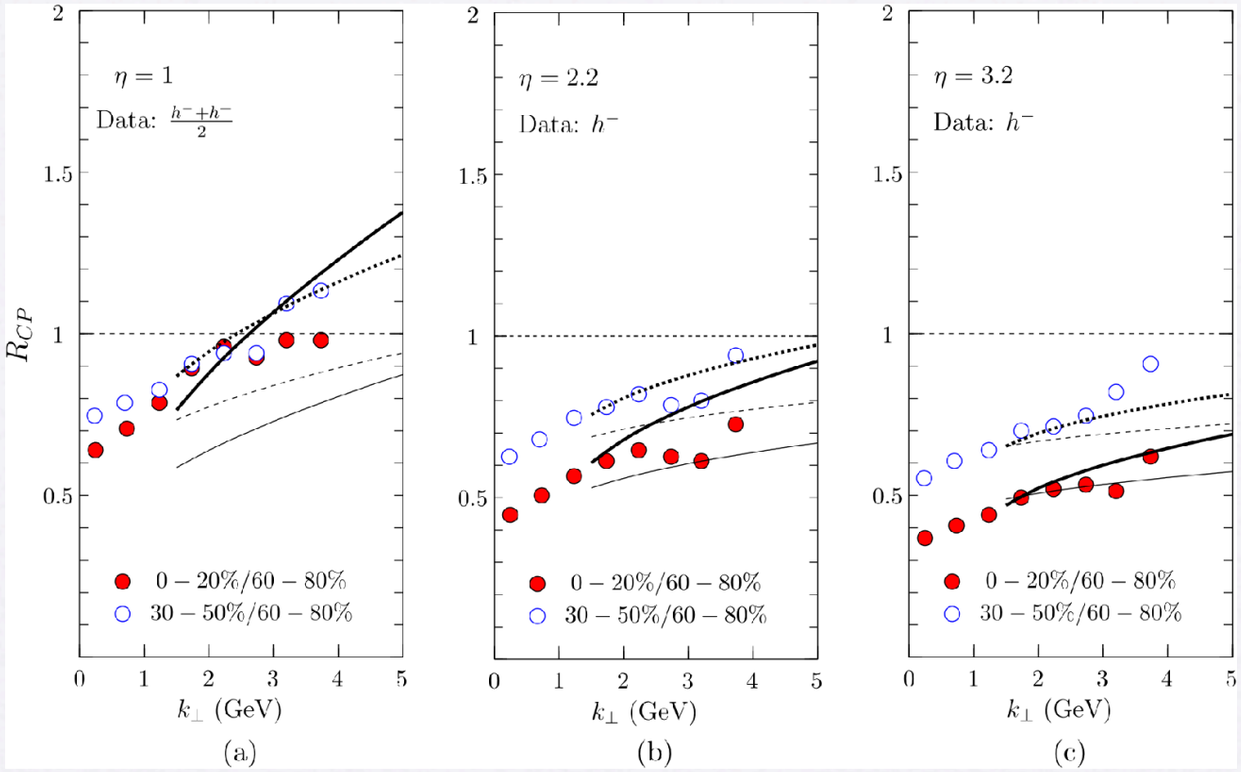

Fig. 4. R_{CP} for the BK parametrization (thick lines) and the BFKL + saturation form (thin lines) at different rapidities $\eta = 1$, 2.2 and 3.2. Full lines correspond to central over peripheral collisions (full experimental dots). Dashed lines correspond to semi-central over peripheral collisions (empty experimental dots). Data from [2].

Dmitri Kharzeev, Yuri V. Kovchegov , Kirill Tuchin, Phys.Lett.B599:23-31,2004.

$$Q_{sA}^2(\mathbf{b}) \simeq Q_{sA}^2(0) N_{\text{part.Au}}(\mathbf{b}) / N_{\text{part.Au}}(0),$$

Rapidity dependence introduced in the quark dipole–nucleus forward scattering amplitude.

$$N_Q(z_T, y) = 1 - \exp\left[-\frac{1}{4}\left(z_T^2 \frac{C_F}{N_c} Q_s^2\right)^{\gamma(y, z_T^2)}\right].$$

Summary

- d+Au collisions at RHIC have been studied thoroughly specially near y=0.
- Cronin enhancement seen at mid-rapidity.
- Enhancement depends on centrality of collisions.
- Protons show stronger enhancement.
- All mesons behave similarly as pions.
- NMFs of pions and kaons show similar suppression at high rapidity.
- NMF of protons and anti-protons shows suppressions as function of rapidity but also a competing Cronin type enhancement.

"Production of Mesons and Baryons at High Rapidity and High Pt in Proton-Proton Collisions at Sqrt{s} = 200 GeV"
Phys. Rev. Lett. 98, 252001 (2007)

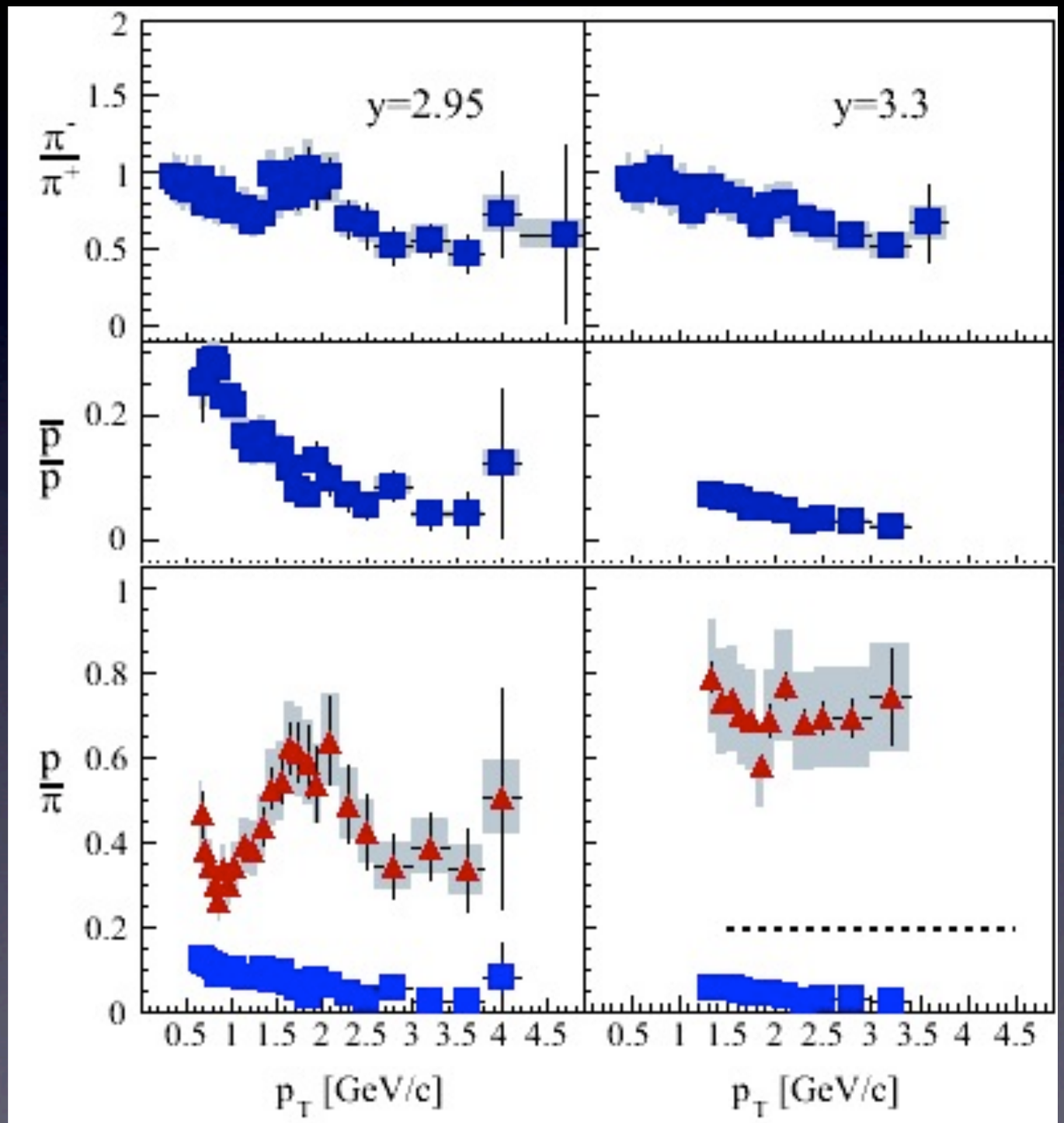

BFKL evolution

Nonlinear evolution

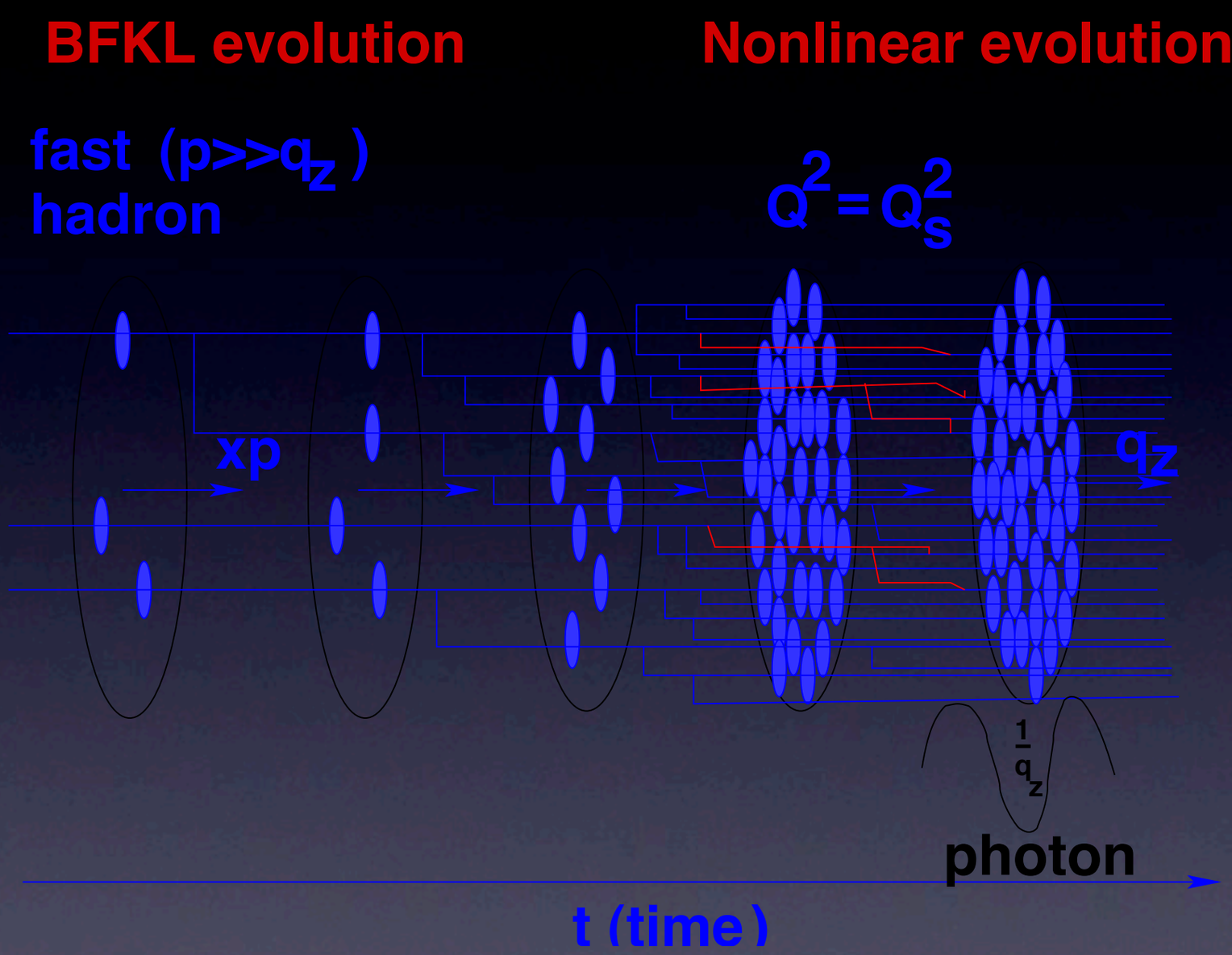

The saturation scale Q_s at $b = 0$ is given for a nucleus of mass number A (Au(197)) as [22]

$$Q_s^2(y_A, b = 0) = A^{1/3} Q_0^2 \left(\frac{x_0}{x_A}\right)^{\lambda} = A^{1/3} Q_0^2 x_0^{\lambda} e^{\lambda y_A}, \tag{6}$$

where $Q_0 \simeq 1$ GeV, $\lambda \simeq 0.3$ and $x_0 \simeq 3.0 \times 10^{-4}$ are fixed by the DIS data [41]. The energy dependence of Q_s is controlled through the constant growth rate $\lambda =$

$$Q_s^2(Y) \simeq Q_0^2 \, \mathrm{e}^{\lambda_s Y} \quad \text{with} \quad \lambda_s \approx 4.9\,\alpha_s \,, \tag{7}$$

where Q_0 is some non-perturbative initial scale. For a large nucleus, Q_0^2 scales like $A^{1/3}$ as does $Q_s^2(Y)$ for any Y. This form of the saturation momentum is

STAR Detector

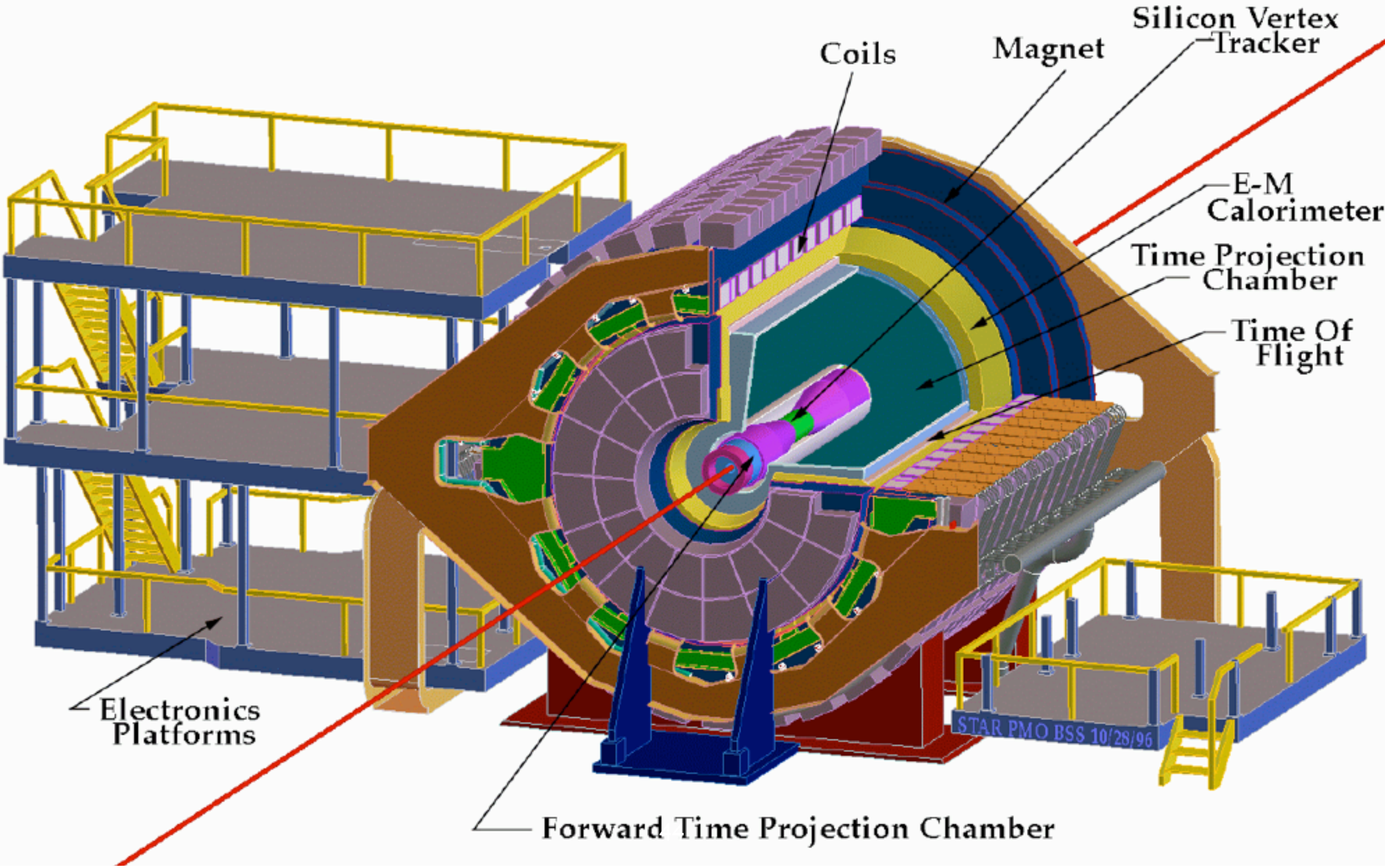

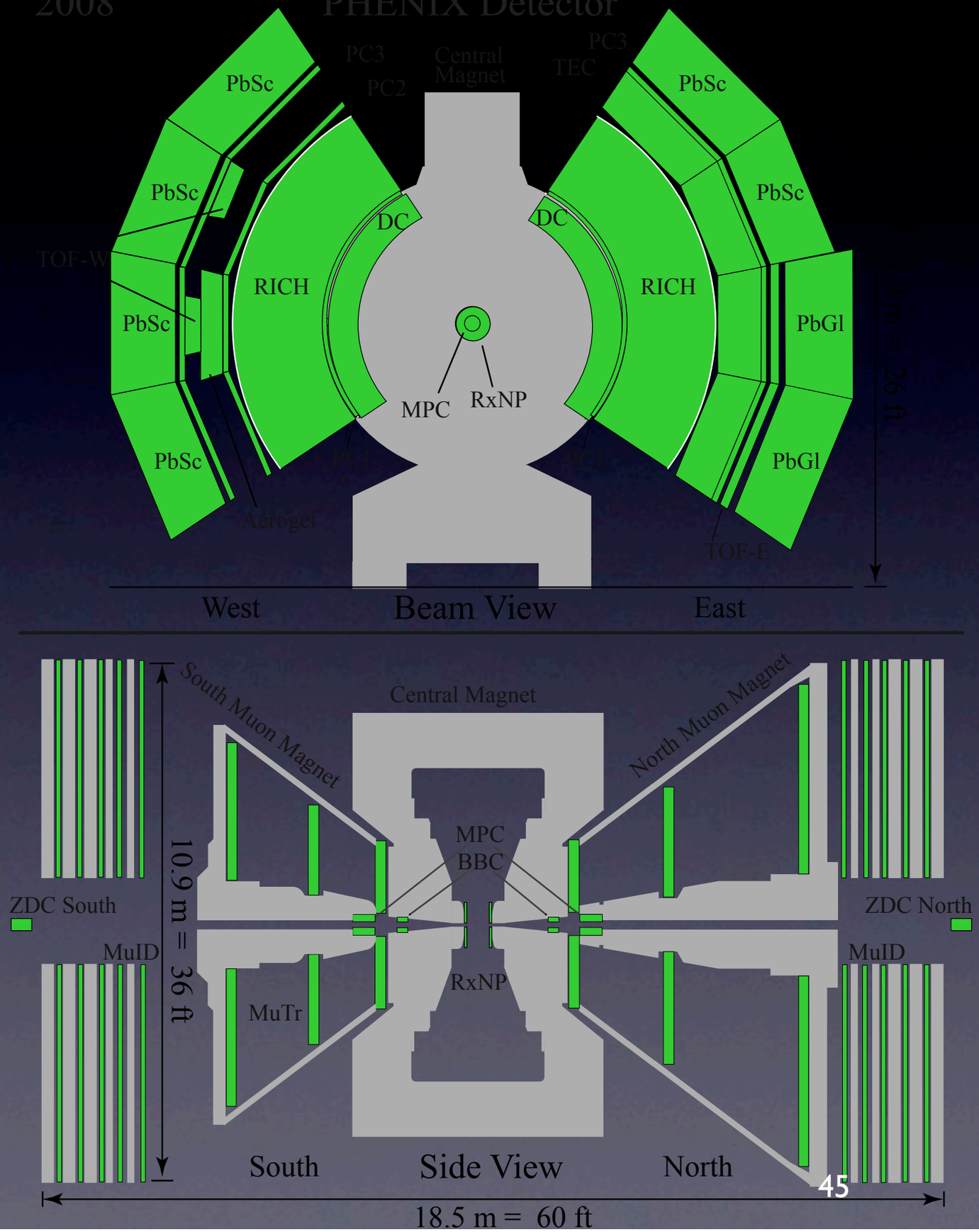
2008
PHENIX Detector
PC3
Central Magnet
PC3
PC2
TEC
PbSc
PbSc
PbSc
PbSc
PbSc
PbSc
DC
DC
TOF-W
RICH
RICH
PbGl
PbGl
MPC
RxNP
PC3
PC1
Aerogel
TOF-E
10.9 m = 36 ft
West
Beam View
East
South Muon Magnet
Central Magnet
North Muon Magnet
MPC
BBC
ZDC South
ZDC North
MuID
MuID
MuTr
RxNP
South
Side View
North
45
18.5 m = 60 ft

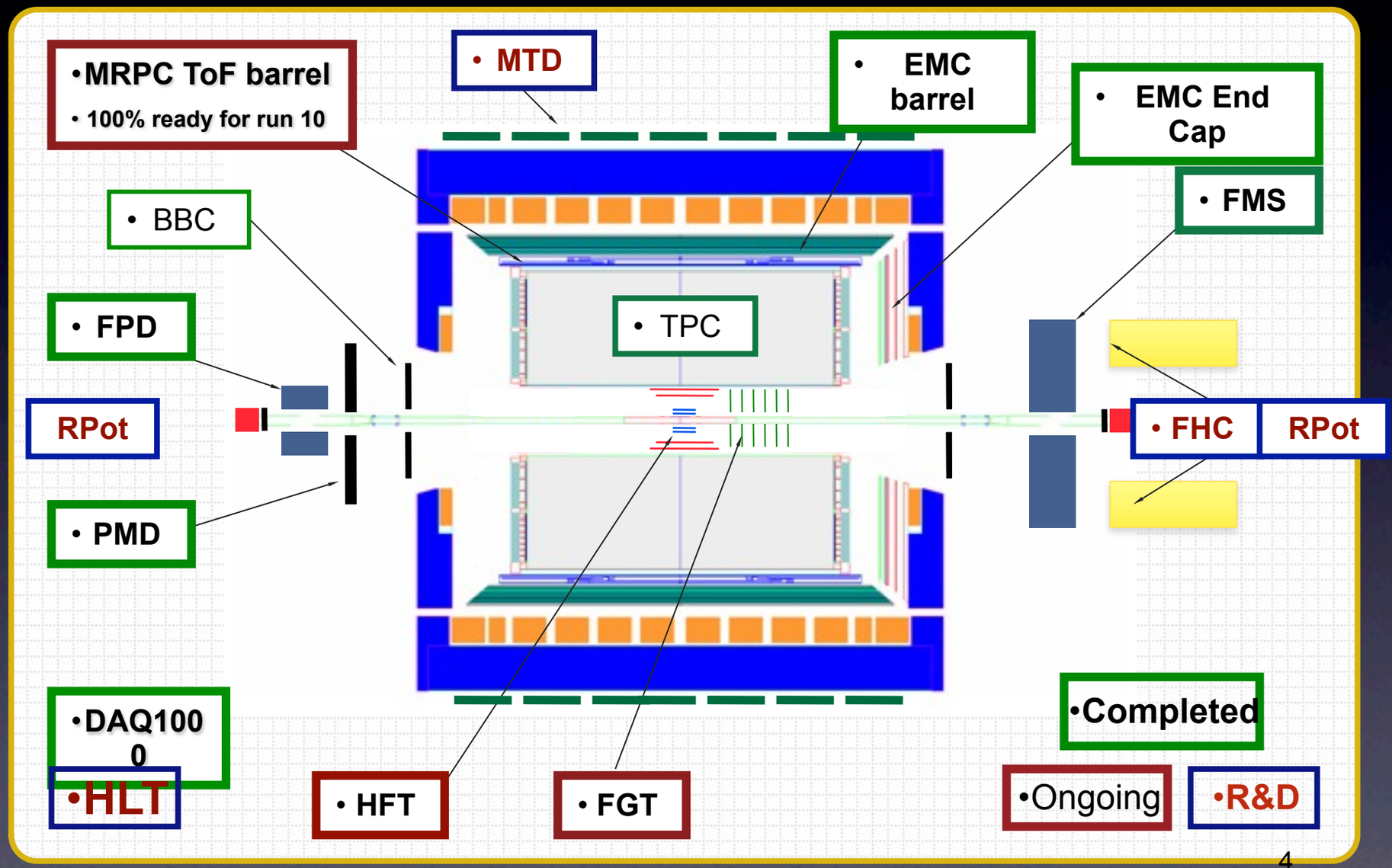
•MRPC ToF barrel
• 100% ready for run 10
• MTD
• EMC barrel
• EMC End Cap
• FMS
• BBC
• FPD
• TPC
RPot
• FHC
RPot
• PMD
•DAQ1000
•HLT
• HFT
• FGT
•Completed
•Ongoing
•R&D

4

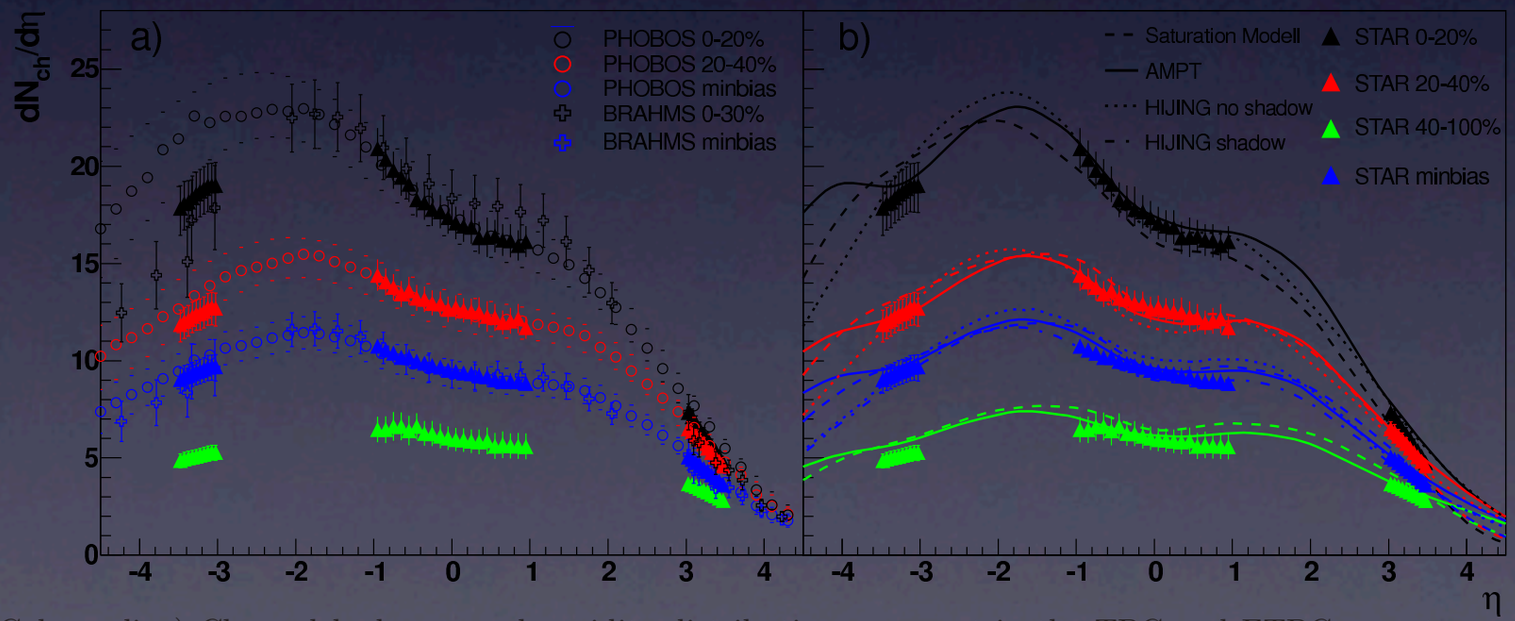

FIG. 3: (Color online) Charged hadron pseudorapidity distribution per event in the TPC and FTPC acceptance for 0-20%, 20-40%, 40-100% central and minimum bias d+Au events (triangles). The error bars include both statistical and systematic error. Also overlayed are measurements from BRAHMS (crosses) [22] and PHOBOS (circles) [23, 24]. In addition predictions from HIJING [19], AMPT [25] and the saturation model [12] are also plotted compared with STAR measurements.

Calculations

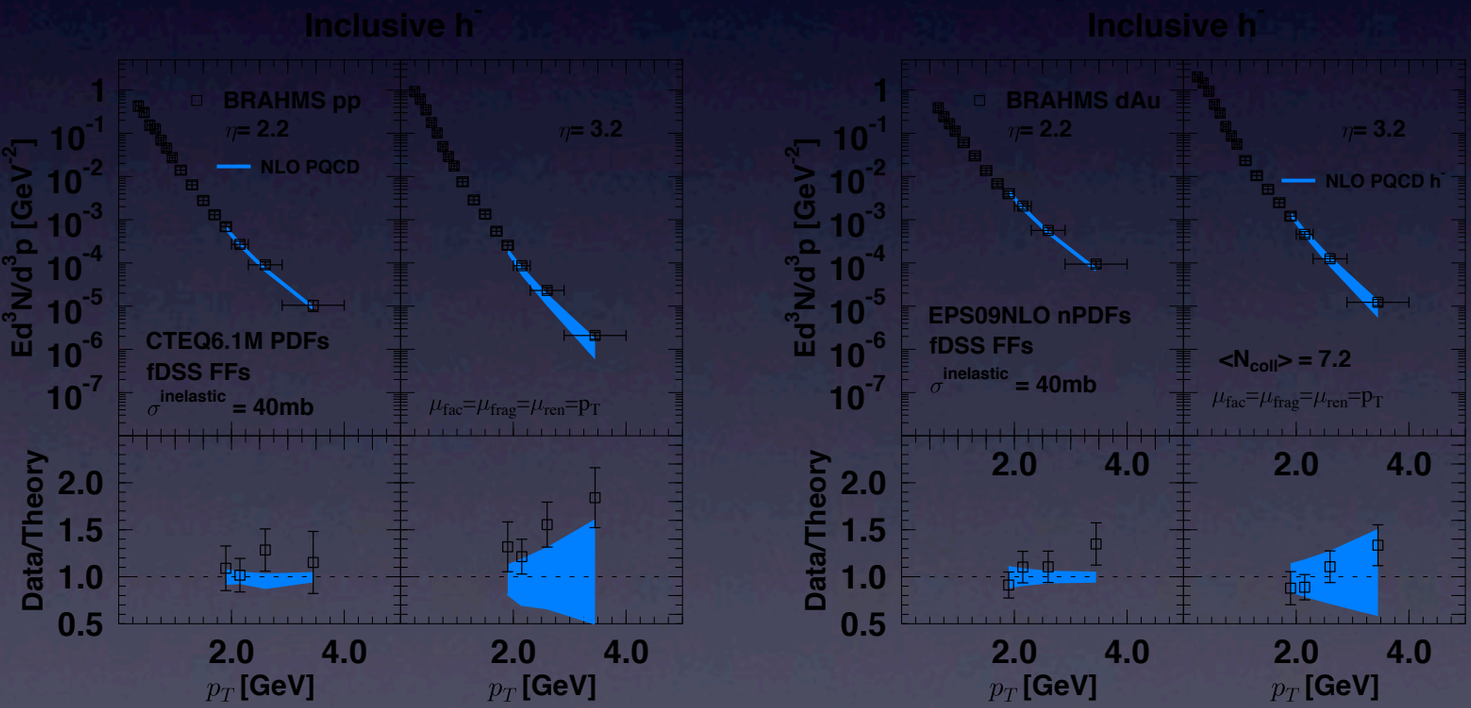

EPS09

Figure 13: Inclusive yield of negatively charged hadrons h^- in pp and dAu collisions. The experimental data shown by open squares is from [37] with statistical and systematical errors added in quadrature, and the horizontal bars indicate the p_T bin. The blue band indicates the 90% confidence range derived from free proton and nPDF uncertainties. The calculated cross-sections have been averaged over the p_T-bin width.

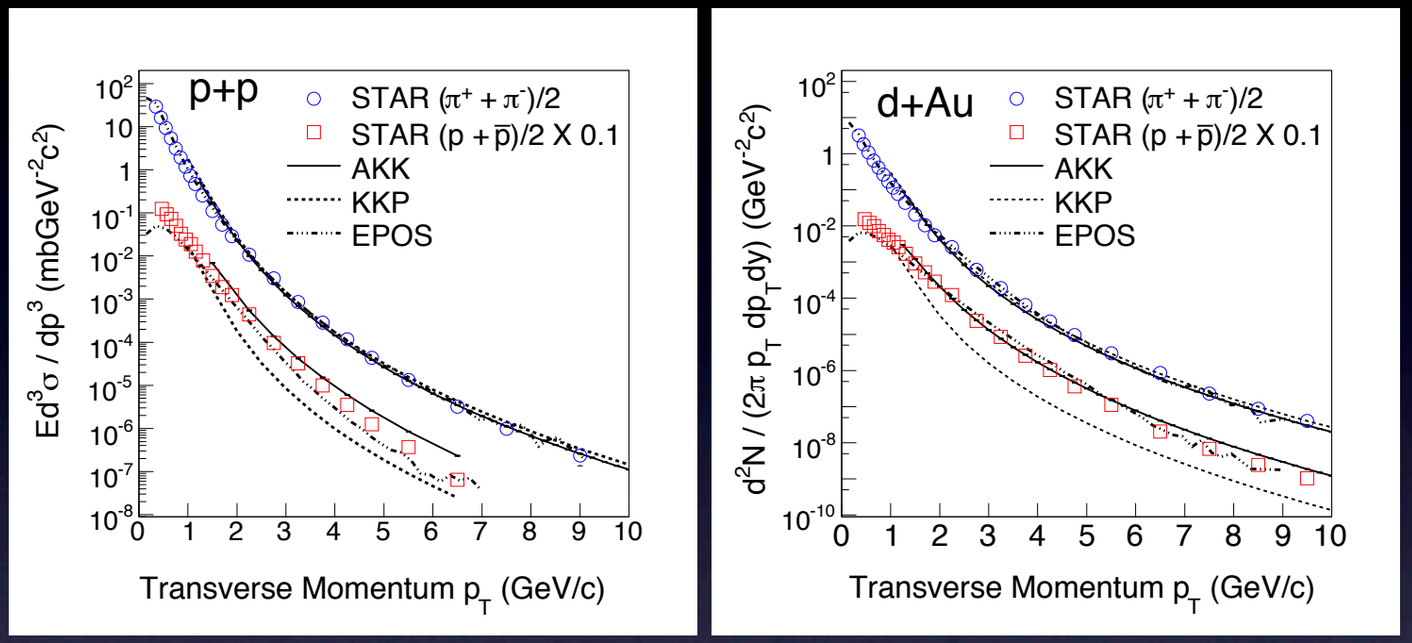

Fig. 6. Midrapidity invariant yields for $(\pi^+ + \pi^-)/2$ and $(p+\bar{p})/2$ at high $p_{\rm T}$ for minimum bias p+p and d+Au collisions compared to results from NLO pQCD calculations using KKP [29] (PDF: CTEQ6.0) and AKK [30] (PDF: CTEQ6M) sets of fragmentation functions and results from the EPOS model [28]. The PDFs for d and Au-nucleus are taken from Refs. [31] and [32] respectively. All results from NLO pQCD calculations are with factorization scale is $\mu = p_{\rm T}$.

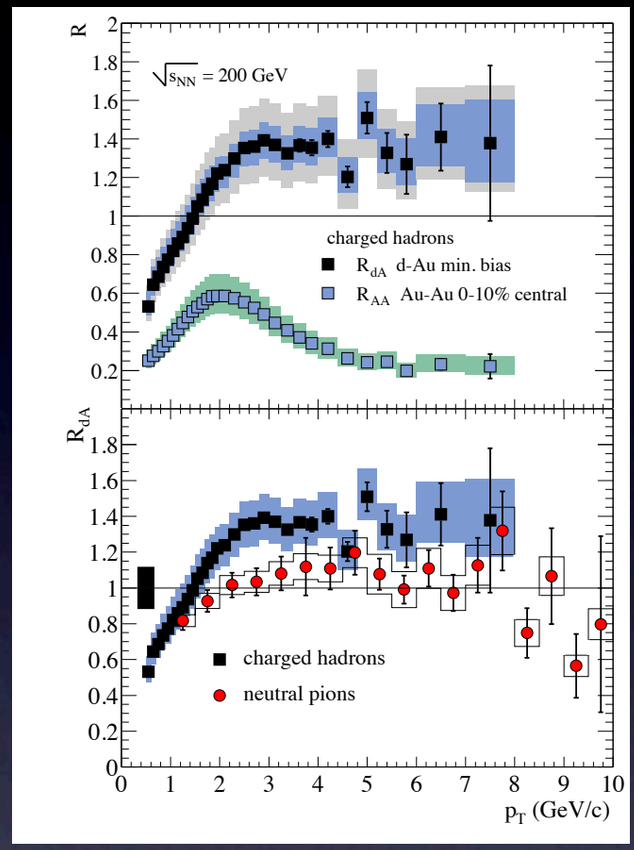

FIG. 3: Top: Nuclear modification factor $R_{\rm dA}$ for $(h^+ + h^-)/2$ in minimum bias d+Au compared to $R_{\rm AA}$ in the 10% most central Au+Au collisions. Inner bands show systematic errors which can vary with p_T, and outer bands include also the normalization uncertainty. Bottom: Comparison of $R_{\rm dA}$ for $(h^+ + h^-)/2$ and the average of the π^0 measurements in d+Au. The bar at the left indicates the systematic uncertainty in common for the charged and π^0 measurements.